

**THERMOCHROMIC AND IR TRANSMITTING OXIDE
GLASSES CONTAINING BISMUTH OXIDE
AND
A NEW DARKENING PHENOMENON IN
OXIDE GLASSES**

**A Thesis Submitted
In Partial Fulfilment of the Requirements
for the Degree of
DOCTOR OF PHILOSOPHY**

**By
AMARNATH SEN**

**to the
MATERIALS SCIENCE PROGRAMME
INDIAN INSTITUTE OF TECHNOLOGY, KANPUR
APRIL, 1985**

**“.....IN KNOWLEDGE IS THE
FEAR OF IGNORANCE”**
: Swami Vivekananda :

10 DEC 1987
CENTRAL LIBRARY
11.7.1
Acc. No. **A** 90195

1885-D-SEN-THE

CERTIFICATE

This is to certify that the thesis entitled "Thermochromic and IR Transmitting Oxide Glasses Containing Bismuth Oxide and a New Darkening Phenomenon in Oxide Glasses" by Mr. Amarnath Sen is carried out under our supervision and has not been submitted elsewhere for a degree.

Jitendra Kumar
Assistant Professor
Materials Science Programme
Indian Institute of Technology
Kanpur

D. Chakravorty
Professor
Materials Science Programme
Indian Institute of Technology
Kanpur

ACKNOWLEDGEMENTS

It is a pleasure for me to express my deep gratitude to Prof. D. Chakravorty and Dr. Jitendra Kumar for their encouragement and guidance throughout the course of this investigation.

I owe much to Dr. A. Ghosh for his valuable help and encouragement.

I am grateful to Mr. B. Sharma for his unassuming help and cooperation.

I wish to thank Messrs. I.D. Sharma, A. Sharma, Narsingh, R.K. Prasad, R.D. Prasad, S. Das, Barthwal, Srivastava, and Dwivedi for extending their helping hands during the work.

I shower a lot of thanks on my colleagues and friends, particularly Drs. S.K. Mukherjee, S. Dutta, A.K. Bag, G.C. Das, D. Bahadur and Messrs. R.K. Dhiman, V. Shrikant, D. Basu, P.K. Das, K. Banerjee, A.K. Bose, D. Banerjee, A. Srivastava and Ms. S. Mukherjee for their cooperation and timely help.

Finally, I acknowledge the help of Messrs. R.N. Srivastava, V.P. Singh, and Bajpae in getting this thesis in a neat form.

- Amarnath Sen

CONTENTS

<u>Chapter</u>		<u>Page</u>
	LIST OF TABLES	v
	LIST OF FIGURES	vi
	SYNOPSIS	ix
1	Thermochromism in Borate Glasses Containing Bismuth Oxide	
	Abstract	2
	1.1 Introduction	3
	1.2 Experimental	8
	1.3 Results and Discussions	13
	1.4 Conclusion	27
	References	29
2	Infrared Transmitting Bismuth Germanate Glasses Containing Zinc Oxide	
	Abstract	33
	2.1 Introduction	34
	2.2 Experimental	55
	2.3 Results and Discussions	59
	2.4 Conclusion	92
	References	95
3	Thermally Generated Darkening of Oxide Glasses	
	Abstract	100
	3.1 Introduction	101
	3.2 Experimental	108
	3.3 Results and Discussions	113
	3.4 Conclusion	133
	References	134

LIST OF TABLES

Number	Title	Page
1.1	Composition of glasses	9
1.2	The wavenumbers in kK of the transitions to the triplet and singlet states in $6s^2$ complexes	21
2.1	Some important properties of different modifications of GeO_2	48
2.2	IR transmitting germanate glasses reported in the literatures	49
2.3	Compositions of the glasses studied	56
2.4	Fifty percent cut-off (IR transmission) wavelengths of glasses	71
2.5	Minimum devitrification temperatures of the glasses	84
3.1	Classification of chromophors in inorganic systems	102
3.2	Types of colour in minerals	104
3.3	Glass compositions in mol %	109
3.4	Summary of heat treatment effects on various glasses	114
3.5	Standard d_{hkl} values for cubic lead and d_{hkl} values calculated from SAD pattern of glass no. 9 after electron beam heating of the sample inside the TEM	131

LIST OF FIGURES

Number	Title	Page
1.1	Block diagram of the set-up used for measuring optical absorption at elevated temperature	11
1.2	Optical absorption of glass 4	14
1.3	Percent change in photodiode resistance (γ) with temperature, reflecting the change in optical transmission characteristics of the glasses in the neighbourhood of 500 nm	15
1.4	A typical electron diffraction pattern of glass samples showing halos characteristic of amorphous materials	17
1.5	A typical electron micrograph of glass samples showing microheterogeneity	17
1.6	Fluorescence spectrum of $\text{MgO}:\text{V}^{2+}$ at various temperatures showing the radiative line and the vibrational satellites	24
2.1	Variation of reflection loss with refractive index	38
2.2	Useful IR transmission regions of important crystalline optical materials	43
2.3	Useful IR transmission regions of important optical glasses	44
2.4	Effect of thickness on transmittance of calcium aluminate glasses	45
2.5	Density of the glasses	61
2.6	Effect of zinc oxide content on molar volume of the glasses	62
2.7	Infrared transmission characteristics of glasses	66
2.8	Infrared transmission characteristics of glasses	67
2.9	Infrared transmission characteristics of glasses	68
2.10	Infrared transmission characteristics of glasses	69

2.11	Vickers microhardness of glasses (load 100 gm)	74
2.12	Weight loss per unit area of the glasses after leaching in 3 N HCl at 30°C for half an hour	77
2.13	Differential thermal analysis of glasses	79
2.14	Differential thermal analysis of glasses	80
2.15	Differential thermal analysis of glasses	81
2.16	Differential thermal analysis of glasses	82
2.17	Optical absorption of glasses	85
2.18	Optical absorption of glasses	86
2.19	Optical absorption of glass 5	87
2.20	Optical absorption of glasses	88
2.21	Optical absorption of glasses	89
2.22	Optical absorption of glass 10	90
3.1	Experimental arrangement for heat treatment in controlled atmosphere	111
3.2	Schematic representation of Lewis acid site in aluminosilicate	118
3.3	Schematic representation of the atomic arrangements in a specific region of the glass surface	120
3.4	Schematic representation of the effect of water addition on the atomic arrangements at the surface	121
3.5	Schematic representation of the effect of water addition on the atomic arrangements at the surface	121
3.6	Schematic representation of three configurations of various atoms that may emerge following heat treatment	122
3.7	Schematic representation of three configurations of various atoms that may emerge following heat treatment	122

3.8	Schematic representation of three configurations of various atoms that may emerge following heat treatment	122
3.9	A typical transmission electron micrograph of the glass samples	129
3.10	Transmission electron micrograph of glass no. 9	129
3.11	Microstructure of glass no. 9 after being heated for a few minutes with the electron beam inside the TEM	130
3.12	Representative electron diffraction pattern of regions emerged in glass no. 9 after electron beam heating of the sample inside the TEM indicative of the presence of the cubic phase of lead (Pb)	130

SYNOPSIS

1. Name of the Student : Amarnath Sen
2. Programme : Ph.D.
3. Department : Materials Science Programme
4. Title of the Thesis : Thermochromic and IR Transmitting Oxide Glasses Containing Bismuth Oxide and a New Darkening Phenomenon in Oxide Glasses
5. Thesis Supervisors : Professor D. Chakravorty and Dr. Jitendra Kumar

The first chapter of the thesis describes thermochromism in borate glasses containing bismuth oxide. New thermochromic glasses have been described in the system $B_2O_3-Al_2O_3-MgO-Na_2O$ containing Bi_2O_3 . Transmission characteristics of the glasses in the visible region have been studied up to $450^\circ C$. Glasses containing 15 mol % (or more) Bi_2O_3 show reversible deepening of colour on heating above $200^\circ C$. Transmission electron micrographs and selected area diffraction pattern of the glasses at room temperature ^{and} at $400^\circ C$ and again on cooling to room temperature have been taken which show no change in microstructure on heating and absence of any crystalline phase in the glasses in all the conditions. Thermogravimetric analysis of the glasses rule out the possibility of oxygen loss on heating. This thermochromic behaviour has been assigned to the temperature dependent vibronic transitions (B band) of Bi^{3+} ions. In this case, B band is redshifted to the blue end of the visible spectrum due to higher content of Bi^{3+} ions and presence of Bi^{3+} aggregates. At the same time, redshift

due to anharmonic vibration of bismuth and oxygen ions and the overlap of their electronic wavefunctions with increase in temperature contribute partly to the thermochromic effect.

The second chapter deals with the development and studies of some new IR transmitting bismuth germanate glasses containing zinc oxide. These glasses contain up to 20 mol % ZnO. The GeO_2 content varies from 60 to 80 mol % and the rest is Bi_2O_3 . The partial substitution of ZnO for GeO_2 (keeping the amount of Bi_2O_3 constant) in the glasses has been found to increase slightly the total cut-off and 50% cut-off wavelengths of the glasses. The molar volumes of the glasses decrease with the increase in ZnO content within them. In general, ZnO improves the hardness of the glasses. All the glasses studied are very resistant to water and the resistance towards 3 N HCl has been found to vary depending on the ZnO and Bi_2O_3 content of the glasses. DTA studies show that ZnO has a tendency to induce devitrification of the glasses at high temperatures. The optical absorption characteristics (in the visible region) of the glasses have also been studied. The results obtained are explained on structural basis taking into consideration the effects of nonbridging oxygen ions (dependent on Bi_2O_3 and ZnO content), change in polarizability of the oxygen ions (after ZnO addition), switching of some of the GeO_4 tetrahedra to GeO_6 octahedra (after ZnO addition) and formation of ZnO_4 tetrahedra (especially in high ZnO containing glasses).

A new darkening effect in oxide glasses, first observed by us, has been described in the third chapter of

the thesis. This effect has been found in oxide glass powders of a wide range of composition when heated in the temperature range 400-600°C with a trace amount of water. Generation of blackening is inhibited when excess water is present. The behaviour is not dependent on the atmosphere in which the heat treatment is carried out. The darkened samples bleach when heated up to 350°C under ordinary atmosphere or treated with oxidising agents. Transmission electron microscopic studies do not reveal any precipitated crystalline phase within the darkened glass matrix. The latter also do not give any specific EPR signal. A model has been proposed which ascribes the darkening to the formation of nonparamagnetic colour centres. The latter forms due to a simultaneous dehydration and reduction reaction, in which, trace amount of water acts as a catalyst.

CHAPTER 1

THERMOCHROMISM IN BORATE GLASSES

CONTAINING BISMUTH OXIDE*

* A paper based on this work has been published in
J. Mat. Sci. Lett. (1983) 2, 677.

ABSTRACT

New thermochromic glasses have been described in the system $\text{B}_2\text{O}_3\text{-Al}_2\text{O}_3\text{-MgO-Na}_2\text{O}$ containing Bi_2O_3 . Transmission characteristics of the glasses in the visible region have been studied upto 450°C . Glasses containing 15 mol % (or more) Bi_2O_3 show reversible deepening of colour on heating above 200°C . Transmission electron micrographs and selected area diffraction pattern of the glasses at room temperature, at 400°C , and again on cooling to room temperature have been taken which show no change in microstructure on heating and absence of any crystalline phase in the glasses in all the conditions. Thermogravimetric analysis of the glasses rule out the possibility of oxygen loss on heating. This thermochromic behaviour has been assigned to the temperature dependent vibronic transitions (B band) of Bi^{3+} ions. In this case, B band is redshifted to the blue end of the visible spectrum due to higher content of Bi^{3+} ions and presence of Bi^{3+} aggregates. At the same time, redshift due to anharmonic vibration of bismuth and oxygen ions and the overlap of their electronic wavefunctions with increase in temperature contribute partly to the thermochromic effect.

1.1 Introduction

Thermochromic materials change colour reversibly with temperature. There are many organic compounds which are thermochromic due to different mechanisms.⁽¹⁾ For example, spiropyrans become deeply coloured on heating due to opening of the spiro rings and formation of a polar structure; in quinoline, equilibrium between hydroxy form and quinone results in thermochromism and the dimers of triphenylimidazole change colour due to dissociation into free radicals. The other organic and metal organic⁽²⁾ thermochromic materials include anils, pyridines, copper bistrifluoroacetylacetonate, alcoholic solutions of the perchlorate salts of the nickel ethylenediamine and propylenediamine complexes, silver allylthiourethan etc.

Long back, Houston⁽³⁾ did systematic studies on many inorganic compounds which change colour on heating. The materials which change colour from red (or reddish) to dark (or black) colour are antimony sulphide, iron oxide, lead oxide etc., from orange to red colour are arsenic sulphide, mercury oxide, lead iodide etc., and, from yellow to orange (orange-red) colour are barium chromate, mercury sulphate, stannic sulphide etc. In most of the cases, the colour change is either due to phase transition (e.g. tetragonal HgI_2 is red whereas rhombic HgI_2 is yellow⁽²⁾) or due to decrease in the band gap with temperature (e.g. ZnO , which is yellow when hot and white when cold⁽⁴⁾). Bismuth oxide also changes colour from yellow to orange (or

brown) on heating, but recovers its original colour on cooling.⁽⁵⁾ Bi_2O_3 is an indirect gap insulator with an energy gap of approximately 2.6 eV at room temperature.⁽⁶⁾ Probably, the change in colour in Bi_2O_3 on heating is due to decrease of band gap with temperature.

Among the metallic systems, β -brass is thermochromic.⁽²⁾ The colour changes in this case is due to the lattice expansion as well as change in Fermi distribution of electrons with temperature.

Mixed oxides of Cr^{3+} with Al, Ga, Mg-Al, La-Ga, La-Al-Ga and Y-Al are thermochromic.⁽⁷⁾ The colour change in these cases has been ascribed to lattice expansion and consequently change in sub-shell energy difference of chromium ion⁽⁸⁾ on heating.

The double salts Ag_2HgI_4 and Cu_2HgI_4 are thermochromic due to an order-disorder transition in which the metal ions may exchange places in the lattice.⁽¹⁾

Boracites $\text{Me}_3\text{B}_7\text{O}_{13}\text{X}$, in which Me is a divalent metal species capable of existing in other valencies, and where X is halogen, are thermochromic.⁽⁹⁾ No mechanism has been suggested to explain this behaviour.

Many solutions also show colour change on heating. Aqueous solutions of some simple metal salts⁽¹⁾ exhibit thermochromicity when heated to 230°C. These include FeCl_3 , CuCl_2 , CoCl_2 , NiCl_2 , UO_2Cl_2 etc. These effects⁽¹⁰⁾ can be correlated with the anharmonic part of the vibrations of the ligands, producing the thermal expansion of the

ion changes rapidly with the ligand metal ion separation distance, the absorption frequency is shifted with temperature.

Hexaphenyldilead and hexacyclohexyldilead in hexane are thermochromic.⁽¹¹⁾ The colour change has been ascribed to temperature dependent broadening of UV band.

The colour of hydrochloric acid solutions of Mo^{5+} changes remarkably with a rise in temperature.⁽¹²⁾ These observations have been explained on the basis of temperature dependence of the monomer $\{\text{MoOCl}_5^{2-}\}$ -dimer $\{(\text{MoOCl}_4)_2\text{O}^{4-}\}$ equilibrium.

Cholesteric liquid crystals also show temperature dependent colour variations. The temperature affects the pitch spacing of the helicoidal structure of cholesteric liquid crystals and, hence, the wavelength of light undergoing Bragg diffraction at a given observation.⁽¹³⁾

Very little work has been reported about noncrystalline thermochromic materials. Amorphous tungsten oxide film has been found to show thermochromic behaviour.⁽¹⁴⁾ This colouring process is associated with the loss of oxygen on heating. A similar colouration band has been observed in oxygen deficient crystals of WO_3 . Total reversibility of thermochromically coloured films (amorphous WO_3) to the transparent state can be achieved by annealing in an oxygen environment for long periods of time.

Weyl⁽¹⁵⁾ reported that glasses containing high PbO are normally colourless but become brown on heating. Accor-

is due to the presence of fairly regular octahedra of PbO_6 in glasses, in contrast to distorted polyhedra in crystalline PbO . The colour change of heavy lead glasses on heating is due to the fluctuation of symmetry with increasing temperature resulting in the shift of the absorption band into the visible region.

Cadmium sulphide glass changes colour from yellow to orange (red) on heating.⁽¹⁵⁾ This colour change is instantaneous and reversible and has been explained on the basis of more intense instantaneous interaction between the polarizable Cd^{2+} and S^{2-} ions with the increase of the amplitude of thermal vibrations. Thermochromic coatings using lead and cadmium salts have already been patented.^(16,17)

Seward⁽¹⁸⁾ reported a new variety of photochromic glasses in the lanthanum borate systems containing copper doped silver halide crystallites. These glasses also show some temperature dependent variation in optical absorption characteristics. Such a glass is normally dark at room temperature, and it gets darker with increasing temperature. Above a certain high temperature, the darkened colour vanishes and the process is reversible. This temperature is believed to be associated with the melting and crystallization of the silver halide particles.

Thermochromism has been observed by Abe et.al.⁽¹⁹⁾ in reduced phosphate glasses in the systems $\text{K}_2\text{O}-\text{B}_2\text{O}_3-\text{Al}_2\text{O}_3-\text{P}_2\text{O}_5$ and $\text{K}_2\text{O}-\text{Al}_2\text{O}_3-\text{P}_2\text{O}_5$. The as cast glasses, which are colourless and transparent, become tinged with red when they are reheated to a temperature in the range 400°C to 600°C .

for a sufficiently long time. The colour can be bleached when the glasses are quenched from above 600°C and the bleached glass is recoloured at room temperature by the irradiation of solar rays. The bleached glasses can be easily coloured by heating at a relatively low temperature ($> 200^{\circ}\text{C}$), the coloured glasses are again bleached thermally. The authors believe that the colouring-bleaching behaviour is due to a phase transformation of colloidal phosphorus formed in these glasses.

The glasses containing Bi^{3+} ions are expected to show interesting optical properties due to the large size and polarizability of Bi^{3+} ions (like Pb^{2+} ions⁽¹⁵⁾). Indeed, we have observed reversible thermochromism in borate glasses ($\text{B}_2\text{O}_3\text{-Al}_2\text{O}_3\text{-MgO-Na}_2\text{O}$) containing Bi_2O_3 . This chapter deals with the studies done on these glasses and a possible mechanism of the thermochromic effect has been suggested.

1.2 Experimental

All the glasses were prepared from reagent grade chemicals. The compositions of the glasses are given in Table 1.1 (and Table 1.1(A)). Proportionate amounts of required components were thoroughly mixed in a porcelain mortar and pestle. Each mixture was melted in a pure alumina crucible using an electrically heated furnace. The glasses were melted at 1050°C and annealing was done at 350°C for 1 hr. In order to get thin samples (order of few mm) the glass was cast on a ^{polished} ~~glazy~~ stainless steel plate and pressed from the top by another ^{polished} ~~glazy~~ stainless steel plate.

Thermogravimetric analyses of the glass samples were carried out in a derivatograph (MOM, Budapest). For this experiment, powdered glass (-100 mesh) was used and heating rate was controlled to 10°C/min. The samples were heated ~~upto~~ 500°C.

For electron microscopic analysis, fine mesh (ASTM 400) copper grids were used. Carbon support films for the grids were initially prepared by vacuum evaporation technique on a precleaned glass slide. The carbon film was then cut into small squares and made to float on the surface of distilled water in a glass dish. These small portions of films were subsequently fished out with copper grids. The grids were then dried in a desiccator. The glass samples to be examined, were thoroughly ground in an agate mortar and pestle and then dispersed in acetone. A drop of acetone containing finely dispersed glass particles was then put on

TABLE 1.1 Composition of glasses

Glass number	B ₂ O ₃ mol %	MgO mol %	Al ₂ O ₃ mol %	Na ₂ O mol %	Bi ₂ O ₃ in mol % over 100 mol composition of the glass no. 1
1	60	15	15	10	0
2	60	15	15	10	2
3	60	15	15	10	5
4	60	15	15	10	15

TABLE 1.1(A) Composition of glasses (here the mole percentage has been calculated by incorporating Bi₂O₃ in 100 mol glass for each case)

Glass number	B ₂ O ₃ mol %	MgO mol %	Al ₂ O ₃ mol %	Na ₂ O mol %	Bi ₂ O ₃ mol %
1	60.00	15.00	15.00	10.00	0.00
2	58.82	14.71	14.71	9.80	1.96
3	57.14	14.29	14.29	9.52	4.76
4	52.18	13.04	13.04	8.70	13.04

the carbon side of the coated grid. After sometime acetone evaporated leaving the fine powder of glass on the grid. One drop of collodion solution (0.5 wt % in amyl acetate) was poured on distilled water to form a very thin film of collodion. The carbon coated grids containing glass particles were then placed on this film such that the particles face the collodion film. Then the grids were fished out by clean glass slides. In doing so, glass particles were sandwiched between carbon and collodion films. The collodion coating kept the particles in a fixed position and also prevented them from falling into the sample chamber during examinations. The grids were then placed on sample holder and observed in a Philips EM 301 transmission electron microscope operated at 100KV. Selected area diffraction and microstructure of the glass samples were recorded. The samples were then heated to around 400°C and their microstructure and selected area diffraction were again recorded.

The optical absorption studies of the glass samples at room temperature were carried out in a Cary 17D spectrophotometer in the range 400-750 nm. Thin glass samples (thickness of the order of few mm) were used for these studies.

For measuring optical absorption at elevated temperature, a special set up was used. The block diagram of the same is given in Figure 1.1. Rectangular glass samples (~ 3 mm thickness) were placed inside an electrically heated minifurnace in which light from a tungsten filament lamp entered from one side and reached the monochromator after

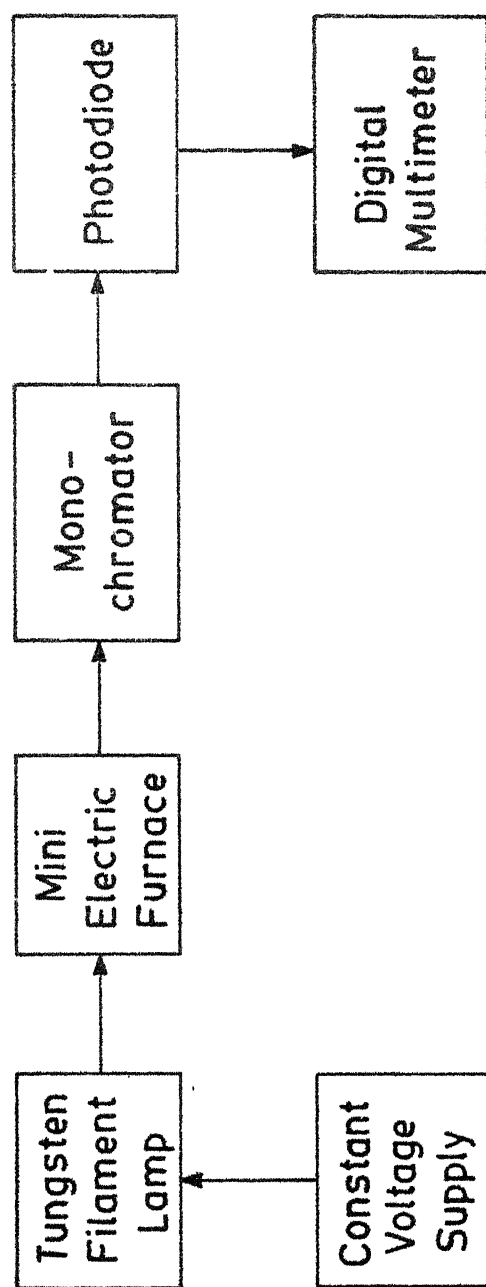


Fig. 1.1. Block diagram of the setup used for measuring optical absorption at elevated temperature.

passing through the sample. The emerging monochromatic beam was then allowed to fall on a photodiode (SI-100, BEL, India), the resistance of which was measured in the forward direction with a digital multimeter (HIL 2102). Thus the change in resistance of the photodiode described the optical transmission characteristics of the glasses. The experiments were carried out at fixed wavelengths in the range 700-500 nm at 50 nm intervals from room temperature to 450°C.

1.3 Results and Discussions

All glasses, except glass no. 4, are transparent and colourless. Glass no. 4 is pale golden yellow at room temperature but becomes deeply coloured (as seen by naked eye) on heating. Figure 1.2 shows the room temperature absorption of glass no. 4 (thickness 2.44 mm) as obtained from Cary 17D spectrophotometer. This glass has a broad absorption in the short wavelength region of the visible spectrum giving it the characteristic golden yellow colour. Glass nos. 1, 2, and 3, do not show any colour change on heating upto 450°C. Further it has been found that the photodiode resistance is constant upto 450°C (above this temperature, glasses begin to soften) throughout the wavelength range 700 to 500 nm for these glasses, indicating an absence of any measurable change in optical transmission characteristics. Figure 1.3 gives the percentage change in the photodiode resistance as a function of temperature.

For semiconductors, it can be shown that the fractional increase in conductivity with illumination is given by⁽²⁰⁾

$$\frac{\Delta\sigma}{\sigma} = \rho q \mu_h (b + 1) \eta E \tau \quad (1.1)$$

where $\rho = \frac{1}{\sigma}$ = Resistivity, q = charge of an electron, μ_h = hole mobility, $b = \mu_e / \mu_h$, where μ_e = electron mobility, η is a factor related to the quantum efficiency, E = incident illumination, τ = carrier life time. Hence the fractional increase in conductivity is directly proportional to the

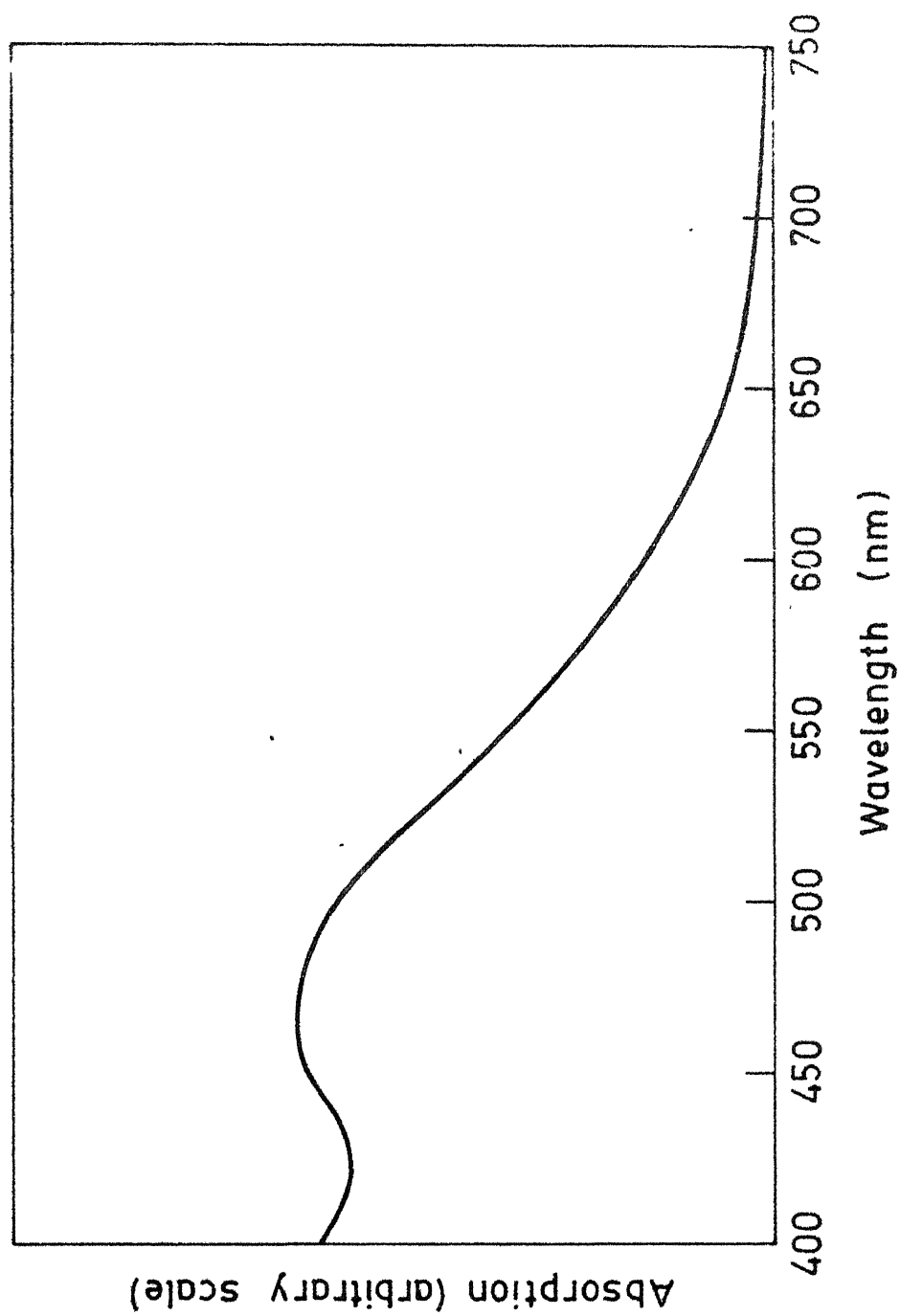


Fig. 1.2. Optical absorption of glass 4.

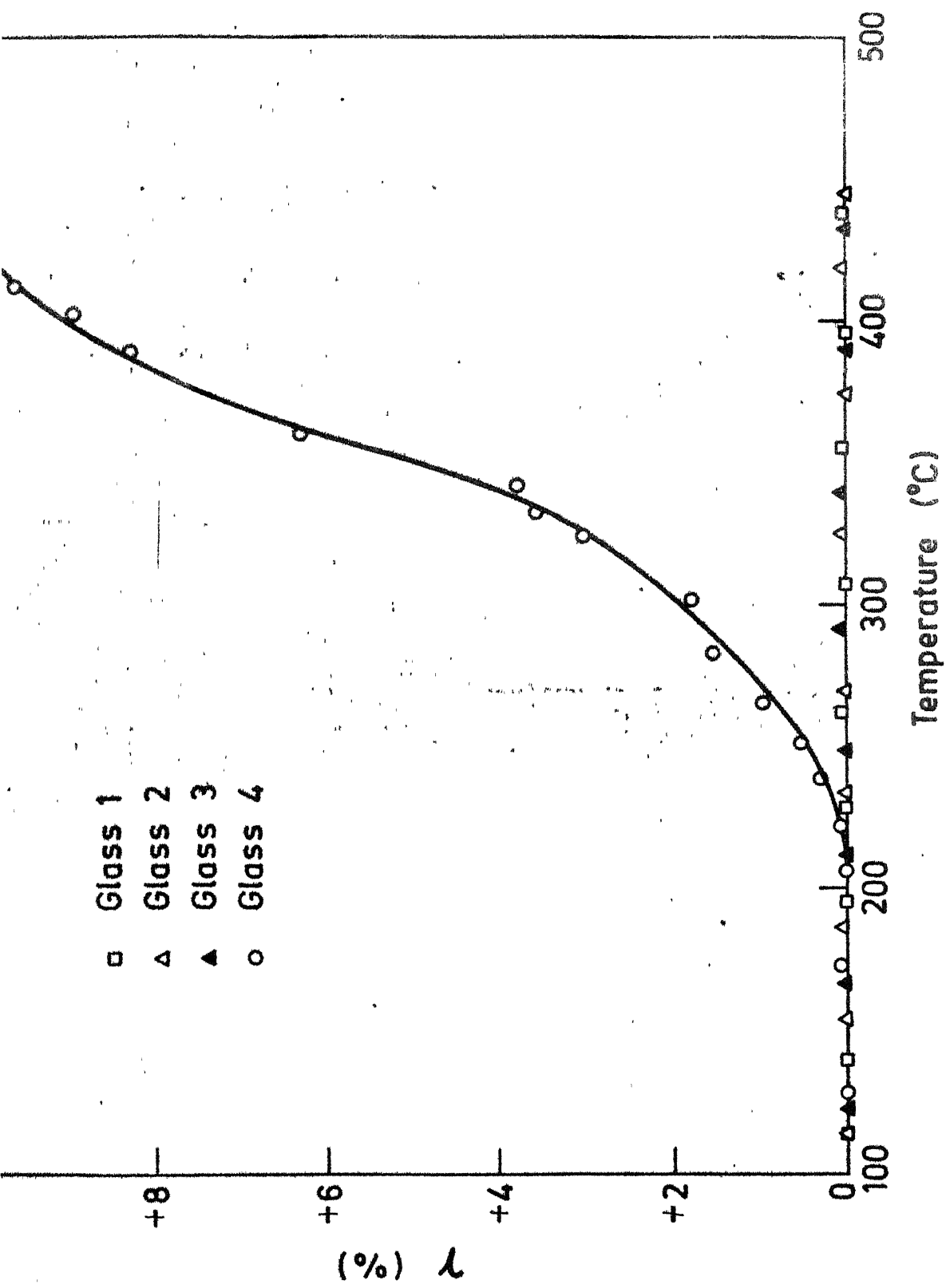


Fig. 1.3. Percent change in photodiode resistance (γ) with temperature reflecting the change in optical transmission characteristics of the glass in the neighbourhood of 500 nm

intensity of radiation incident on the sample. In our case, if I_0 is the intensity of the incident beam falling on the glass sample and I the intensity of the transmitted beam falling on the photodiode, then, we can write,

$$\frac{\Delta\sigma}{\sigma} \propto I \quad (1.2)$$

In other words, change in the photodiode resistance will be proportional to I .

So from Figure 1.3, it is clear that glass no. 4 shows an increase in absorption around 500 nm above 200°C. Due to poor sensitivity of the photodiode in the low wavelength region of the visible spectrum, change in absorption (if any) around 400 nm could not be measured, but change in absorption around 500 nm (as shown in Figure 1.3) is sufficient to prove that there is an appreciable thermochromicity in this glass especially above 350°C.

No visible change in the microstructure is observed in a TEM for all these glasses on heating. Moreover, selected area electron diffraction patterns at room temperature and on heating to 400°C show halos characteristic of amorphous materials. Representative photographs of the electron diffraction pattern and microstructure have been given in Figures 1.4 and 1.5 respectively. These results indicate that the process is not controlled by crystallization or phase change phenomena. Further, thermogravimetric analysis of all the glasses show no loss in weight on heating upto 500°C. This rules out the possibility of any

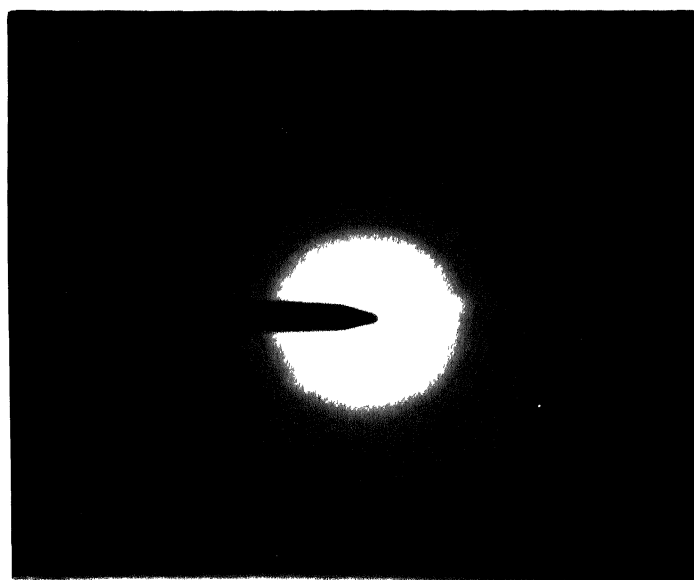


Figure 1.4

A typical electron diffraction pattern of glass samples showing halos characteristic of amorphous materials.

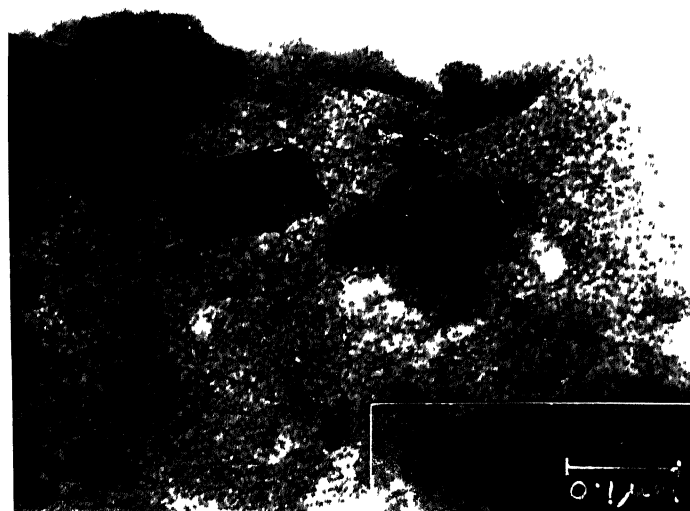


Figure 1.5

A typical electron micrograph of glass samples showing microheterogeneity.

loss of oxygen and hence formation of colour centres due to generation of defects.

The electronic spectra of compounds of main group elements can be classified in three groups.⁽²¹⁾ They are (1) Molecular spectra, (2) Charge transfer spectra, and (3) Rydberg spectra.

Molecular spectra involve transitions between molecular orbitals in covalently bonded molecules. The spectra of such solids may be best discussed in terms of a band structure. Example of compounds showing such spectra are the halogen vapours, NO_2 (brown), yellow Se_4^{2+} , red Te_4^{2+} and orange S_4N_4 .

Intense absorption bands resulting from excitation of electrons from orbitals localized mainly on the metal to an orbital localized mainly on the ligands, or vice versa are called charge transfer bands. Charge transfer spectra may be of three types.⁽²²⁾

(a) Ligand to metal transfer spectrum: It is due to a transfer of an electron originally localized in a ligand orbital to the central ion (e.g. IrCl_4^{2-} , MnO_4^- , CrO_4^{2-} etc.).

(b) Metal oxidation spectrum: It is due to a transfer of an electron localized in the central ion to an excited ligand orbital that is not much mixed with orbitals of the central ion (e.g. Ru^{2+} and Ir^{3+} complexes with pyridine and phenanthroline).

(c) Intraligand spectrum: It is due to a transfer of an electron from a ligand orbital to another ligand

orbital in a polyatomic ligand group. In this process only molecular orbitals of the ligands are involved (e.g. thiocyanate ion SCN^-).

In many compounds of the heavy post transition metal elements (e.g. Tl, Pb, Bi) the outermost s-orbital is only weakly involved in bonding. If the s-orbital is occupied, then transitions to the empty p-orbital above it are allowed, and directly analogous to the allowed $s \rightarrow p$ Rydberg transitions of atomic spectra. The Rydberg spectrum is thus due to a transfer of an electron localized in the central metal ion to an excited orbital that is not much mixed with the ligand orbitals (e.g. Tl^{1+} , Pb^{2+} , Bi^{3+} (configuration $\{\text{Xe}\} 4f^{14}5d^{10}6s^2$)).

The transitions of Bi^{3+} ions can therefore be interpreted as constituting Rydberg spectra. As far as free ions are concerned, the ground state term for Bi^{3+} (also Pb^{2+} and Tl^{1+}) is 1S_0 and the terms for the excited states of the configuration sp are in the order of increasing energy, 3P_0 , 3P_2 , 3P_1 (A band) and 1P_1 (C band). The transitions to 3P_2 and 3P_0 are forbidden by electronic selection rules for the cubic groups.⁽²³⁾ Some forbidden transitions may violate the selection rule due to coexcitation of electronic and vibrational levels and such transitions are called vibronic transitions.⁽²¹⁾ From symmetry considerations, it can be shown that 3P_2 (B band) transition is possible in case of Bi^{3+} (also Pb^{2+} and Tl^{1+}).⁽²³⁾ However, these transitions are quite sensitive to the local environment of the ion. It

has been observed that as the covalency increases in the metal ion-ligand interaction, there is a redshift, that is, a decrease in the s-p separation. This has been indicated in Table 1.2.⁽¹⁰⁾ So it is clear from Table 1.2 that, with the increase in polarizability of the ligands, that is, with the increase in covalency of the metal ion-ligand interaction, there is a redshift. O^{2-} ion with a polarizability close to that of Br^- ($Br^- = 42.4 \times 10^{-25} \text{ cm}^3$ and $O^{2-} = 39.0 \times 10^{-25} \text{ cm}^3$)⁽²⁴⁾ is expected to show similar effects as that of Br^- . Indeed $^1S_0 \rightarrow ^3P_1$ transition energy of Bi^{3+} in alkaline earth metal oxide is nearly 25 kK,⁽²⁵⁾ whereas for Br^- ligand this value is 26.3 kK.

In glasses (sulphate, phosphate and silicates), Bi^{3+} ion has been found to show absorption in the UV region and the transition energy in this case is greater than that of Bi^{3+} in alkaline earth metal oxide. This is due to the presence of dinegative oxygen ions in the latter, instead of chains and networks in the glasses where the oxygens suffer a reduction in electron charge density which in turn reduces their ability to form covalent bonds with the metal ions.⁽²⁵⁾

The above discussion is valid when the concentration of the metal ions is very low in the matrix. As the concentration increases, a pairing effect may occur.⁽²³⁾ In case of Tl^{1+} in KI, when the concentration of $Tl^{1+} \geq 0.01 \text{ mol } \%$, bands due to Tl^{1+} pairs are observed.⁽²⁶⁾ Bands of higher aggregates of Tl^{1+} are redshifted with respect to that of single ion species (e.g. in $KCl:Tl$, A band peak frequency is at 247 nm, B band at 210 nm and C band at 196 nm, while for Tl^{1+} aggregates, the

TABLE 1.2 The wavenumbers in kK^* of the transitions to the triplet and singlet states in $6s^2$ complexes⁽⁴⁾

	Gaseous	H_2O	OH^-	Cl^-	Br^-	I^-
<hr/>						
Tl^{1+}						
$^1\text{S}_0 \rightarrow ^3\text{P}_1$	52.39	46.7	-	40.5	38.1	35.5
$^1\text{S}_0 \rightarrow ^1\text{P}_1$	75.66	-	-	51.0	47.2	43.0
<hr/>						
Pb^{2+}						
$^1\text{S}_0 \rightarrow ^3\text{P}_1$	64.39	48.0	41.65	36.8	33.2	27.6
$^1\text{S}_0 \rightarrow ^1\text{P}_1$	95.34	-	-	51.0	44.9	-
<hr/>						
Bi^{3+}						
$^1\text{S}_0 \rightarrow ^3\text{P}_1$	75.93	45.0	-	30.5	26.8	22.2
$^1\text{S}_0 \rightarrow ^1\text{P}_1$	114.60	-	-	45.0	38.5	29.8

* kK . (Kilokayser = 1000 cm^{-1} , range of visible spectrum:
12-22 kK)

peak frequency is at 260 m).⁽²⁷⁾ Similarly in NaCl:Pb crystals, with increase of Pb^{2+} concentration, bands due to Pb pairs have been observed.⁽²⁸⁾

From NMR studies of borate glasses containing Tl^{1+} , Momii et.al.⁽²⁹⁾ concluded that with the increase of Tl_2O (> 18 mol %) there is more covalent interaction of Tl ions with nearest oxygen ions. They also suggested the possibility of the presence of thallium ion pairs. These observations explain the redshift in high Tl_2O containing glasses (thallium borate glasses acquire a distinct yellow colour at about 18 mol % Tl_2O concentration, while they are colourless at low concentration of Tl_2O).⁽²⁹⁾

In glasses containing small amounts of bismuth oxide, bands in the UV region are found due to transitions in Bi^{3+} as discussed earlier. But as the concentration of bismuth oxide increases, clustering of Bi^{3+} ions is likely to occur. In glasses, this type of microheterogeneity due to clustering of modifier ions is a common phenomenon.⁽³⁰⁾ The glasses in our system also show microheterogeneities which is evident from the electron micrograph shown in Figure 1.5.

Also, with the increase of Bi_2O_3 , more covalent interaction of bismuth ions with the neighbouring oxygen ions is expected as is found in the case of Tl_2O containing glasses. The increase in covalency can be understood as a loosening of structure by more network modifier ions (Bi^{3+} in this case) and formation of more polarizable nonbridging oxygen ions.⁽¹⁵⁾

So, as discussed earlier, with the increase in covalency of the metal ion ligand interaction (that is, with the increase of Bi_2O_3 content in our case), as well as clustering of Bi^{3+} ions, optical absorption should show an appreciable redshift. This explains the pale golden yellow colour of glass no. 4 (containing 15 mol % Bi_2O_3) due to absorption in the blue region of the visible spectrum as shown in Figure 1.2, while lower amount of Bi_2O_3 cannot impart any colour to the glasses.

It is a well known fact in absorption spectroscopy of ionic crystals that, the width of a band becomes larger as the temperature increases which is comprehensible from the configurational coordinate diagrams.⁽²²⁾ For vibronic transitions, as thermal vibrations are involved, the strength of absorption becomes strongly temperature dependent. A typical vibronic spectrum, appearing on both sides of a purely radiative line for $\text{MgO}:\text{V}^{2+}$ is shown in Figure 1.6.⁽³¹⁾ It is evident from the figure that with increasing temperature, the continuum of the spectrum expands more to wavelengths further removed from that of the no phonon line and grows in intensity, whereas the peaks tend to smooth out and disappear. As discussed earlier, $^1\text{S}_0 \rightarrow ^3\text{P}_2$ transition in Bi^{3+} (also Pb^{2+} and Tl^{1+}) is vibronic and hence expected to be temperature sensitive. Indeed this has been found in case of Tl^{1+} in KI. Seitz⁽³²⁾ first observed a weak band at 2440 Å for Tl^{1+} in KI. Yuster et.al.⁽²⁶⁾ found that the intensity of absorption to the weak 2440 Å band is strongly dependent on temperature. Since it is between the bands previously

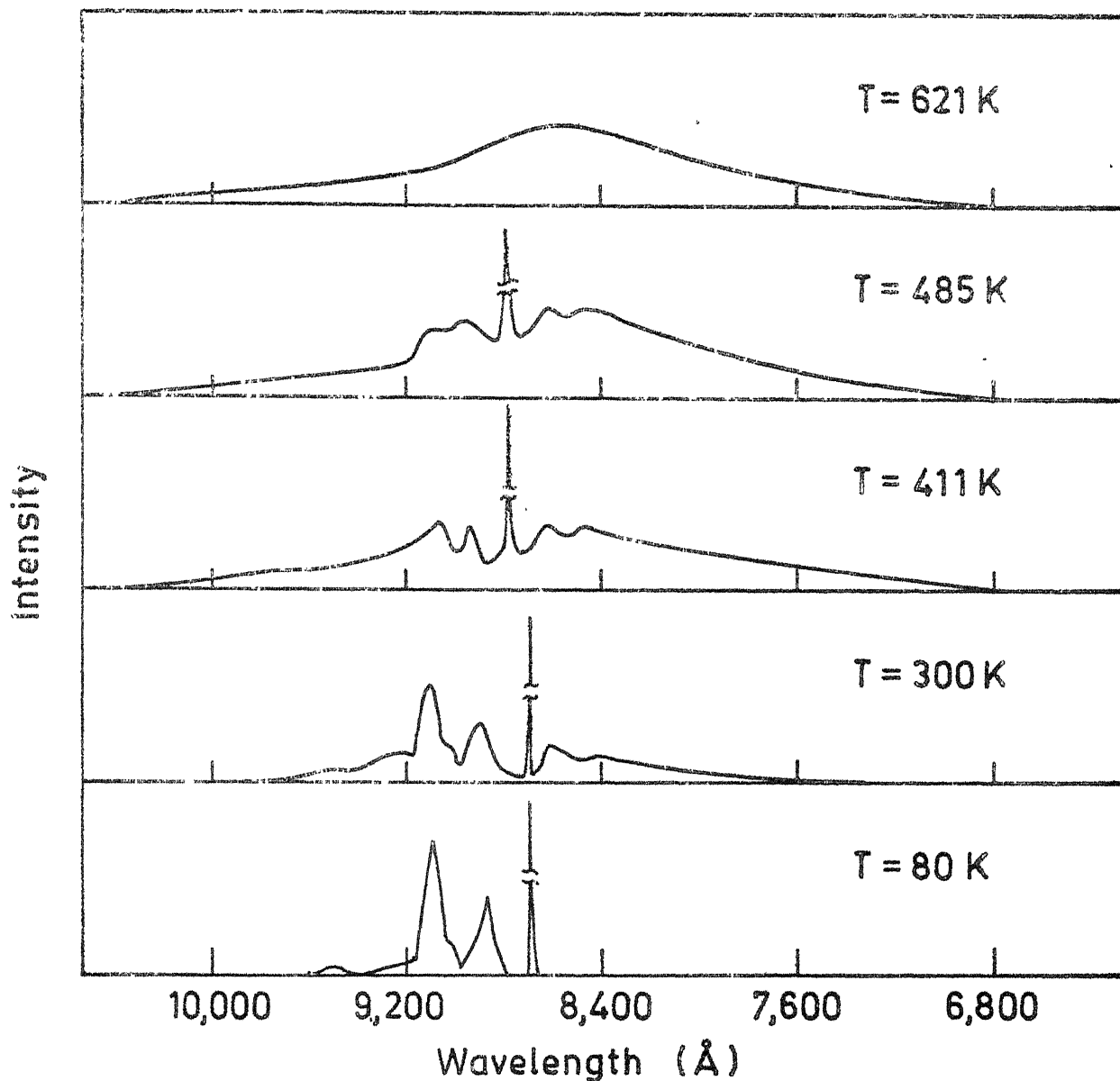


Fig. 1.6. Fluorescence spectrum of $\text{MgO} : \text{V}^{2+}$ at various temperatures showing the radiative line and the vibrational satellites⁽³¹⁾.

identified as 1P_1 and 3P_1 and has the temperature dependence expected for a vibrationally induced transition, it has been assigned as 3P_2 band.

From the above considerations, it seems that the main contribution to the thermochromic effect in glass no. 4 (containing 15 mol % Bi_2O_3) arises from the increased absorption with temperature due to the vibronic transitions (B band) of bismuth ions, which is redshifted to the blue end of the visible spectrum (like A and C bands) with respect to single Bi^{3+} ion species due to higher content of Bi^{3+} ions and presence of Bi^{3+} aggregates.

Anharmonicity of vibrations, which is significant in case of bismuth and oxygen ions (due to their large difference in masses, and to some extent due to large polarizability of bismuth ions) plays a significant role in vibronic spectra. It leads to a temperature shift and increase in the widths of the excited vibrational levels.⁽³³⁾ At the same time, a positive contribution to the thermochromicity should come from the increased vibrational overlap (due to increase in temperature) of the electronic wavefunctions of bismuth ions and neighbouring oxygen ions leading to an increased covalency and hence redshift.

As depicted in Figure 1.3, for glass no. 4, there is a measurable change in the absorption around 500 nm, which starts from 200°C. Above 300°C, there is a sharp increase in the absorption. Below 200°C and in higher wavelength regions, there is practically no change in absorption

or, at least, the change (if any), is too small to be measured by our set up.

The shape of the curve (Figure 1.3) for glass no. 4 should follow Beer's law, which states that⁽³⁴⁾ $I = I_0 e^{-\alpha t}$, where I is the intensity of the transmitted beam, I_0 is the intensity of the incident beam, α is the absorption coefficient and t is the thickness of the material. In our case, I_0 and t are constants. The ordinate of the curve (Figure 1.3) is proportional to I . So the shape of the curve for glass no. 4 will be governed by an exponential function of α , where α is dependent on temperature and hence is a complicated function of phonon density, band broadening and redshift.

1.4 Conclusion

Thermochromic behaviour has been found in B_2O_3 - Al_2O_3 - MgO - Na_2O glasses containing 15 mol % Bi_2O_3 . The deepening of colour with temperature is prominent above $300^\circ C$. This behaviour has been explained on the basis of temperature dependent intensity variations of vibronic transitions in bismuth ion and bismuth ion aggregates. At the same time, redshift due to anharmonic vibration of bismuth and oxygen ions and the overlap of their electronic wavefunctions with increase in temperature have been taken into account.

It should be mentioned that glasses containing more than 15 mol % Bi_2O_3 also show thermochromism. But initially due to their strong colour, they do not seem to be of much practical interest.

As Bi^{3+} ions can be incorporated in sufficient amounts in silicate, phosphate and borosilicate glasses,^(35,36) these glasses are also expected to show thermochromic behaviour. Detailed studies in various systems are needed to choose the right glass composition showing the optimum thermochromic effect.

Although reversible thermochromic materials are not of much practical use, whereas, irreversible thermochromic materials⁽¹⁾ like salts and organic complexes of cobalt, nickel, copper, manganese, iron etc. are used as temperature indicators in difficult-to-reach places in complex electrical equipment or moving parts of an engine or a reaction vessel, yet these glasses may be of practical use due to

their transparency and the ease with which they can be prepared.

These and related glasses can be used as a temperature sensitive filter, which may find application in control devices. The intensity of the beam of right wavelength transmitted through the glass will be changed with temperature and this change in intensity may be manipulated in a suitable way to shift a system from the on state to the off state (or vice versa) with temperature.

REFERENCES

- (1) Day, J.H. (1979) in Kirk-Othmer Encyclopaedia of Chemical Technology, Vol. 6, p.129, John Wiley & Sons, New York.
- (2) Day, J.H. (1968), Chem. Rev. 68(6), 649.
- (3) Houston, E.J. (1871), Chem. News. 24, 177, 188.
- (4) Moore, W.J. (1967), Seven Solid States - An Introduction to the Chemistry and Physics of Solids, p. 145, W.A. Benjamin Inc., New York.
- (5) Samsonov, G.V. (1932), The Oxide Handbook, pp. 225, 227, IFI/Plenum, New York.
- (6) Dolocan, V. and Iova, F. (1981), Phys. Stat. Solid. A, 64(2), 755.
- (7) Poole, C.P., Jr. (1964), J. Phys. Chem. Solids, 25, 1169.
- (8) Jorgensen, C.K. (1971), Modern Aspects of Ligand Field Theory, p. 344, North-Holland Publishing Co., Amsterdam.
- (9) Schmid, H. (1965), Phys. Chem. Solids, 26, 973.
- (10) Jorgensen, C.K. (1962), Absorption Spectra and Chemical Bonding in Complexes, pp. 145, 186, Pergamon Press, Oxford.
- (11) Drenth, W., Willemsons, L.C. and VanderKerk, G.K.M. (1964), J. Organometal. Chem. 2, 279.
- (12) Yoshino, Y., Taminaga, I. and Uchida, S. (1971), Bull. Chem. Soc. Jpn., 44, 1435.
- (13) Fergerson, J., Goldberg, N., Nadalin, R. (1966), Mol. Cryst., 1, 315.
- (14) Goulding, M.R., Thomas, C.B. and Hurditch, R.J. (1983), Solid State Commun., 46(6), 451.
- (15) Weyl, W.A. and Marboe, E.C. (1962), The Constitution of Glasses - A Dynamic Interpretation, Vol. 1, pp. 315, 45, 60, 41, Interscience Publishers, New York.
- (16) Spaethling, W. and Seidel, H. (June 1976), USSR Patent 514 945.
- (17) Brom, M.P. and Devris, R.C. (Oct. 1973), German Patent 2 314 722.

- (18) Seward, T.P. (1975), J. Appl. Phys., 46(2), 689.
- (19) Abe, Y., Kawashima, K. and Suzuki, S. (1981), J. Amer. Ceram. Soc. 64, 206.
- (20) Levi, L. (1980), Applied Optics - A Guide to Optical System Design, Vol. 2, p. 455, John Wiley & Sons, Inc., New York.
- (21) Williams, A.F. (1979), A Theoretical Approach to Inorganic Chemistry, pp. 144, 133, Springer-Verlag, Berlin, Heidelberg.
- (22) DiBartolo, B. (1968), Optical Interactions in Solids, pp. 415, 421, John Wiley & Sons, Inc., New York.
- (23) McClure, D.S. (1959), Electronic Spectra of Molecules and Ions in Crystals, pp. 165, 173, Academic Press, New York.
- (24) Harvey, K.B. and Porter, G.B. (1963), Introduction to Physical Inorganic Chemistry, p. 251, Addison-Wesley Publishing Co., Massachusetts.
- (25) Duffy, J.A. and Ingram, M.D. (1970), J. Chem. Phys. 52, 3752.
- (26) Yuster, P. and Delbecq, C. (1953), J. Chem. Phys. 21, 892.
- (27) Paterson, D.A. and Klick, C.C. (1957), Phys. Rev. 105, 401.
- (28) Burstein, E., Oberly, J.J., Henvis, B.W., and Davisson, J.W. (1951), Phys. Rev. 81, 459.
- (29) Momii, R.K. and Nachtrieb, N.H. (1968), J. Phys. Chem., 72(10), 3416.
- (30) Porai-Koshits, E.A. (1966) in The Structure of Glass - Properties, Structure and Physical-Chemical Effects, Ed. E.A. Porai-Koshits (Trans. E. Boris Uvarov), Vol. 6, p. 3, Consultant Bureau, New York.
- (31) Imbusch, G.F., Yen, W.M., Schawlow, A.L., McCumber, D.E. and Sturge, M.D. (1964), Phys. Rev. 133, A1029.
- (32) Seitz, F. (1938), J. Chem. Phys. 6, 150.
- (33) Rebane, K.K. (1970), Impurity Spectra of Solids - Elementary Theory of Vibrational Structures (Trans. J.S. Shier), p. 132, Plenum Press, New York.

- (34) Kingery, W.D. (1960), Introduction to Ceramics, p. 514, John Wiley & Sons, Inc., New York.
- (35) Das, G.C. (1982), Ph.D. Thesis, I.I.T. Kanpur.
- (36) Bhargava, S. (1984), M.Tech. Thesis, I.I.T. Kanpur.

CHAPTER 2

INFRARED TRANSMITTING BISMUTH GERMANATE

GLASSES CONTAINING ZINC OXIDE*

* Applied for a patent.

ABSTRACT

Some new IR transmitting bismuth germanate glasses containing zinc oxide have been developed. These glasses contain upto 20 mol % ZnO. The GeO_2 content varies from 60 to 80 mol % and the rest is Bi_2O_3 . The partial substitution of ZnO for GeO_2 (keeping the amount of Bi_2O_3 constant) in the glasses has been found to increase slightly the total cut-off and 50% cut-off wavelengths of the glasses. The molar volumes of the glasses decrease with the increase in ZnO content within them. In general, ZnO improves the hardness of the glasses. All the glasses studied are very resistant to water and the resistance towards 3N HCl has been found to vary depending on the ZnO and Bi_2O_3 content of the glasses. DTA studies show that ZnO has a tendency to induce devitrification of the glasses at high temperatures. The optical absorption characteristics (in the visible region) of the glasses have also been studied. The results obtained are explained on structural basis taking into consideration the effects of nonbridging oxygen ions (dependent on Bi_2O_3 and ZnO content), change in polarizability of the oxygen ions (after ZnO addition), switching of some of the GeO_4 tetrahedra to GeO_6 octahedra (after ZnO addition) and formation of ZnO_4 tetrahedra (especially in high ZnO containing glasses).

2.1 Introduction

Infrared radiation is electromagnetic in nature. It is generated by vibration and rotation of the atoms and molecules within any material whose temperature is above absolute zero. The infrared region is bounded on the short wavelength side by visible light and on the long wavelength side by microwaves. As a result of developments in detectors and optical materials, three quite natural though purely arbitrary divisions of the IR spectrum are commonly used.⁽¹⁾ These are (a) the near-IR region from approximately 0.7 to 1.5 μm , (b) the intermediate or middle IR region from approximately 1.5 to 5.6 μm and (c) the far-IR region from approximately 5.6 to 1000 μm .

The infrared techniques have a large number of applications.^(1,2) Starting from their use in scientific research (like measurement of temperature, meteorological applications, remote sensing of astronomical bodies, infrared photography, space communication, spectroscopic applications in basic science research etc.), they have extensive industrial (like non-destructive testing, temperature measurement, photography etc.) and military applications (like search, track, ranging, weapon guidance, infrared photography, reconnaissance etc.). Now a days, infrared systems have also become important diagnostic tools in the medical field.

Since the 1930s a great deal of effort has been made in the search for materials having optical and physical

properties suited to IR imagery. Infrared transmitting materials are required in a number of applications ranging from infrared lenses and related optical components, to windows and domes that may function primarily to protect detecting systems from the environment. For the material selection, four primary properties should be studied.⁽¹⁾ They are (a) optical properties, (b) mechanical properties, (c) thermal properties and (d) chemical properties.

(a) Optical properties: The primary requirement of an IR optical material is that it should have maximum transmission of IR radiation in the desired wavelength band. Optical homogeneity is very desirable. Refractive index is also an important parameter, which controls reflection losses, aberrations etc.

(b) Mechanical properties: A high mechanical strength is essential especially in the case of optical materials employed for IR air-borne and missile applications, where severe vibration and shock conditions exist. For windows and domes exposed to the severe erosion problems, which occur in air-borne applications, the surface hardness of the material is an important parameter. Certain optical materials require special surface coatings to prevent scratching and erosion, which cause pitting of the polished surface, forming local 'hot spots' or sources of radiation which produce false target images and sharp background-radiation gradients.

(c) Thermal properties: Thermal shock resistance should be good enough to withstand aerodynamic heating in irldomes and windows used in missiles and high speed aircraft. A high softening point, a low thermal coefficient of expansion, and good thermal conductivity are desirable properties under these conditions.

(d) Chemical properties: In the optical materials used for many industrial applications of IR, such as pyrometers, process-stream analyzers, etc., their chemical resistance to the various solvents and gases encountered in industrial processes must be considered. In windows and irldomes exposed to atmospheric environments, optical materials used should be non-hygroscopic and water insoluble.

Besides these properties, in dual-mode systems, that is, those combining infrared and radar and using a common protective dome (irradome), it is necessary to know the RF properties of the material as well.

Unfortunately, there exist no such optical material which possesses all the desirable features described above. The choice of an optical material for a particular application is therefore a matter of compromise for the designer.

Before describing the optical materials, we will briefly discuss the theoretical considerations for infrared transmission and other relevant properties.

The proportion of incident radiation transmitted by a material is a function of absorption and scattering within the bulk of the material, and of reflection at the external

surfaces. The intensity of transmitted radiation, I_t , through a sample of thickness t , may be estimated from the Lambert-Bouger law⁽³⁾:

$$I_t = I_i e^{-\alpha t} \quad (2.1)$$

where I_i is the intensity of the incident radiation and α is the absorption coefficient (reflection losses at the surfaces are neglected).

If reflection at the two interfaces is taken into account, the ratio of transmitted to incident intensity, I_t/I_i is given by:

$$\frac{I_t}{I_i} = (1 - R)^2 e^{-\alpha t} \quad (2.2)$$

where R , the reflectivity at normal incidence, is dependent on the refractive index n , of the material, and for reflection by a transparent medium in air is given by:

$$R = \frac{(n_\lambda - n_{\text{air}})^2 + K_{\text{air}}^2}{(n_\lambda + n_{\text{air}})^2 + K_{\text{air}}^2} \quad (2.3)$$

where K is the extinction coefficient and is given by $K = \lambda\alpha/4\pi n$ (λ stands for wavelength). For air, $\alpha \sim 0$, so $K \sim 0$ and also $n_{\text{air}} \sim 1.0$, hence

$$R \sim \left(\frac{n_\lambda - 1}{n_\lambda + 1} \right)^2 \quad (2.4)$$

Figure 2.1 shows the variation of percentage reflection loss with refractive index of the optical materials.

The absorption of incident radiation may be due to

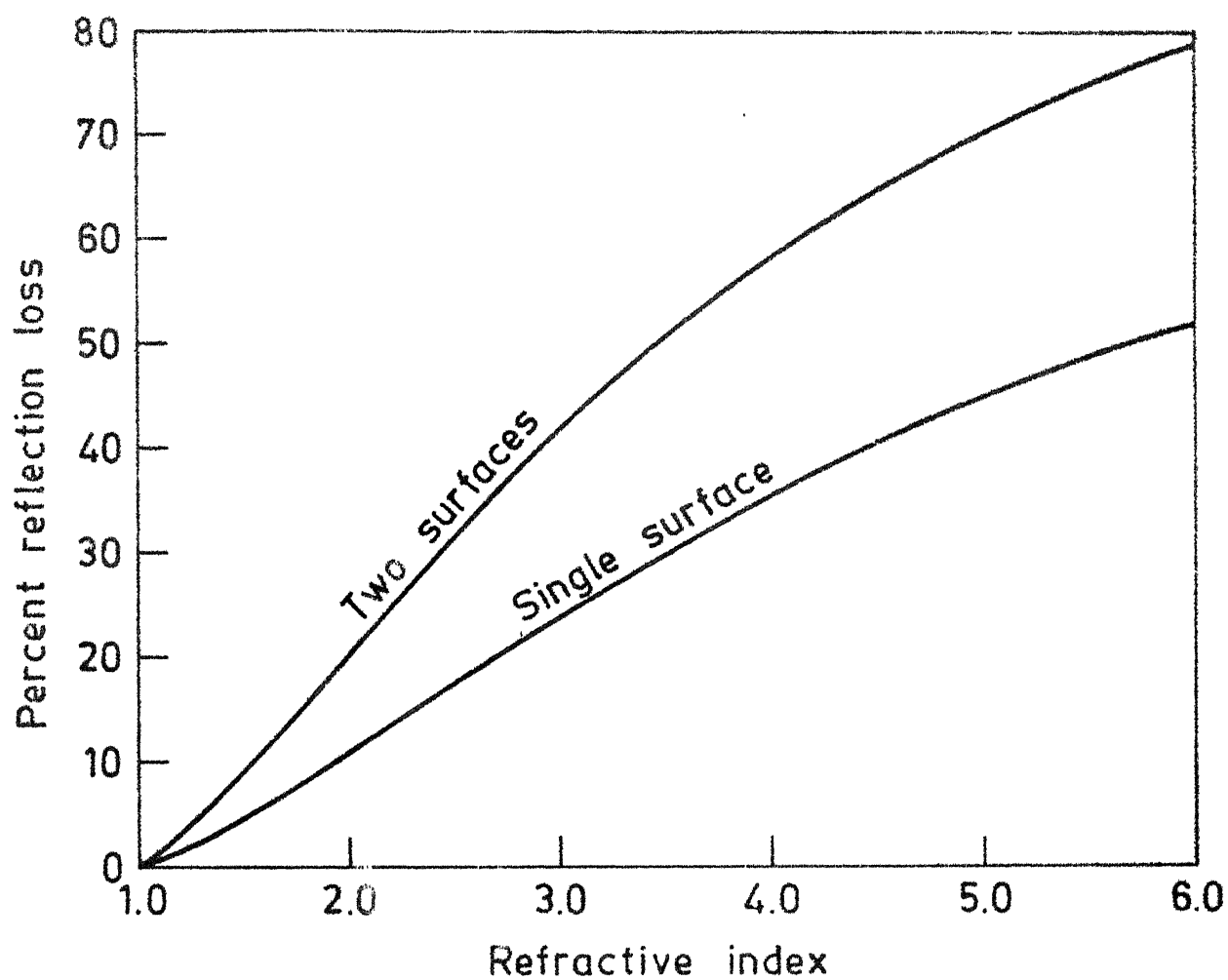


Fig. 2.1. Variation of reflection loss with refractive index⁽²⁾.

(a) Intrinsic absorption mechanisms: Absorption at short wavelengths is due to transitions between electronic states and is a function of the energy gap, E_g , of the material. The short wavelength cut-on λ_c is given by the relationship:

$$\lambda_c = \frac{hc}{E_g} \quad (2.5)$$

The long wavelength cut-off is due to infrared active lattice absorption, and depends on the vibrational modes of the atoms or ions of the material. For the electromagnetic radiation to excite vibrational modes, the molecules must possess a permanent dipole moment which can be activated by the oscillating electric field of the incident radiation. This first order effect occurs in ionic crystals only, and is known as reststrahlen absorption. A non-ionic crystal can have an effective charge, and consequently a dipole moment, if the atoms are not identical. Second order electric moment due to multiphonon interactions can also induce dipole moments in elemental materials such as diamond and silicon. The simplest mode of vibration of a linear diatomic molecule consisting of two point masses m_1 and m_2 , is a simple harmonic oscillation of the two masses along the line joining them. This is the classical description of a linear polar diatomic molecule, and the frequency of the vibration according to this model is given by⁽⁴⁾:

$$\nu \text{ (cm}^{-1}\text{)} = \frac{1}{2\pi c} \left(\frac{K}{\mu} \right)^{1/2} \quad (2.6)$$

where the reduced mass $\mu = \{m_1 m_2 / (m_1 + m_2)\}$ and K is the restoring force, or force constant.

This simple equation is very effective in predicting the fundamental absorption frequency of many polar diatomic molecules, as well as some multi-atomic systems, and even some homopolar systems. For harmonic oscillators, the selection rule for absorption is $\Delta v = \pm 1$, where v is the vibrational quantum number of the atomic system. In real cases (anharmonic oscillators), $\Delta v = \pm 2, \pm 3$ etc. are allowed. The frequency of ± 2 band is approximately double that of the fundamental band, and is known as overtone, or harmonic. The long wavelength limit may often be set by the first overtone of the fundamental.

The interpretation of IR spectra of amorphous materials is complicated by the fact that no long range structural order exists. One must rely on the results obtained from the theory of crystals.⁽⁵⁾ This is justified, to some extent, by the observation that the vibrational spectra of glasses are determined largely by the nearest neighbour interactions and thus are essentially similar to the spectra of crystals of the same composition and possessing the same type of short range order. But, the concept of an average or most probable structural unit (related to the crystalline state) must be introduced, as the structural unit may vary locally both in shape and size.⁽⁶⁾

(b) Extrinsic absorption mechanisms: Absorption or scattering of incident radiation may occur due to impurities in the matrix, including solid solutions or second phase inclusions or due to inhomogeneities like grain boundaries, dislocation networks, porosity and local variations in composition, density etc.

Donation of the free carriers by dissolved impurity atoms in semiconductors can displace the short wavelength cut-on of the material. H_2O in the form of entrapped molecular water or as bound hydroxyl groups can show absorption due to their fundamental vibrations. These are a few examples of extrinsic absorption in materials.⁽³⁾

Unfortunately, the conditions required for high IR transmission run counter to those of good mechanical properties. Equation (2.6) suggests that heavy elements interacting by weak force constants will show good transmission in the high wavelength regions, whilst light masses and strong force constants generally favour high strength, high melting point, and low thermal expansion. Several methods have been employed by different workers for strengthening infrared optical materials. Some of the examples are strengthening of single crystal alkali halides by divalent ion additions (Ca^{2+} , Ba^{2+} , Sr^{2+})⁽⁷⁾; strengthening of polycrystalline alumina, titania etc. by quenching⁽⁸⁾; surface application of low thermal expansion materials at high temperature⁽⁹⁾; ion exchange for glasses,⁽¹⁰⁾ surface crystallisation in glasses⁽¹¹⁾ (with little loss in IR transmission) etc.

Infrared optical materials may be broadly classified into two groups: (1) Crystalline materials and (2) Glasses. Figure 2.2 gives the useful IR transmission regions of some of the crystalline materials and Figure 2.3 gives the same for glasses. Fifty percent transmission is usually taken as the minimum useful transmission. This 50% cut-off changes to some extent with the sample thickness. Figure 2.4 shows the effect of thickness on transmittance of calcium aluminate glasses.⁽¹²⁾

Glasses as infrared optical materials have certain advantages over the crystals. Unlike many crystals, they are not subject to cleavage and therefore have superior shock resistance characteristics. They can be produced with relative ease and speed. Larger sizes of windows, lenses, and prisms can be produced. They are easily shaped and polished, and generally have superior surface hardness and thermal and mechanical properties. They also possess superior moisture resistance properties.

From equation (2.6), it is clear that glass formers of high reduced mass and low field strength are required for maximum transmission in higher wavelengths. Hence, oxide glass formers may be placed in a series of decreasing cation charge to mass ratio, in which oxides higher in the series (like Bi_2O_3 , La_2O_3) are expected to exhibit improved infrared transmission relative to those lower in the series⁽⁶⁾:

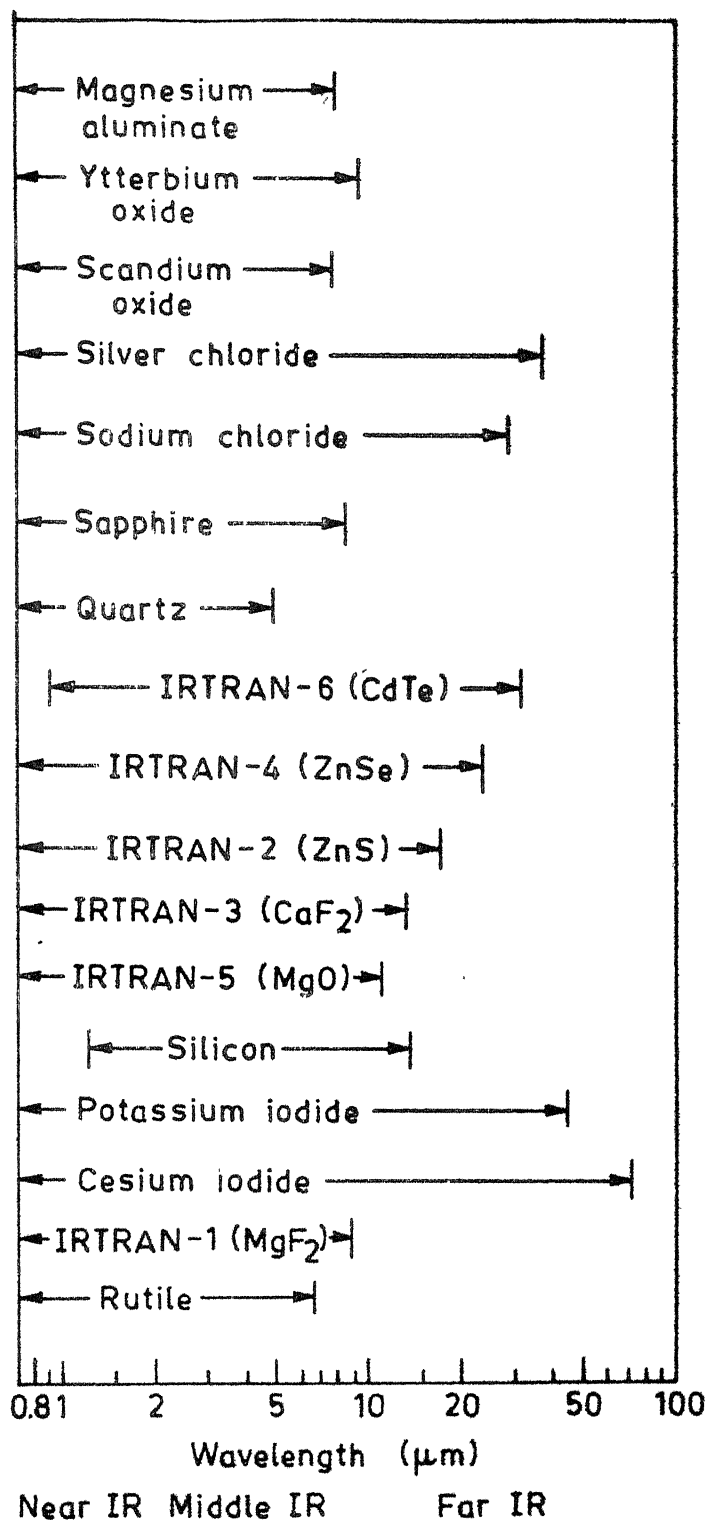


Fig. 2.2. Useful IR transmission regions of important crystalline optical materials.

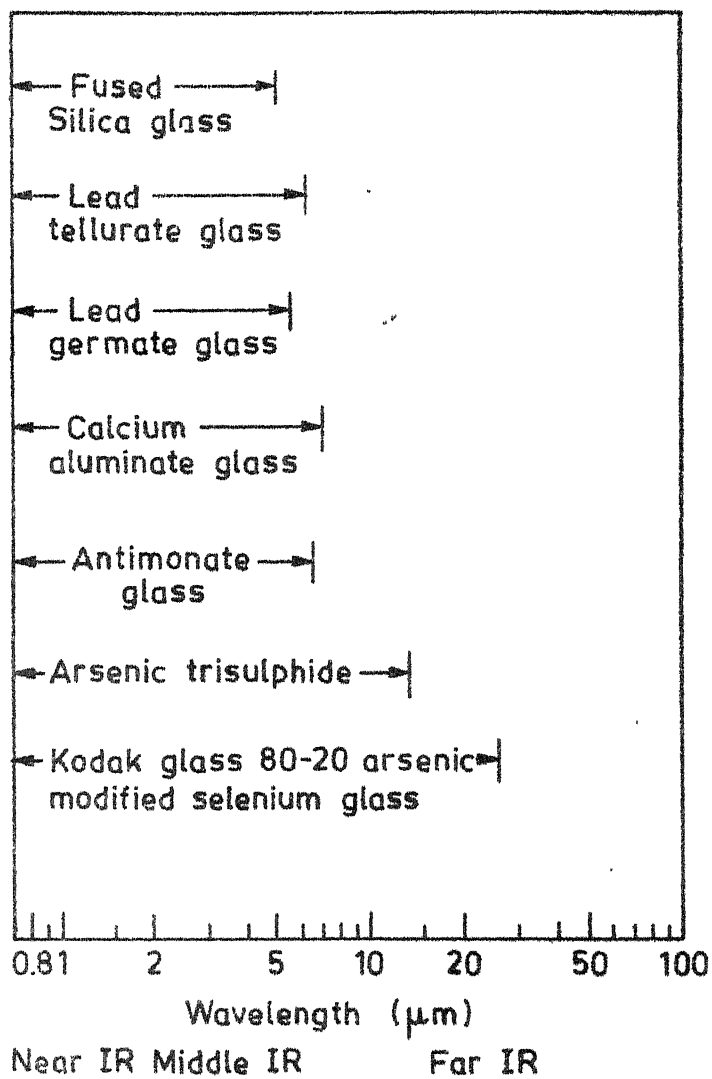


Fig. 2.3. Useful transmission regions of important optical glasses.

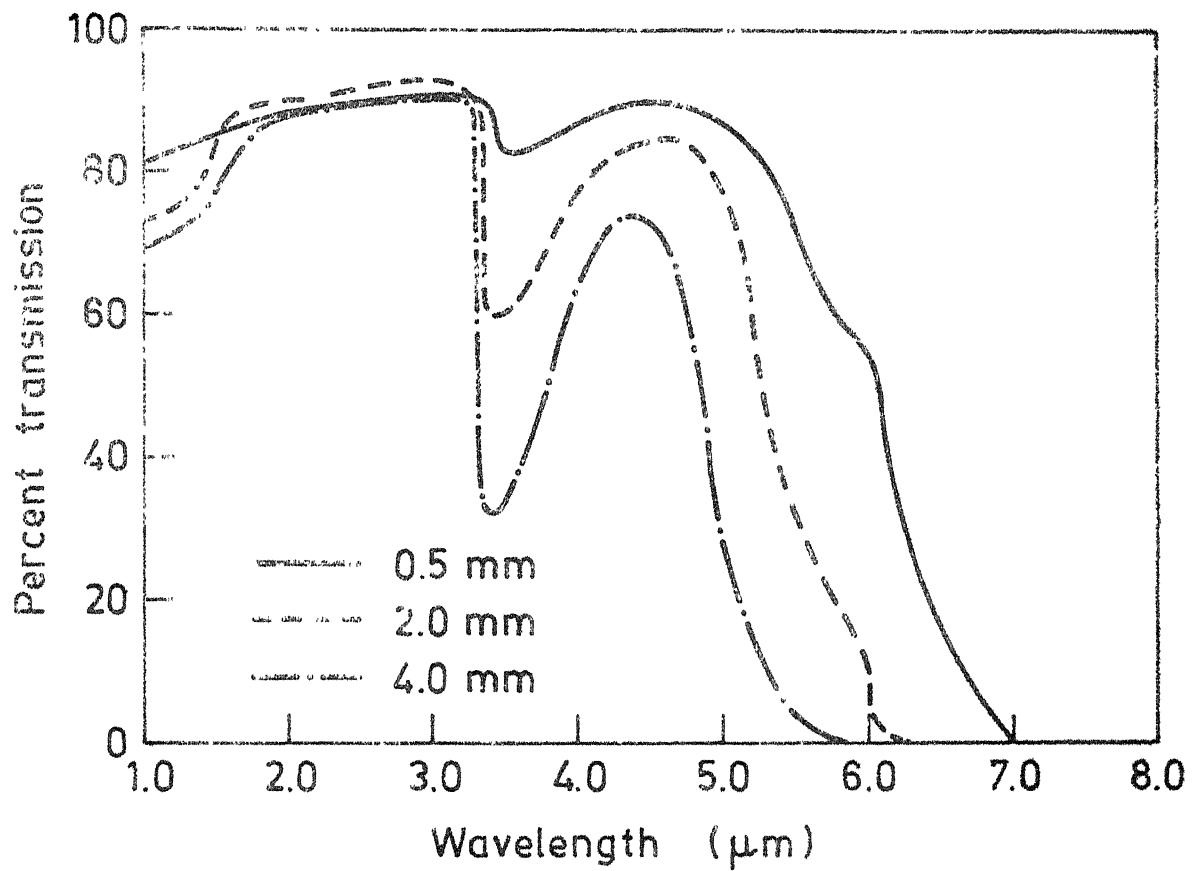
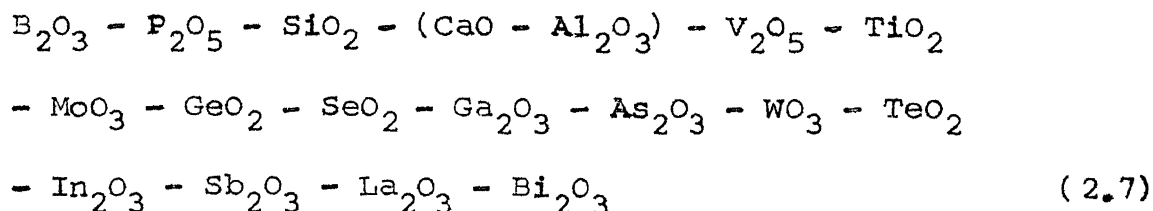


Fig. 2.4. Effect of thickness on transmittance of calcium aluminate glasses⁽¹²⁾.



Glasses based on B_2O_3 and P_2O_5 exhibit very limited infra-red transmission due to the high vibrational frequencies associated with the B-O and P-O bonds. Glasses for infra-red transmission can be broadly classified into the following groups⁽⁶⁾: (a) Glasses based on SiO_2 , (b) Glasses based on GeO_2 , (c) Glasses based on Ga_2O_3 - SrO , (d) Glasses based on TeO_2 , (e) Glasses based on Sb_2O_3 , (f) Glasses based on Bi_2O_3 , (g) Glasses based on $\text{CaO-Al}_2\text{O}_3$, (h) Miscellaneous oxide glasses (e.g. $\text{PbO-CdO-Fe}_2\text{O}_3\text{-Ti}_2\text{O}$, $\text{As}_2\text{O}_3\text{-PbO-Bi}_2\text{O}_3$ etc.) and (i) Non oxide glasses (e.g. As_2S_3 , As_2Se_3 etc.).

No particular glass can be said to be the best from the point of view of practical applications. For example, a glass showing better IR transmission may have poor mechanical properties and vice versa. A compromise should be made according to the need.

Glasses based on SiO_2 have a limit of useful transmission $< 4.8 \mu\text{m}$, $\text{MoO}_3/\text{WO}_3 < 5.1 \mu\text{m}$, $\text{GeO}_2 < 5.7 \mu\text{m}$, $\text{Ga}_2\text{O}_3 < 6 \mu\text{m}$, $\text{As}_2\text{O}_3 < 5.7 \mu\text{m}$, $\text{TeO}_2 < 6.3 \mu\text{m}$, $\text{Bi}_2\text{O}_3 < 7.5 \mu\text{m}$, $\text{CaO-Al}_2\text{O}_3 < 5.5 \mu\text{m}$. But glasses based on $(\text{MoO}_3\text{-WO}_3)$, SeO_2 , TeO_2 , Sb_2O_3 and As_2O_3 are limited due to their relatively low softening temperature. Bi_2O_3 based glasses also have relatively low softening points. Glasses based on chalcogenides or on the halides, are not generally suitable for application in the $1\text{-}6 \mu\text{m}$ spectral range due to a combination

of high thermal expansion, high water solubility, low softening point and poor mechanical properties. Hence the useful glass formers are probably limited to $(\text{CaO-Al}_2\text{O}_3)$, GeO_2 , Ga_2O_3 , WO_3 , La_2O_3 and possibly In_2O_3 and Bi_2O_3 systems.⁽⁶⁾

The long wavelength cut-off of germanate glasses is greater than that of the silicates because the fundamental stretching band of Ge-O-Ge is at 878 cm^{-1} , whilst that of Si-O-Si is at 1100 cm^{-1} .⁽¹³⁾ However the limitations of the germanates may be their high cost and water solubility. Some important physical and chemical properties of the different modifications of GeO_2 are given in Table 2.1.⁽¹⁴⁾

So far, infrared transmitting germanate glasses containing different oxides have been studied by various workers.⁽¹⁵⁻³³⁾ Table 2.2 gives a brief survey of the work reported in the literatures. General trends predicted by theory, such as increase in thermal expansion with addition of higher expansion oxides were observed by Colburn et al.⁽³⁴⁾ in case of germanate glasses containing different oxides. The effect of hydroxyl absorption may be prominent in germanate glasses. However, this can be minimized by methods appropriate to silicate systems including halide additions to the batch, or by melting and casting in vacuum or in a flowing dry atmosphere. The decrease in the water absorption band observed when halides are used as a batch ingredient may be explained in a number of ways.⁽³⁵⁾ One is that the volatilization of some compounds of

TABLE 2.1 Some important properties of different modifications of GeO_2

	Soluble	Insoluble	Vitreous
Structure	Hexagonal	Tetragonal	Amorphous
Density at 25°C, g/cc	4.228	6.239	3.637
Melting point (°C)	1116	1086	-
Coordination number of germanium	4	6	4
Solubility in water at 25°C (g/L solution)	4.53	Insoluble	5.18
Same at 100°C	13	Insoluble	-
Solubility in HCl, HF and NaOH solutions	Soluble	Insoluble	Soluble

TABLE 2.2 IR transmitting germanate glasses reported in the literatures

Glass	Comments	References
GeO ₂ -PbO, GeO ₂ -CaO-Al ₂ O ₃ , GeO ₂ -BaO-BeO-PbO	Transmission total cut-off is around 6 μm. Transmission 50% cut-off lies between 5-5.5 μm (Sample thickness ~ 2 mm)	Florence et al. (15)
PbO-GeO ₂ -La ₂ O ₃ (ZrO ₂ , Al ₂ O ₃)	Good IR transmission (20-35% at 6 μm)	Blau (16) (1955)
Ternary systems containing GeO ₂ , PbO and AlF ₃ , PbF ₂ , TiO ₂ , As ₂ O ₃ , Sb ₂ O ₃ , Bi ₂ O ₃ or TeO ₂	Similar IR transmission like GeO ₂ has been reported	Nielsen et al. (17) (1961)
GeO ₂ -BaO-TiO ₂ -La ₂ O ₃	Transmission 50% cut-off is at 5.3 μm (Sample thickness 2 mm)	Cleek et al. (18) (1962)
GeO ₂ -BaO-TiO ₂ -ZnO and GeO ₂ -BaO-TiO ₂ -ZnO-BaF ₂	Transmission 50% cut-off is around 5.7 μm (Sample thickness ~ 2 mm. Intensity of water absorption band is reduced in BaF ₂ containing glass	Cleek et al. (19) (1964)
PbO-GeO ₂	This glass exhibited useful transmission up to 6 μm	Phillips et al. (20) (1965)

Contd...

TABLE 2.2 (continued)

Glass	Comments	References
$\text{GeO}_2\text{-PbO-Ga}_2\text{O}_3$	Transmission 50% cut-off is at 5.5 μm (sample thickness 2 mm)	Burton et al. (21) (1965)
$\text{GeO}_2\text{-PbO-Bi}_2\text{O}_3\text{-PbF}_2\text{-Tl}_2\text{O}_3$	High transmittance up to 5 μm	Leitz (22) (1968)
$\text{GeO}_2\text{-Al}_2\text{O}_3\text{-CaO}$	Useful transmission up to 5.2 μm (sample thickness 2 mm). Water absorption band was removed by CaF_2 addition and flowing dry gases	Dumbaugh (23) (1970)
$\text{GeO}_2\text{-Al}_2\text{O}_3\text{-La}_2\text{O}_3$ with small additions of Nb_2O_5 , Ta_2O_5 , SrO , BaO , PbO and (or) ZnO	Useful transmission to about 5.3 μm , coupled with relatively low thermal expansion and high abrasion resistance	Dumbaugh (24) (1973)
$\text{GeO}_2\text{-La}_2\text{O}_3\text{-Ta}_2\text{O}_5\text{-ZnO}$	Better transmission than $\text{GeO}_2\text{-Al}_2\text{O}_3\text{-La}_2\text{O}_3$ glasses	Dumbaugh (25) (1975)
$\text{GeO}_2\text{-La}_2\text{O}_3\text{-Ta}_2\text{O}_5\text{-ZnO}$, with little addition of B_2O_3 , SiO_2 , P_2O_5	Substantial IR transmission up to 6 μm	Dumbaugh (26) (1976)

Contd...

TABLE 2.2 (continued)

Glass	Comments	References
GeO ₂ -Al ₂ O ₃ -Ta ₂ O ₅ -BaO, alkali metal oxides and SrO, CaO, MgO, ZnO, PbO, La ₂ O ₃ , ZrO ₂ , TiO ₂ , Nb ₂ O ₅ , WO ₃ , Sb ₂ O ₃ , As ₂ O ₃ are also added in different glasses	Good IR transmission coupled with high water proofness	Hodogaya Chemical Co., Ltd. (27) (1980)
GeO ₂ -PbO-Al ₂ O ₃ and Bi ₂ O ₃ , Sb ₂ O ₃ and/or TeO ₂	Very good IR transmission (70% at 6 μm)	Tokyo Shibaura Electric Co. Ltd. (28) (1981)
GeO ₂ -Sb ₂ O ₃	For IR transmitting optical fibres	Furukawa Electric Co. Ltd. (29) (1981)
GeO ₂ -Sb ₂ O ₃ (NH ₄ HF ₂ was added in the batch)	Transparent glass having high IR transmission	Agency of Industrial Sciences and Technology (30) (1982)
CaO-Ga ₂ O ₃ -GeO ₂ -La ₂ O ₃ -Ta ₂ O ₅ -TiO ₂ -ZrO ₂	High IR transmission	Agency of Industrial Sciences and Technology (31) (1982)

Contd...

TABLE 2.2 (continued)

Glass	Comments	References
<p>$\text{GeO}_2\text{-Al}_2\text{O}_3\text{-CaO}$-alkali metal oxides (CaO content may be partially or totally replaced by other metal oxides)</p>	<p>52% transmission at 5 μm (Sample thickness 4 mm)</p>	<p>Boudot et al. (32) (1982)</p>
<p>$\text{GeO}_2\text{-BaO-CaO-Ga}_2\text{O}_3$ (Ga_2O_3 can be partially replaced by ZnO, GeO_2 by ZrO_2 and BaO and CaO by MnO)</p>	<p>IR transmission characteristics were studied; the IR transmission was increased by chemical dehydration with BaF_2 or physical dehydration by increasing the melt temperature, extending the melting time and using dry argon as the melting atmosphere</p>	<p>Khalilev et al. (33) (1984)</p>

bubbling of a dry gas through the melt would do. Water may also be removed as volatile HF.⁽³⁶⁾ Another possibility⁽³⁵⁾ is that the fluoride reacts with a hydroxyl group forming a bifluoride and oxide, thus reducing the hydroxyl content of the melt.

In the present studies, we have chosen Bi_2O_3 - GeO_2 systems. We have selected bismuth oxide because it is at the top of the series (2.7). So the combination of Bi_2O_3 and GeO_2 is expected to give good IR transmission. The bismuth oxide based glasses reported so far contain either PbO , or As_2O_3 (Sb_2O_3) or both. These oxides have toxic effects on human beings. So a combination of GeO_2 and Bi_2O_3 will be better in this respect. Riebling⁽³⁷⁾ has studied glasses in the system GeO_2 - Sb_2O_3 and GeO_2 - Bi_2O_3 . He found that at least 60 mol % of GeO_2 is needed for glass formation. Topping et al.⁽³⁸⁾ also studied in detail glasses in the system Bi_2O_3 - GeO_2 and Bi_2O_3 - SiO_2 - GeO_2 . They found that less than 60% GeO_2 will form glass provided equivalent amount of SiO_2 is added. Nassau et al.^(39,40) studied the glass formation regions in Bi_2O_3 - GeO_2 - PbO and PbO - GeO_2 - Tl_2O systems. In these cases, lower amount of GeO_2 (< 60%) can form glass provided PbO and (or) Tl_2O are used.

As in the Bi_2O_3 - GeO_2 system 60 mol % GeO_2 is the minimum required for glass formation, we started from 40 Bi_2O_3 .60 GeO_2 composition (in another set, higher GeO_2 was used). Our main objective was to lower the amount of GeO_2 by replacing it by other oxides. The lower the

time, the durability is also expected to be better (note that vitreous GeO_2 is soluble in water). But it should be kept in mind that the added oxide should not hamper IR transmittance and other pertinent properties.

From our past experience on bismuth oxide based glasses, we found that ZnO has a stabilizing effect on such glasses. At the same time, ZnO will increase the refractoriness of the glasses (melting point of ZnO is 1975°C) and is also expected to increase the chemical durability (ZnO increase chemical durability of silicate glasses⁽⁴¹⁾). So the effects of ZnO on IR transmittance of $\text{Bi}_2\text{O}_3\text{-GeO}_2$ glasses will be interesting as $\text{Bi}_2\text{O}_3\text{-GeO}_2\text{-ZnO}$ glasses are expected to be better in other respects than $\text{Bi}_2\text{O}_3\text{-GeO}_2$ glasses as IR transmitting windows.

2.2 Experimental

The compositions of the glasses studied are given in Table 2.3. All the chemicals used were of reagent grades except GeO_2 which was of electronic grade. Proportionate amounts of the required components were thoroughly mixed in a porcelain mortar and pestle. The crucibles used for melting were of pure alumina (pore free). All the glasses were melted in a global furnace with an air atmosphere. The glasses were melted at 1200-1250°C and quenched on an aluminium plate kept at room temperature ($\sim 30^\circ\text{C}$). In order to get thin samples (0.5-1 mm) the glasses were cast on a ^{polished} ~~glazy~~ stainless steel plate and pressed from the top by another ^{polished} ~~glazy~~ stainless steel plate.

Densities of the glasses were determined by using a Sartorius balance (sensitive upto fourth decimal place). Distilled water (at $\sim 25^\circ\text{C}$) was used as the immersion fluid. As discussed later, these glasses do not dissolve (or react) in water. Initially, the weight of the glass sample was taken in air (W_1 gm) and then the weight was again noted after immersing in water (W_2 gm). The density was calculated as $W_1/(W_1 - W_2)$ gm/cc. The molar volumes of the glasses were calculated from the mole percentage of their compositions and corresponding densities.

The microhardness of the glass samples was noted from the standard chart by measuring the diagonal of the impression formed after indentation with Vickers diamond pyramid indenter using a load of 100 gm. The model used

TABLE 2.3 Compositions of the glasses studied

Glass no.	Composition (mol %)	Melting temperature	Glass no.	Composition (mol %)	Melting temperature
1	60 SiO ₂ .40 Bi ₂ O ₃	1200°C	6	80 GeO ₂ .20 Bi ₂ O ₃	1200°C
2	60 GeO ₂ .40 Bi ₂ O ₃	1200°C	7	75 GeO ₂ .20 Bi ₂ O ₃ .5 ZnO	1200°C
3	55 GeO ₂ .40 Bi ₂ O ₃ .5 ZnO	1200°C	8	70 GeO ₂ .20 Bi ₂ O ₃ .10 ZnO	1200°C
4	50 GeO ₂ .40 Bi ₂ O ₃ .10 ZnO	1200°C	9	65 GeO ₂ .20 Bi ₂ O ₃ .15 ZnO	1250°C
5	45 GeO ₂ .40 Bi ₂ O ₃ .15 ZnO	1250°C	10	60 GeO ₂ .20 Bi ₂ O ₃ .20 ZnO	1250°C

For measurement of chemical durability, thin glass pieces (thickness 0.5-0.8 mm) of area approximately 1 cm^2 were taken. They were weighed in a balance and the area of each glass piece was noted by placing them on a millimeter graph paper and finding the number of squares covered by the glass piece. As the glass pieces were very thin, the area along the thickness can be neglected. These glass pieces were then kept in boiling distilled water for half an hour and weight loss (if any) was noted. 'Accelerated' chemical durability test was done by keeping the glass pieces in 3 N HCl at around 30°C for half an hour. The weight loss was noted. From the weight loss and surface area data, weight loss per unit area for each glass was calculated.

Differential thermal analysis of the glass samples was carried out in a derivatograph (MOM, Budapest). For this experiment, powdered glass (-100 mesh) was used and heating rate was controlled to $10^\circ\text{C}/\text{min}$. The samples were heated upto 800°C .

The optical absorption studies of the glass samples were done in a Cary 17D spectrophotometer in the range 400-750 nm. Thin glass samples (0.35-0.63 mm) were used for these studies.

Infrared transmittance of the glasses were measured in an infrared spectrophotometer (Perkin-Elmer 377). A square hole (5 mm x 5 mm) was made in a rectangular cardboard (9 cm x 5 cm). One such cardboard was put in the reference slot of the spectrophotometer. Another such

cardboard was placed in the sample slot. The spectrum was taken upto 8 μm wavelength region. Obviously a straight line will come, as the hole in the cardboard is empty. This straight line will indicate 100% transmission in our standard condition. Now the cardboard from the sample slot was taken out and the glass to be studied was placed in the square hole and kept at that position by using adhesive tapes at the sides. Then the cardboard with the glass in the square hole was placed exactly at the same position in the sample slot of the spectrophotometer. The spectrum was recorded upto 8 μm wavelength region. This procedure was repeated for all the glass samples and their transmittances were then calculated with respect to 100% transmission line of our standard case. The thickness of the glass samples was measured by using Mitutoyo (Japan) micrometer.

2.3 Results and Discussions

Glass 1 is a silicate glass which contains 40 mol % Bi_2O_3 , rest are the germanate glasses. This glass was also studied with the germanate glasses to have an appreciation of the difference in properties between the silicate and the germanate glasses containing 40 mol % Bi_2O_3 .

After preparation of the glasses, it was found that ZnO can replace some of ^{the} GeO_2 in Bi_2O_3 - GeO_2 glasses without inducing crystallisation. In ^{the} case of 60 GeO_2 .40 Bi_2O_3 composition, up to 15 mol % GeO_2 can be replaced by ZnO, keeping the amount of Bi_2O_3 constant. The melt containing 15 mol % ZnO (no. 5), after quenching ^{on} ~~in~~ an aluminium plate (at $\sim 30^\circ\text{C}$) was found to be devitrified at the top surface (due to slower heat transfer from the top). Visually it was found that upto 3 mm thickness a good glass had been formed. So glass 5 can be used upto 3 mm thickness only. In this context, it should be noted that the practical useful thickness for IR transmitting windows is nearly 2-3 mm in most of the cases.

In ^{the} case of 80 GeO_2 .20 Bi_2O_3 composition, up to 20 mol % ZnO can be substituted for GeO_2 . The glass containing 20 mol % ZnO (no. 10) was found to have a surface devitrified layer in thickness above 5 mm. In the later part of our discussion, for brevity, germanate glasses containing 40 mol % Bi_2O_3 (nos. 2, 3, 4 and 5) will be described as Set A and germanate glasses containing 20 mol % Bi_2O_3 (nos. 6, 7, 8, 9 and 10) will be described as Set B

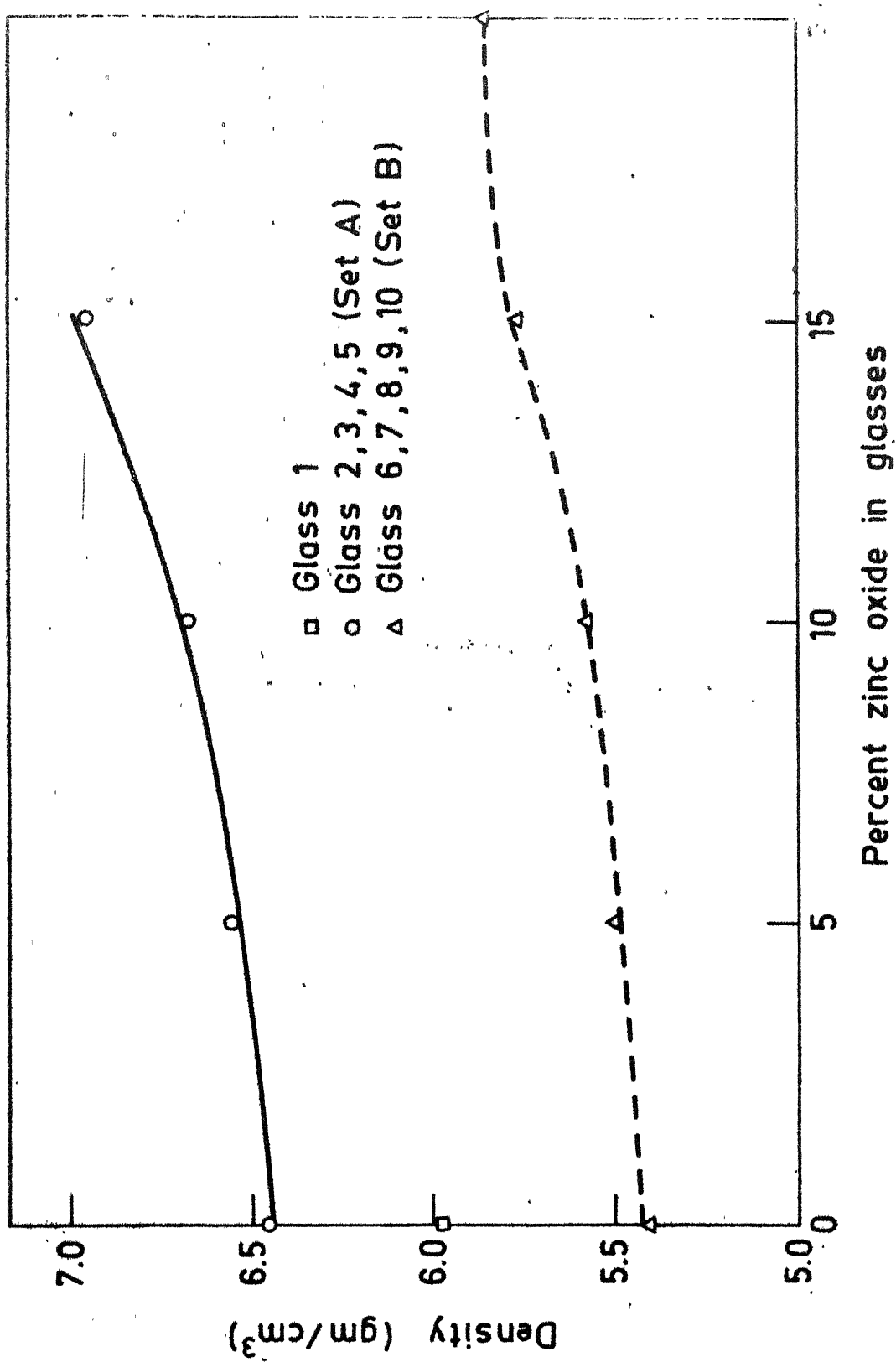


Fig. 2.5. Density of glasses.

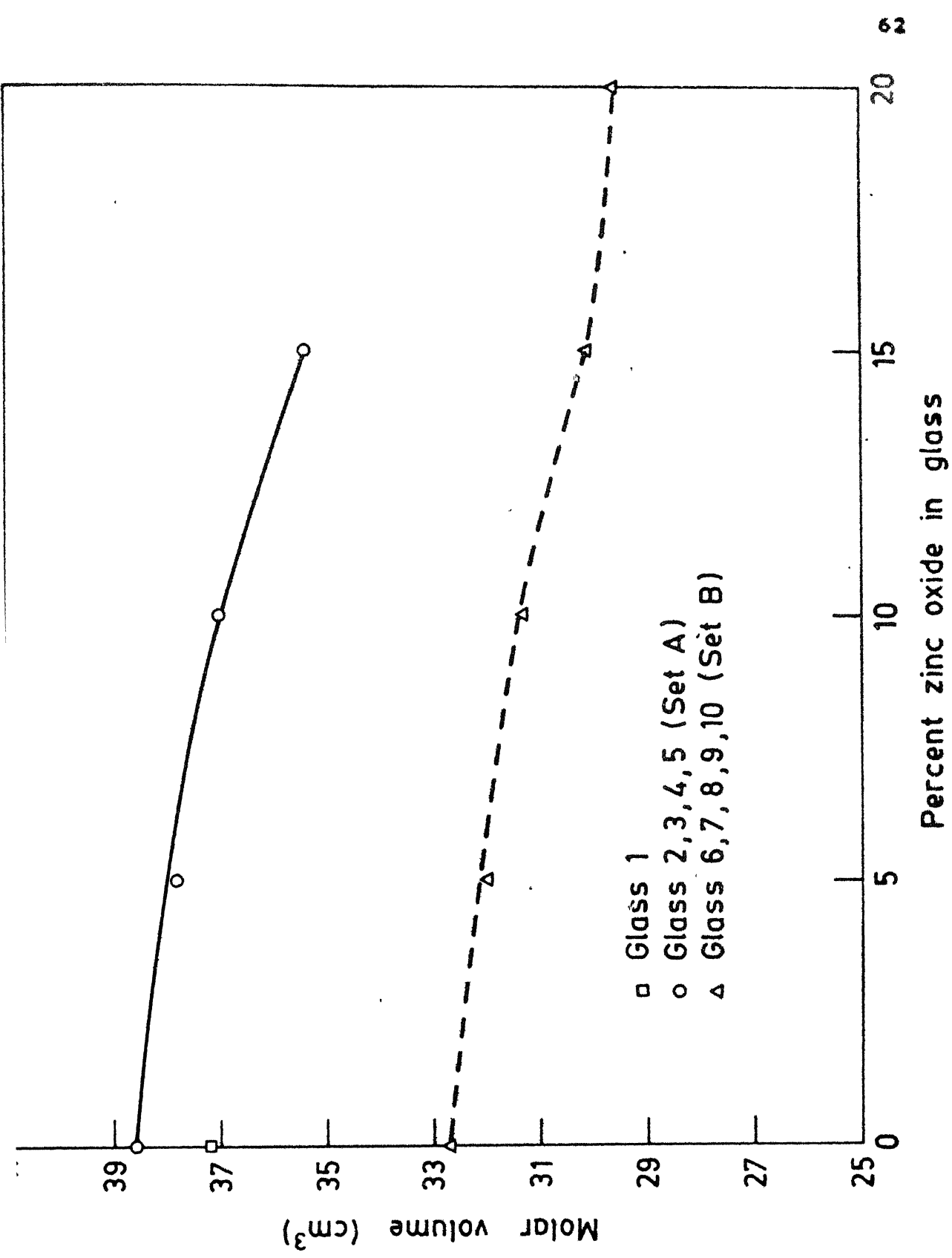


Fig. 2.6. Effect of zinc oxide on molar volume of the glasses.

in different ways. It participates in the structure by forming four pyramidal BiO_3 groups, it introduces some nonbridging oxygens in the structure and it gives part of its oxygen to boron to create four coordinated sites. It has also been reported that in the system $(\text{M}_2\text{O or M}'\text{O})-\text{Bi}_2\text{O}_3-\text{Al}_2\text{O}_3$, where M is Na or K and M' is Sr, Ba, Zn etc., BiO_4 , AlO_4 polyhedra act as network formers.⁽⁴⁸⁾ BiO_5 , BiO_6 and BiO_7 units have also been reported in different bismuth germanates and silicate crystals.^(49,50,51) So from the above studies, it is clear that Bi_2O_3 in glasses will act as both network former (especially when the concentration of Bi_2O_3 is high) as well as network modifier, the relative contribution as network former and as network modifier will depend on the amount of Bi_2O_3 and the type of the glass concerned.

ZnO in glass is known to act as an intermediate oxide. The chemistry of zinc is appreciably covalent due to poor shielding by the 3d electrons in Zn^{2+} with consequent delocalisation of charge.⁽⁵²⁾ ZnO has been reported to form ZnO_4 tetrahedra and can act as a network former, especially when present in sufficient amount.^(53,54)

According to Riebling,⁽³⁷⁾ with the addition of Bi_2O_3 to GeO_2 glass, depolymerization of the three dimensional network of GeO_4 tetrahedra takes place and discrete GeO_4 tetrahedra start forming. This depolymerization, according to the same worker, is complete at 40 mol % Bi_2O_3 . In our case, as the amount of Bi_2O_3 in Set A glasses is high (40 mol %), so most of the Bi_2O_3 will act as network

former and the rest as network modifier. In case of Set B glasses (containing 20 mol % Bi_2O_3), most of the Bi_2O_3 is expected to act as network modifier and will create sufficient nonbridging oxygen ions.

When ZnO is added to Set A glasses, the following effects are expected to occur: (a) It will create some nonbridging oxygen ions by breaking some of the Bi-O-Ge (and/or Bi-O-Bi if any) linkages. (b) Like other divalent metal oxides, it will change some of the GeO_4 tetrahedra to GeO_6 octahedra. This will make the structure more close-packed and dense (six coordinated GeO_2 is denser than four coordinated GeO_2 , see the Table 2.1). (c) Some of the Zn^{2+} ions will go inside empty sites⁽³⁷⁾ and can increase the packing slightly.

For Set B glasses, the second (b) and the third (c) effects will be the same as that of Set A glasses. The first effect will be somewhat different as Bi_2O_3 in this case (Set B glasses) is acting mostly as network modifier oxide. In this case, although Zn^{2+} will introduce some nonbridging oxygen ions, it will eliminate the most polarizable nonbridging oxygen ions formed due to the presence of Bi_2O_3 as a network modifying oxide in GeO_2 structure. This is almost similar to the effect of CaO addition in $\text{Na}_2\text{O-SiO}_2$ glasses.⁽⁵⁵⁾ This is because, Zn^{2+} , being a non-noble gas-like cation is not screened properly by its electrons, so it has a strong polarizing power (even more than Ca^{2+} ion) on the anions.

Except ^{for} the above three effects, when ZnO will be sufficient in amount, it can form ZnO_4 tetrahedra and act as a network former for both Set A and Set B glasses.

Mainly the second (b) and to some extent the third (c) effects (discussed above) are responsible for lowering the molar volume of the glasses with the increase in ZnO content. In Figure 2.6, the deviation of the molar volume from linearity, especially around 15 mol % ZnO compositions, may be due to the formation of some ZnO_4 tetrahedra resulting in further packing of the structure. The decrease in molar volume with the addition of ZnO explains the increase in density of the glasses with the increase in ZnO content as shown in Figure 2.5.

Figures 2.7 to 2.10 show the infrared transmission characteristics of the glasses. In Figure 2.7, IR transmittance of vitreous silica has also been given so that a comparison can be made with the transmittance (and cut-off) of other glasses. The initial ^{transmission} transmittance (at $2.5 \mu\text{m}$) of vitreous silica is more than that of both glass 1 ($60 \text{ SiO}_2 \cdot 40 \text{ Bi}_2\text{O}_3$) and glass 2 ($60 \text{ GeO}_2 \cdot 40 \text{ Bi}_2\text{O}_3$). Glasses 1 and 2 contain high amount of Bi_2O_3 and Bi^{3+} , being highly polarizable, increases the refractive indices of the glasses. GeO_2 also increases the refractive indices of the glasses more than that of SiO_2 .⁽⁵⁶⁾ As discussed earlier (see equation (2.4) and Figure 2.1), the higher the refractive index, the more will be the reflection loss. This explains the initial low ^{transmission} transmittance of glass 1 (and much lower

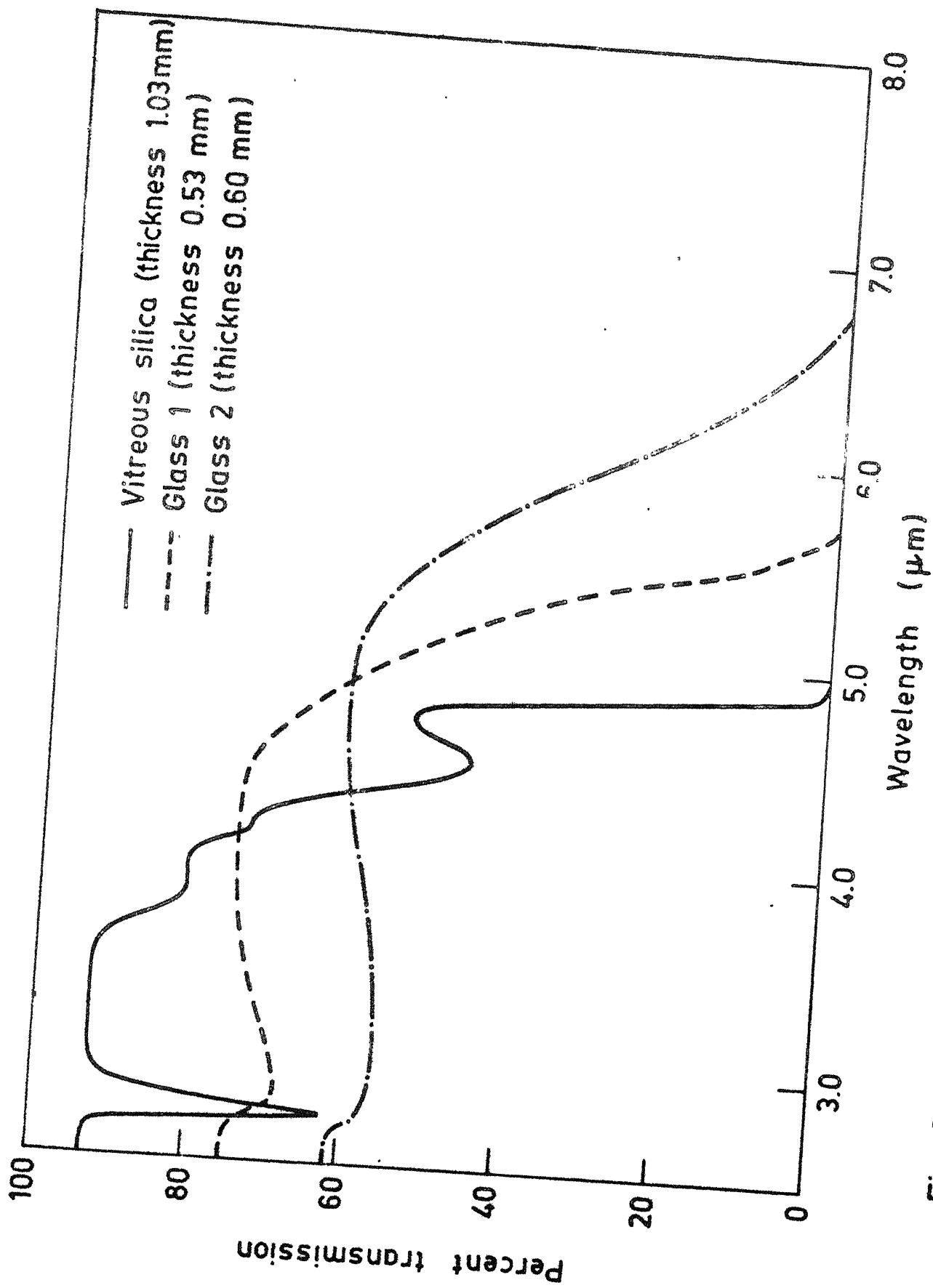


Fig. 2.7. Infrared transmission characteristics of glasses.

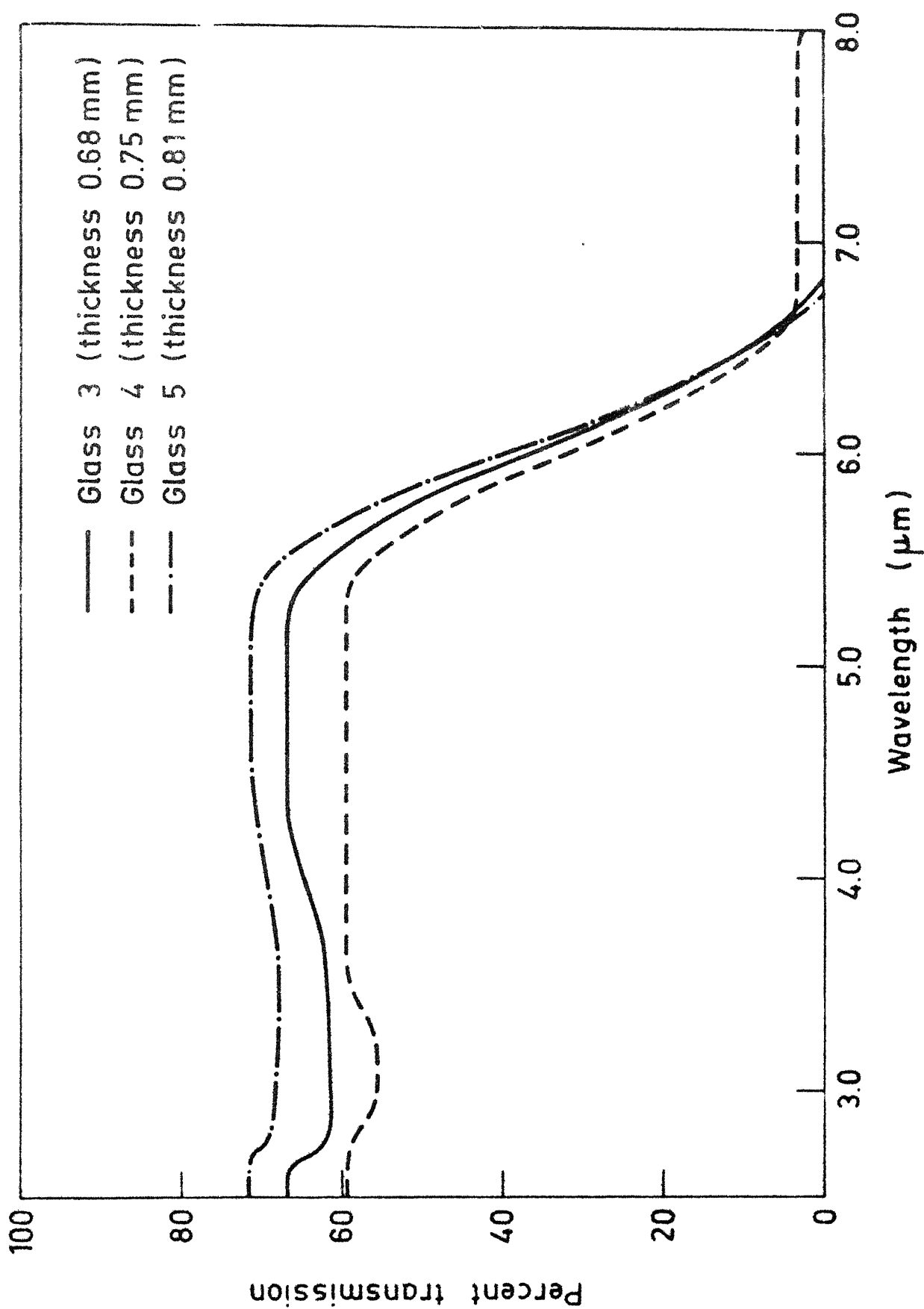


Fig. 2.8. Infrared transmission characteristics of glasses.

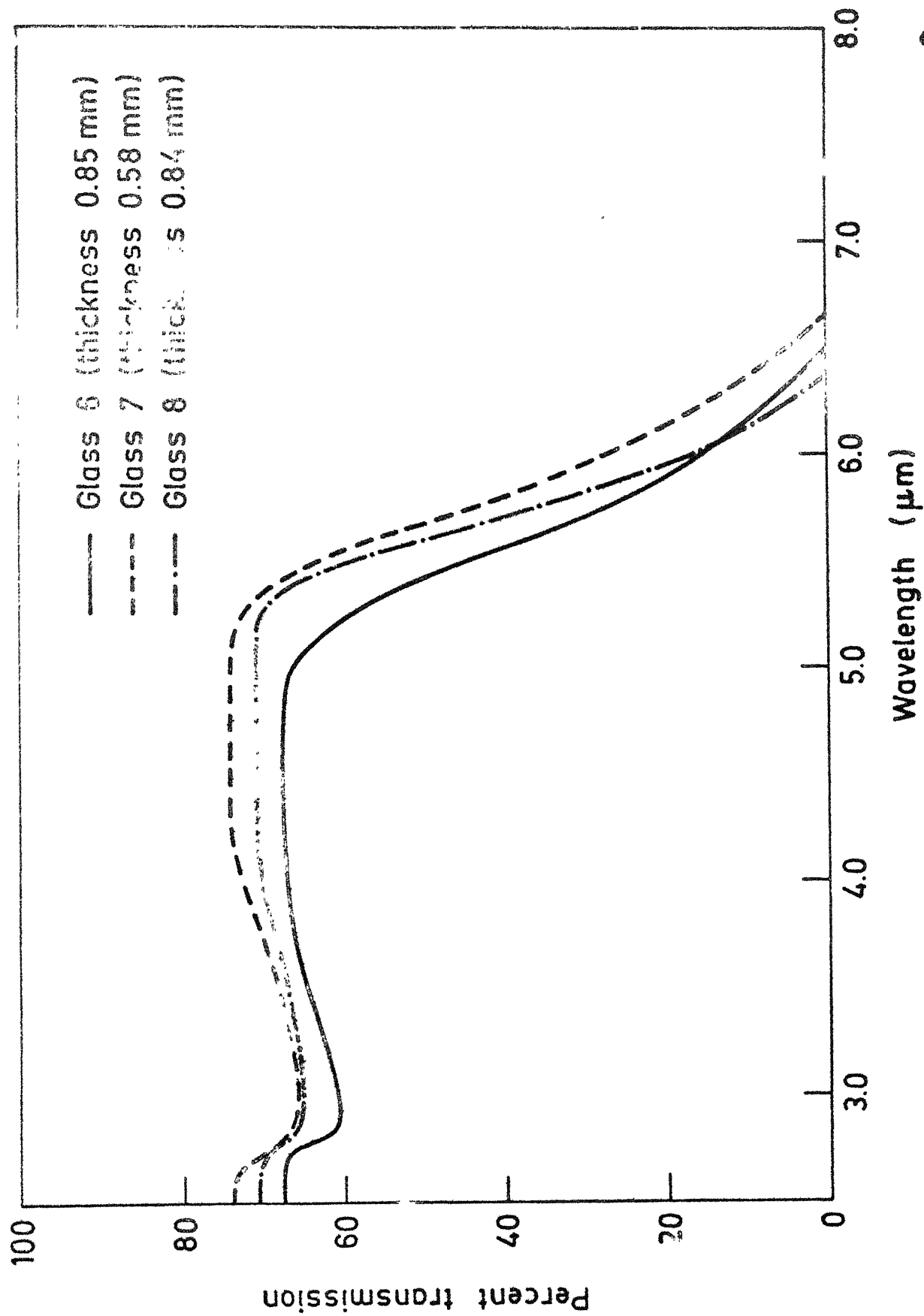


Fig. 2.9. Infrared transmission characteristics of glasses.

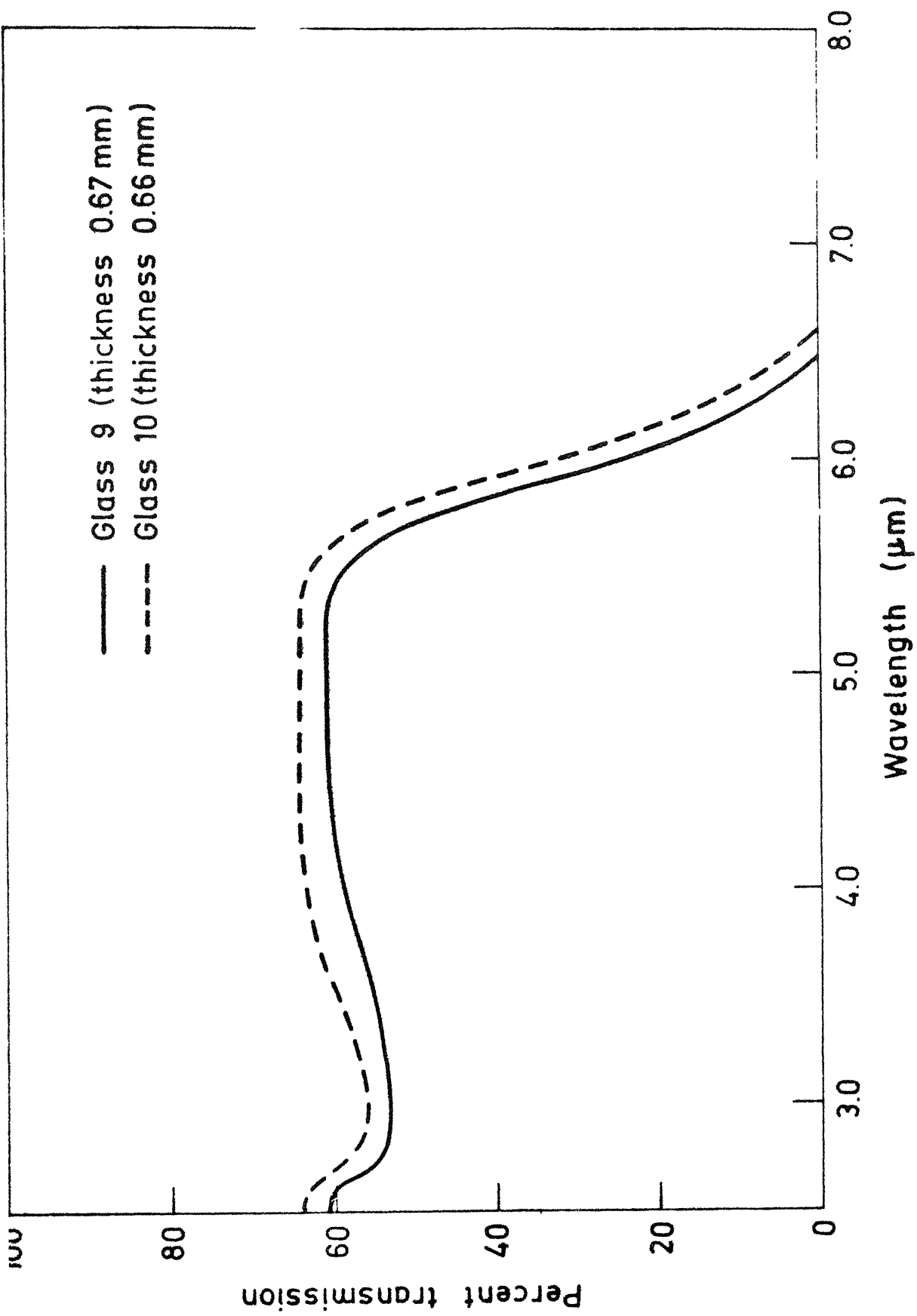


Fig. 2.10. Infrared transmission characteristics of glasses.

for glass 2, which contains GeO_2) in comparison to that of vitreous silica.

IR absorption dip around $2.5\text{--}3.5\ \mu\text{m}$ has been found in different glasses and has been attributed to the vibration of OH groups and the exact position of the absorption dip depends on the type of glass, presence of other ions near the OH groups and degree of association (if any) of the OH groups. ^(36,57)

The absorption dip at around $2.75\ \mu\text{m}$ in vitreous silica is due to the presence of unassociated OH groups. ⁽⁵⁸⁾ In all our glasses (Set A, Set B and glass 1), the absorption band around the region $2.75\text{--}3.50\ \mu\text{m}$ is due to the presence of OH groups. In case of vitreous silica, the other absorption dips are due to the glass network itself. ⁽⁵⁸⁾ The total cut-off wavelength of vitreous silica is less than that of glass 1 ($60\ \text{SiO}_2\text{--}40\ \text{Bi}_2\text{O}_3$) and much more so than that of glass 2 ($60\ \text{GeO}_2\text{--}40\ \text{Bi}_2\text{O}_3$). From the series (2.7), it is clear that replacing SiO_2 by Bi_2O_3 will increase IR transmission at higher wavelengths and similarly replacing SiO_2 by GeO_2 will have the same effect. This explains our observed trend of cut-off wavelengths (and also 50% cut-off wavelengths) for vitreous silica, glass 1 and glass 2 (see also Table 2.4).

It has been observed ⁽⁶⁾ that the fundamental Ge-O absorption can be shifted to lower frequencies either by inducing GeO_2 to switch from four-fold to six-fold coordination so that the structure contains GeO_6 octahedra

TABLE 2.4 Fifty percent cut-off (IR transmission) wavelengths of glasses

Glass	Thickness (mm)	Transmission 50% cut-off (μm)	Glass	Thickness (mm)	Transmission 50% cut-off (μm)
Vitreous silica	1.03	4.4	Glass 6	0.85	5.4
Glass 1	0.53	5.1	Glass 7	0.58	5.7
Glass 2	0.60	5.5	Glass 8	0.84	5.6
Glass 3	0.68	5.8	Glass 9	0.67	5.7
Glass 4	0.75	5.7	Glass 10	0.66	5.8
Glass 5	0.81	5.9	-	-	-

network so that the GeO_4 tetrahedra become isolated. Riebling⁽³⁷⁾ observed^a similar shift of Ge-O absorption to higher wavelength (that is, lower frequency) with the addition of Bi_2O_3 , which according to him, is due to depolymerization of Ge-O network and formation of discrete GeO_4 tetrahedra. As explained earlier, ZnO in Bi_2O_3 - GeO_2 glasses^{is} are expected to create some GeO_6 octahedra and hence the total cut-off (as well as 50% cut-off) wavelength of the glasses should increase (at least slightly) with the increase in ZnO content of the glasses. From the Figures 2.7 to 2.10 and Table 2.4, it can be said that there is a slight increase in the total cut-off (and also 50% cut-off) wavelengths in all the glasses (Set A and Set B) with the increase in ZnO content of the glasses. No definitive statement can be made about the relative change in total cut-off and 50% cut-off wavelengths for glasses containing different amounts of ZnO, because the thickness of the glass samples are not uniform in these cases. As discussed earlier, the total cut-off and 50% cut-off wavelengths are dependent to some extent on the thickness of the samples (see Figure 2.4). Glass 4 shows very little transmission ($\sim 3\%$) beyond $7\text{ }\mu\text{m}$. Detailed structural studies can throw light on the mechanisms for this unexpected behaviour, of course, such a low transmission has no practical usefulness. Another interesting though quite natural observation is that, in general, the total cut-off wavelengths of Set B glasses are lower than that of Set A glasses. This

is due to a lower Bi_2O_3 content in Set B glasses as compared to that in Set A glasses.

Figure 2.11 depicts the effect of ZnO on the micro-hardness of the glasses. Hardness is a property which depends on many parameters. It is a misconception to relate hardness solely to lattice energy. The very soft AgCl has a higher lattice energy (214 Kcal/mol) than the much harder rock salt (180 Kcal/mol). According to Weyl et al.⁽⁵⁵⁾ any hardness test involves partial unscreening of cations. The greater the polarizability of the ions, the easier it will be to deform them and the lower will be the hardness of the material.

As discussed earlier, glass 6 ($80 \text{ GeO}_2 \cdot 20 \text{ Bi}_2\text{O}_3$) contains sufficient number of nonbridging oxygen ions. With the increase of ZnO content in Set B glasses, though the total number of nonbridging oxygen ions will increase to some extent, the relative increase in the total number of nonbridging oxygen ions will not be much and above all Zn^{2+} will decrease the net polarizability of the already existing nonbridging oxygen ions (discussed earlier). At the same time ZnO will create some GeO_6 octahedra resulting in a denser packing. So both lowering of the polarizability of the oxygen ions and increase in packing of the structure explain the increase in hardness of the Set B glasses with the increase in ZnO content.

In case of Set A glasses, with the addition of ZnO, the relative increase in the total number of non-bridging oxygen ions will be appreciable. This is due to

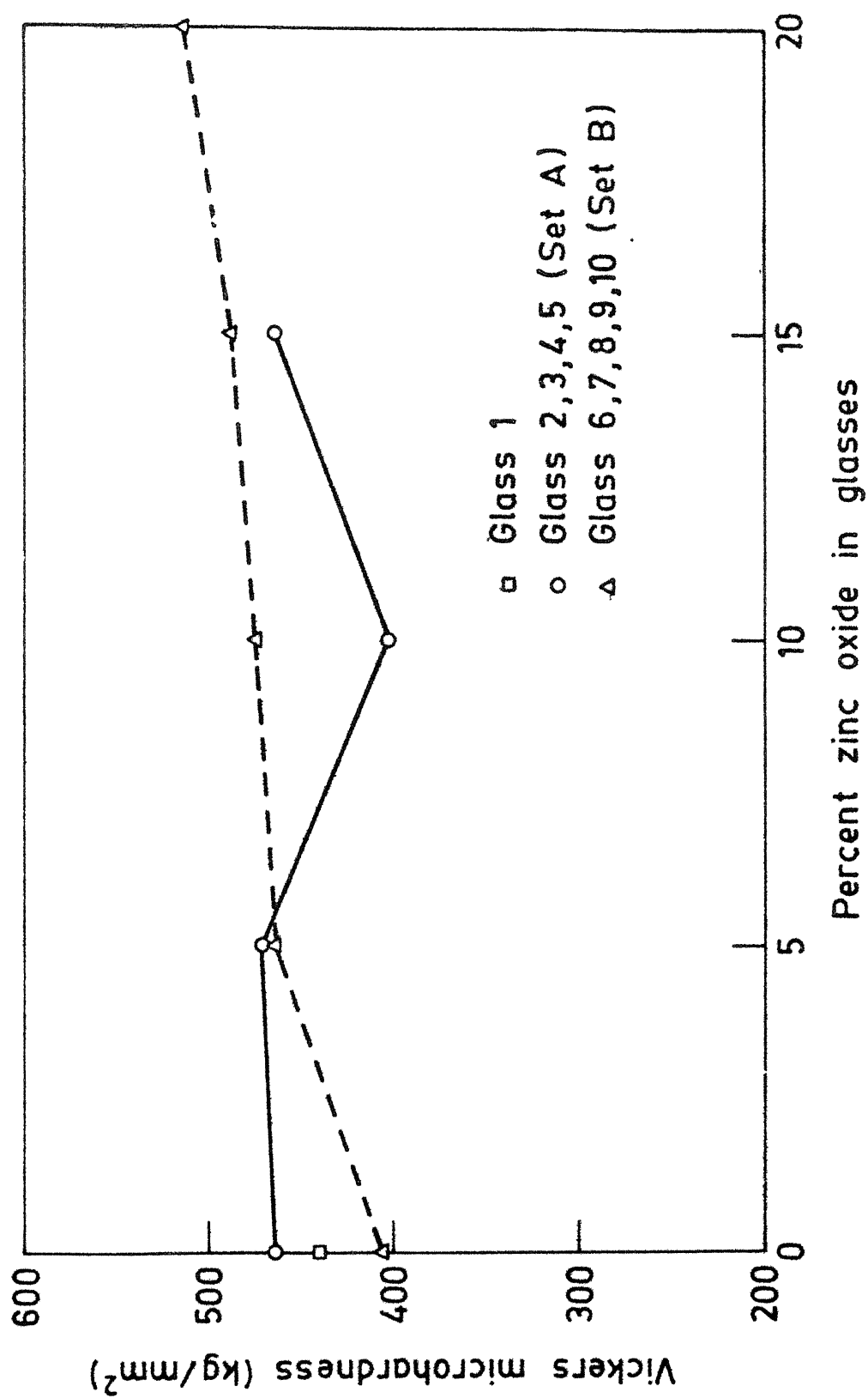


Fig. 2.11. Vickers microhardness of glasses (load 100 gm).

the initial low amount of nonbridging oxygen ions present in 60 GeO_2 .40 Bi_2O_3 glass. At the same time, the number of GeO_6 octahedra created by the addition of ZnO may not be as much in this case as that in Set B glasses. This is because the probability of GeO_4 to GeO_6 transformation, after the addition of ZnO , will be dependent to some extent on the initial amount of GeO_4 present in the glass, which is lower in the case of Set A glasses (Set A glasses in general contain lower amount of GeO_2 than Set B glasses). So for Set A glasses, the lowering of hardness due to the increase in the number of nonbridging oxygen ions and the increase in hardness due to the formation of GeO_6 octahedra will counteract each other. Indeed, a minimum in hardness has been found for 10 mol % ZnO containing glass (glass 4). The improvement in hardness for glass 5, containing 15 mol % ZnO , may be due to the formation of ZnO_4 tetrahedra with consequent lowering of the number of nonbridging ions and denser packing of the structure.

As the chemical durability of a glass is controlled by many parameters, it is very difficult to predict it accurately. The important controlling factors are: (a) the surface characteristics of the glass, (b) reactivity of the individual constituents of the glass towards the solvent, (c) the structure of the glass concerned, (d) solubility (or inertness) of the surface film formed after reacting with the solvent, (e) concentration of the leachant (solvent), (6) rate of proton penetration (for water and acid solutions only). It should be noted that the rate

of proton penetration increases with the increase in polarizability of the oxygen ions.⁽⁵⁵⁾

Besides the above factors, many other parameters can control the chemical durability of a glass, which may be specific for the particular glass concerned.

In our case, no change in weight of the glasses (both Set A and Set B, and also glass 1) is detected after boiling in water for half an hour. This proves that these glasses are very resistant to water. Figure 2.12 depicts the weight loss per unit area of the glasses after leaching them in 3 N HCl ($\sim 30^\circ\text{C}$) for half an hour.

For Set B glasses, with the increase in ZnO content, the durability (towards HCl) has improved except in the case of glass 9 containing 15 mol % ZnO. As discussed earlier, the addition of ZnO lowers the net polarizability of the oxygen ions (for Set B glasses), so the rate of proton penetration will decrease with the increase of ZnO content. Also ZnO will create some GeO_6 octahedra. These octahedra are stable towards acid (tetragonal GeO_2 containing GeO_6 octahedra are insoluble in acids, see Table 2.1). So both of these effects seem to be responsible for the improvement in acid resistance of the Set B glasses with the increase in ZnO content. The unexpected fall in durability of glass 9 (containing 15 mol % ZnO) is a bit intriguing. Detailed studies are needed to find out the reason(s) in this case.

For Set A glasses, ZnO will appreciably increase the number of nonbridging oxygen ions and the creation of

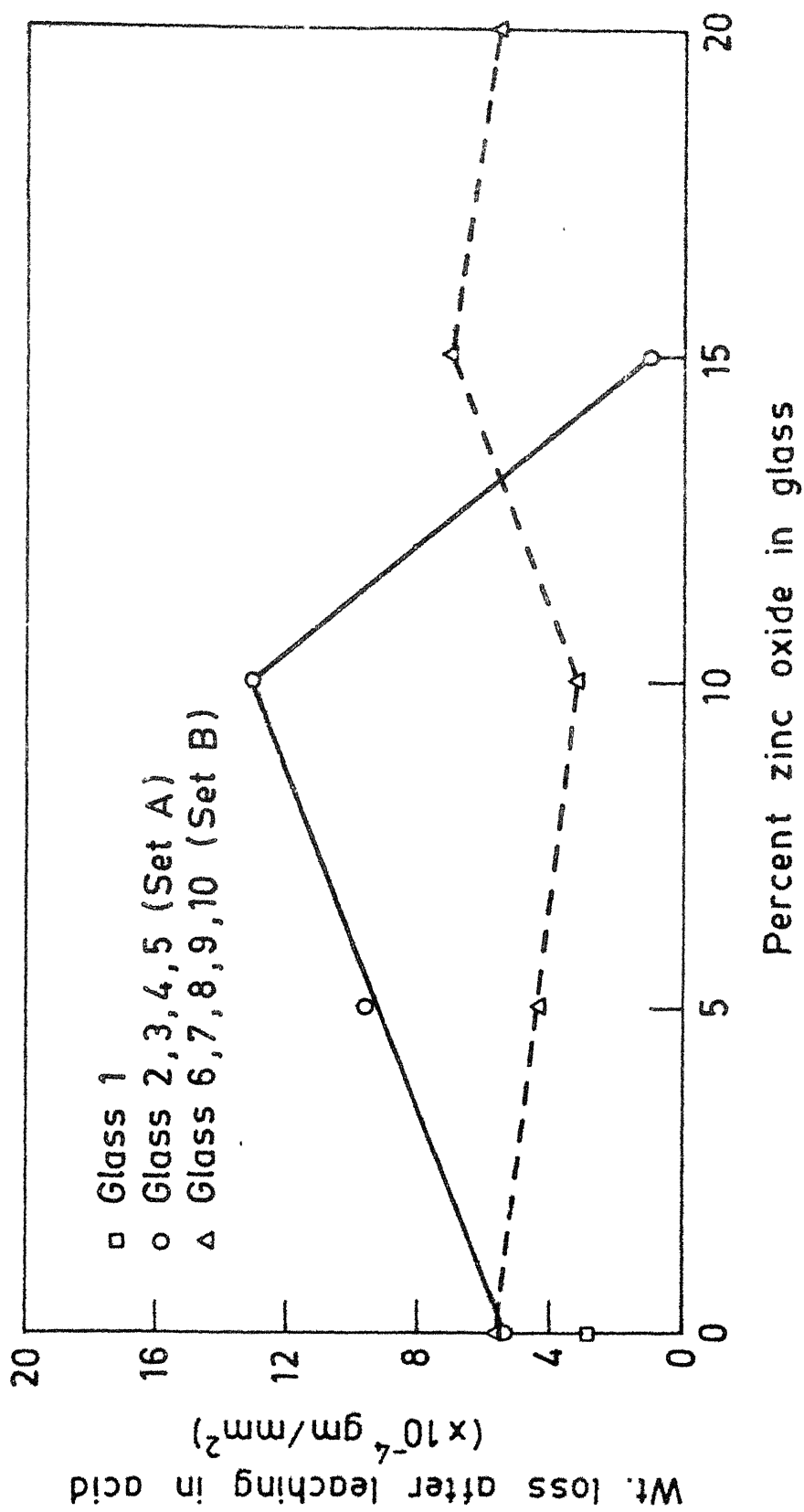


Fig. 2.12. Weight loss per unit area of the glasses after leaching in 3N HCl at 30 °C for half an hour.

GeO_6 octahedra will be less in this case than that of Set B glasses (already discussed). So it is quite likely that the lowering of durability due to the formation of polarizable nonbridging oxygen ions will more than counterbalance the improvement of durability due to the formation of GeO_6 octahedra. Indeed, we have found that for Set A glasses, durability has gone down with the increase in ZnO content in the glasses (Figure 2.12). The drastic improvement of durability in case of glass 5 (containing 15 mol % ZnO) may be due to the formation of ZnO_4 tetrahedra with consequent lowering of the number of nonbridging oxygen ions.

Figures 2.13 to 2.16 show the differential thermal analysis curves for the glasses. As the IR transmitting windows are subjected to aerodynamic heating, it is worthwhile to do DTA studies in order to find out whether the glasses have tendencies to devitrify at higher temperatures and if so, up to what temperature they can be used safely. Differential thermal analysis (DTA) is a well known tool to find out the devitrification temperature of a glass by noting the exothermic peak(s) in the curves.⁽⁵⁹⁾ It is to be noted that with devitrification, there may be marked changes in IR transmitting characteristics of the glasses like appearance of new bands, scattering losses (depending on the size of the crystals) etc.⁽⁶⁰⁾

All the set A glasses devitrify above 500°C (note that $60\text{ SiO}_2 \cdot 40\text{ Bi}_2\text{O}_3$ glass do not show any tendency towards devitrification). Multiple number of exothermic peaks indicate the formation of different crystals. The mild

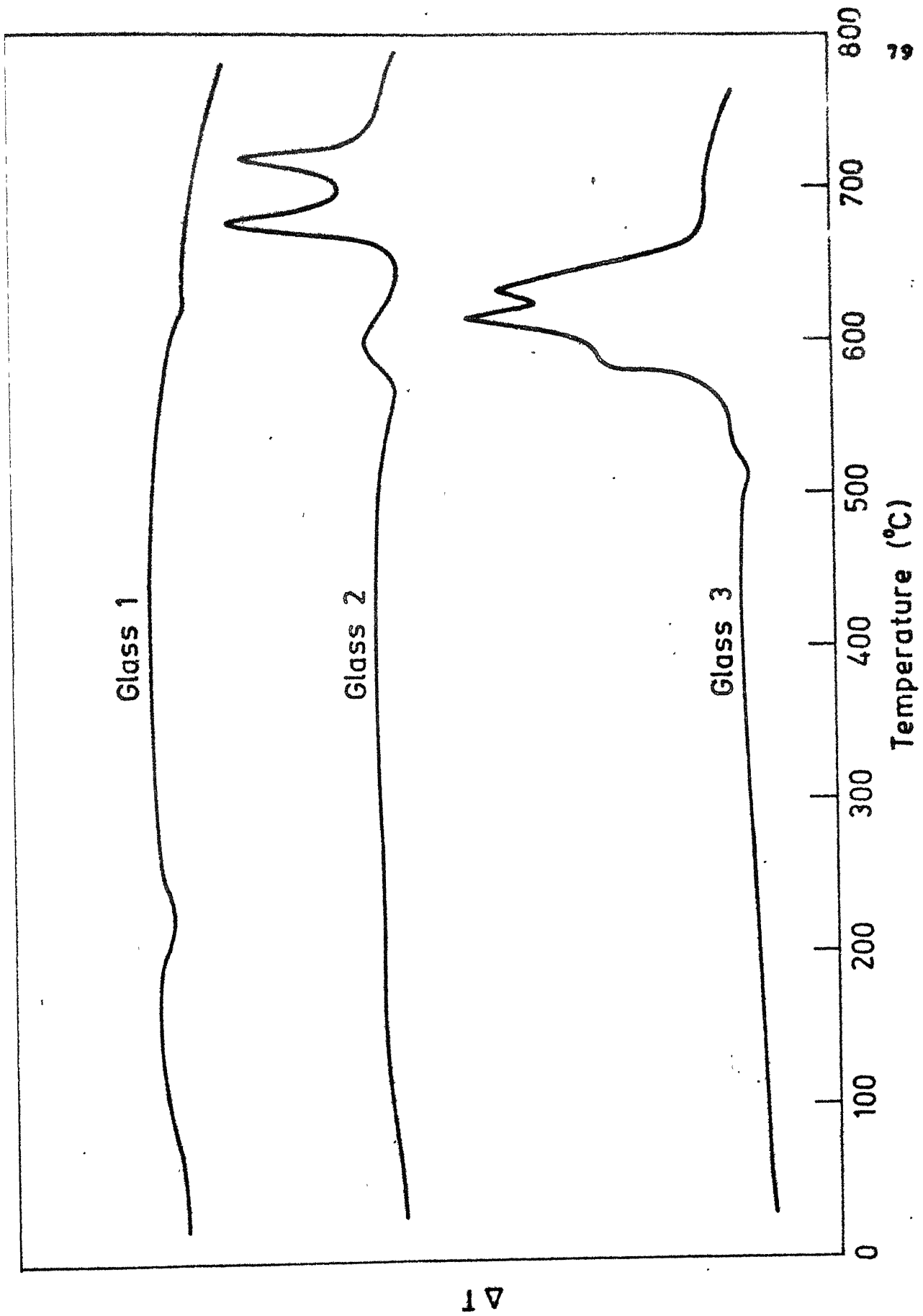


Fig. 2.13. Differential thermal analysis of glasses.

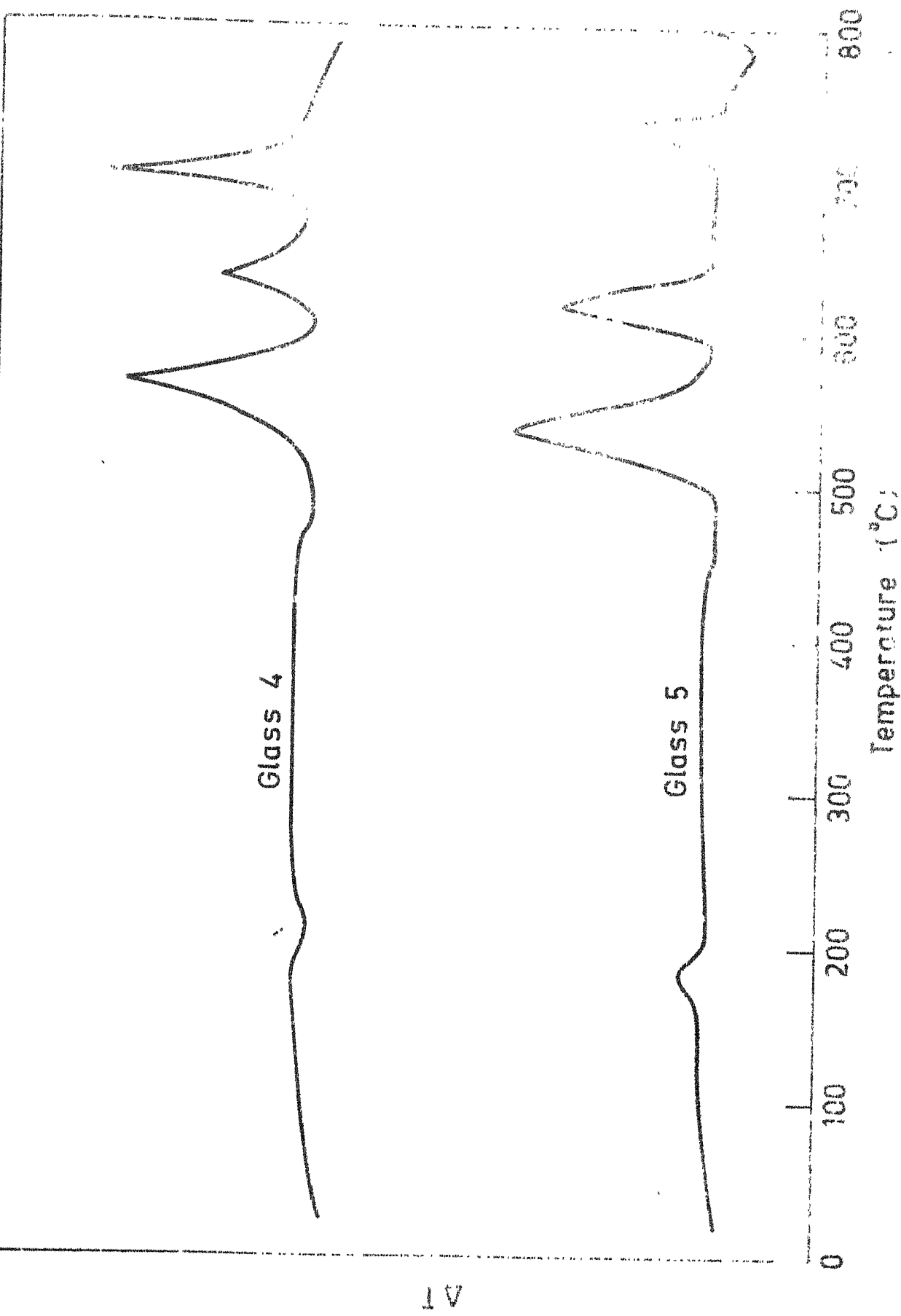


Fig. 2.14. Differential thermal analysis of glasses

Glass 6

Glass 7

Glass 8

ΔT

Temperature ($^{\circ}\text{C}$)

0 100 200 300 400 500 600 700 800

Fig. 2.15. Differential thermal analysis of glasses.

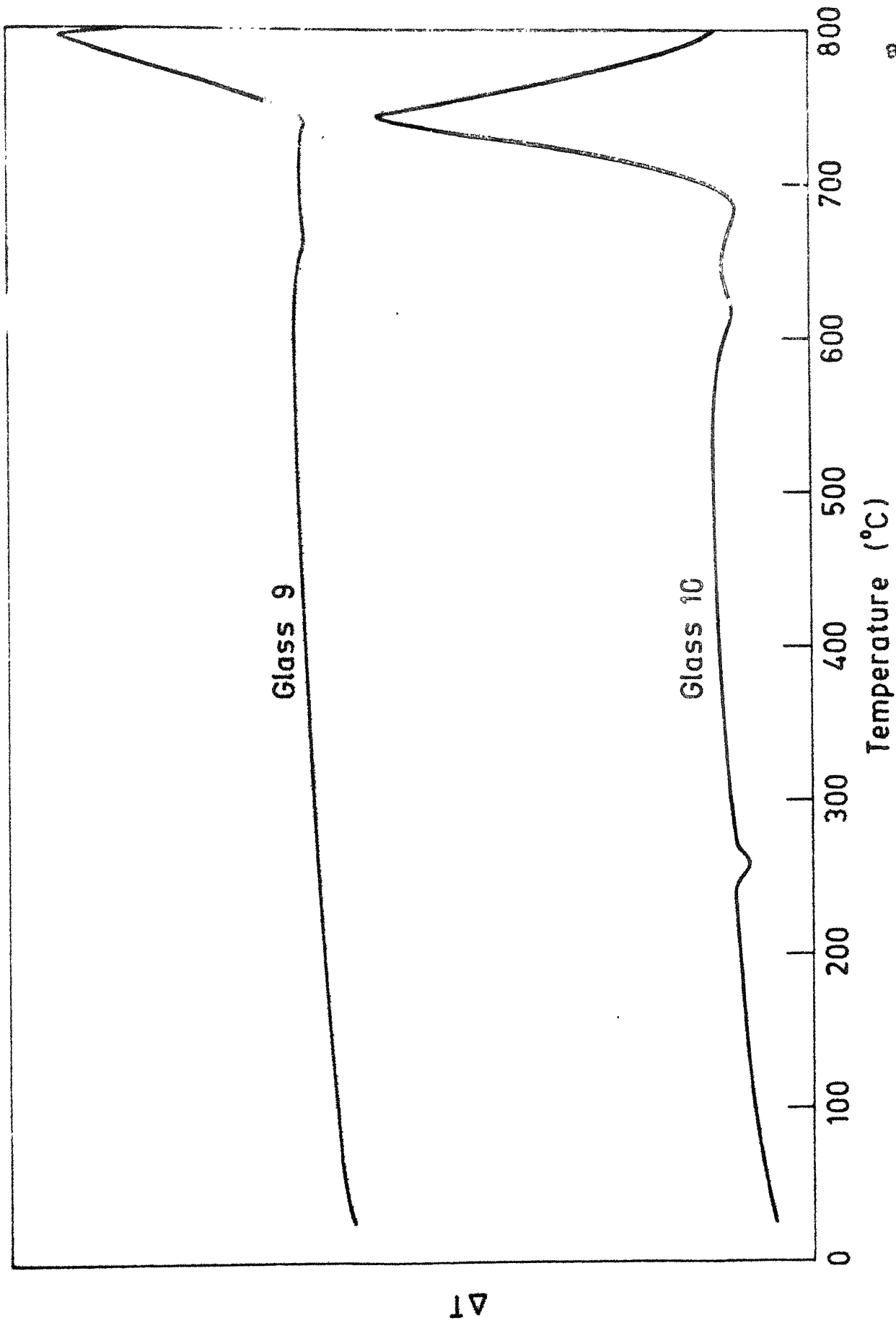


Fig. 2.16. Differential thermal analysis of glasses.

exothermic peak at 180°C for glass 5 is somewhat ambiguous. From the Figures 2.13 and 2.14 it can be said that ZnO enhances the tendency towards devitrification which is evident from the multiplicity of the peaks in high ZnO containing glasses and progressive lowering of the devitrification temperature with the increase in ZnO content of the glasses.

ZnO increases the tendency towards devitrification in case of Set B glasses too. Glass 6, containing no ZnO, does not show any tendency towards devitrification, and the intensity of the exothermic peak increases with the increase in ZnO content in the glasses (see Figures 2.15 and 2.16). Table 2.5 gives the minimum devitrification temperatures for all the glasses.

Figures 2.17 to 2.22 depict the optical absorption characteristics of the glasses in the visible region of the electromagnetic spectrum. As discussed in Chapter 1 of this thesis, the colour in high Bi_2O_3 containing glasses is due to Rydberg transition in Bi^{3+} ion pairs (and clusters). As the addition of ZnO induces better packing of the glass structure (which is evident from the decrease in molar volume, see Figure 2.6), the interaction between Bi^{3+} ion pairs (and clusters) is expected to be stronger. So with the increase in ZnO content of the glasses, their colour should become deeper.

The Set B glasses are of reddish orange colour and the colour deepens with the addition of ZnO. Figures 2.20 to 2.22 also impart the same idea, the absorption peak

TABLE 2.5 Minimum devitrification temperatures of the glasses

Glass number	Figure number	Minimum devitrification temperature	" " " "	Glass number	Figure number	Minimum devitrification temperature
1	2.13	-	" " " "	6	2.15	-
2	2.13	600°C	" " " "	7	2.15	700°C
3	2.13	583°C	" " " "	8	2.15	667°C
4	2.14	566°C	" " " "	9	2.16	793°C
5	2.14	537°C	" " " "	10	2.16	743°C

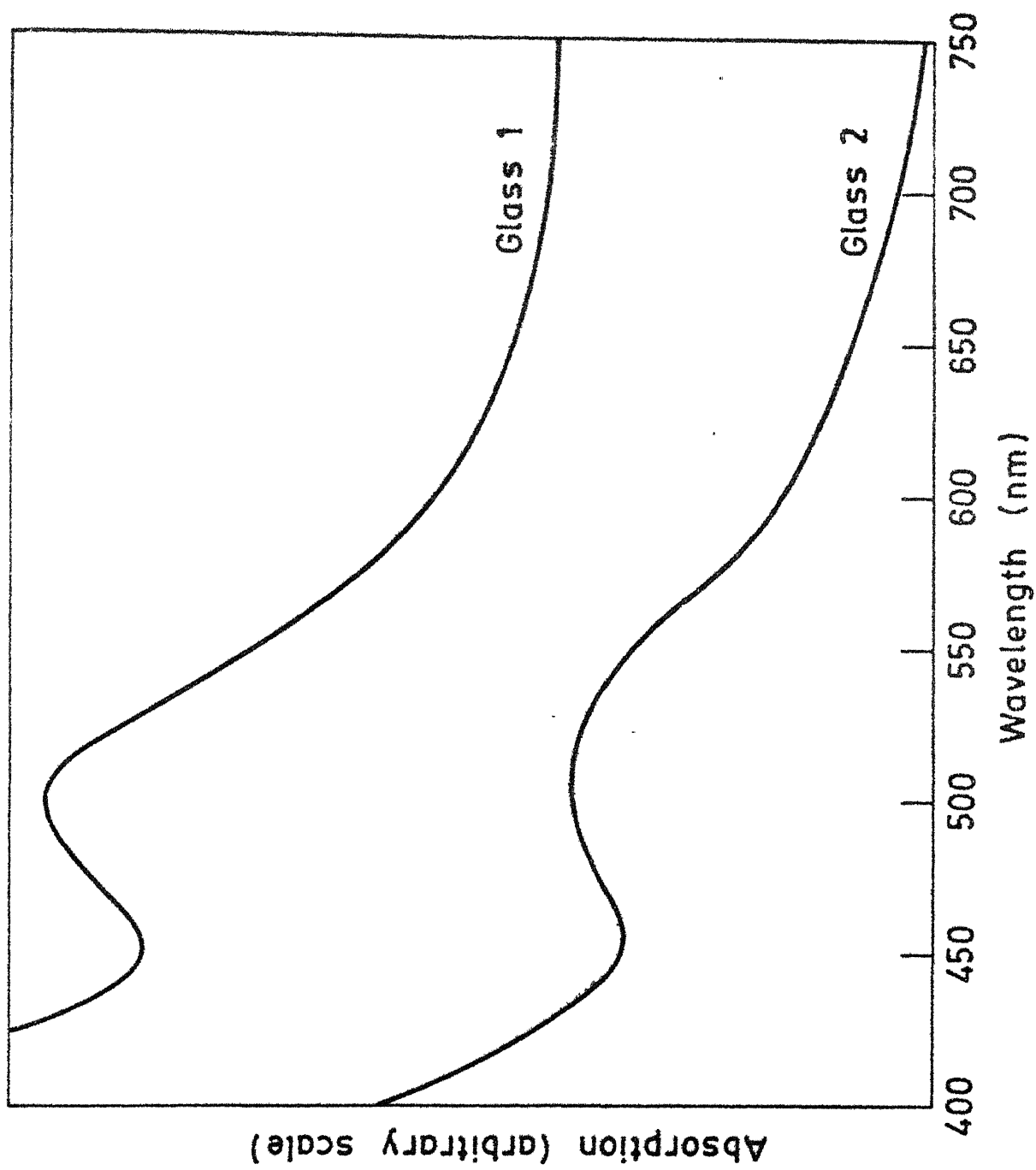


Fig. 2.17. Optical absorption of glasses.

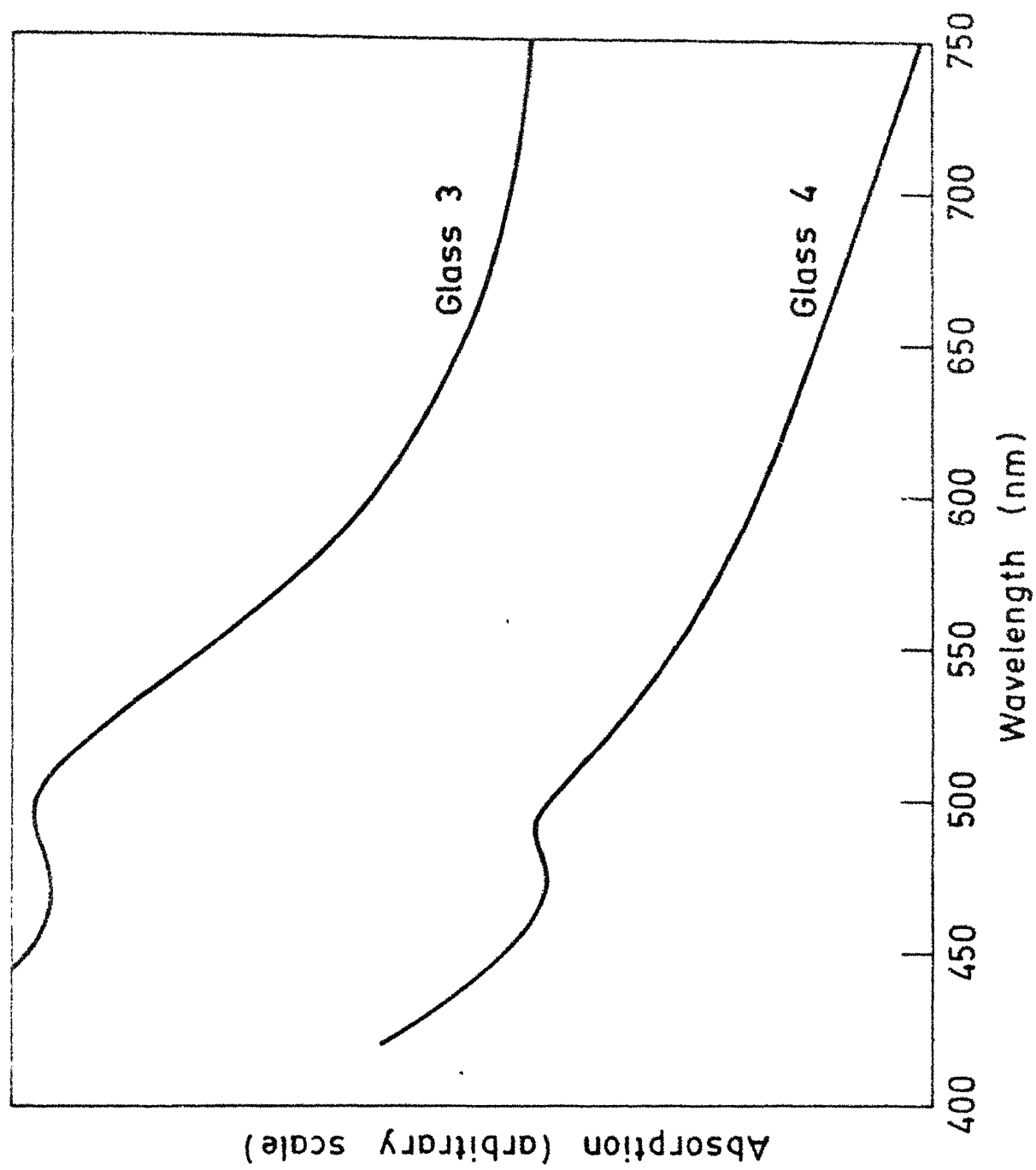


Fig. 2.18. Optical absorption of glasses.

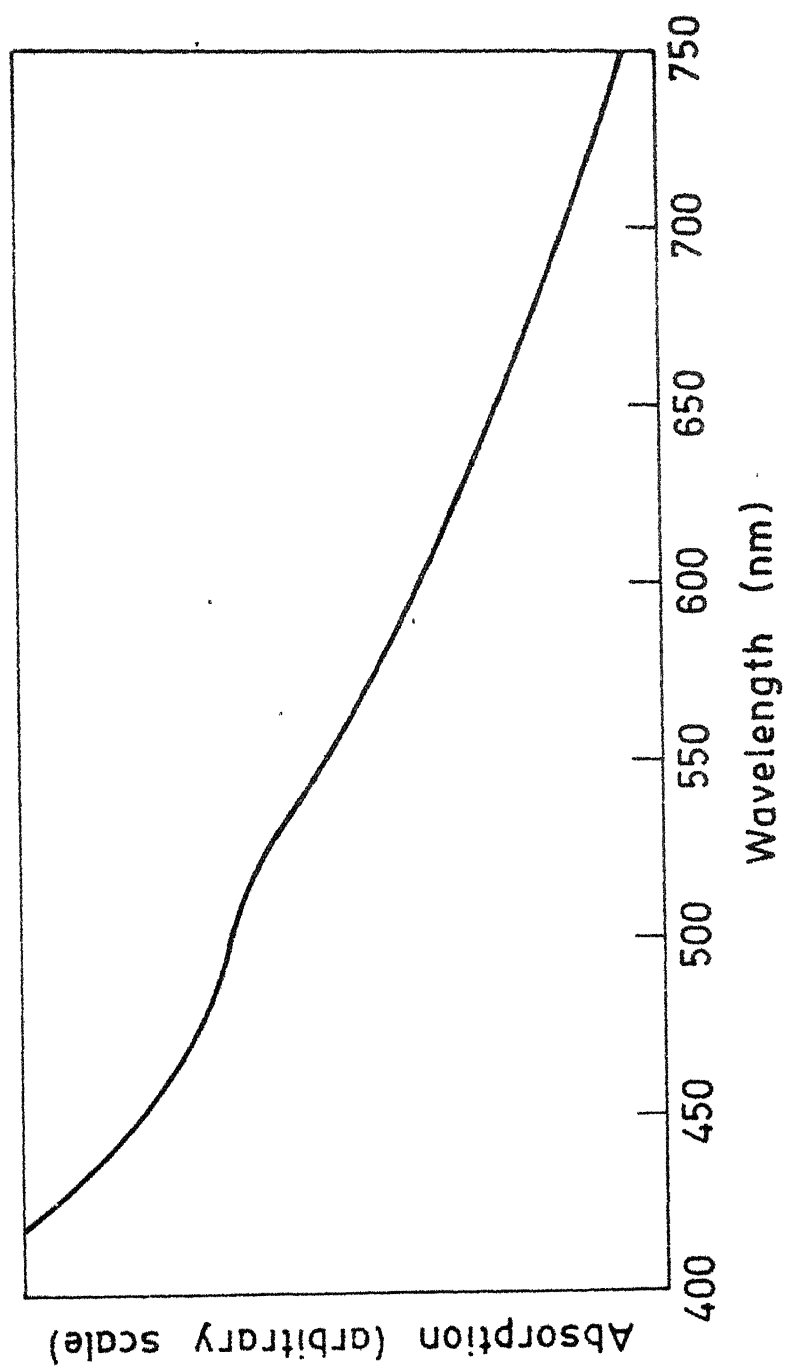


Fig. 2.19. Optical absorption of glass 5.

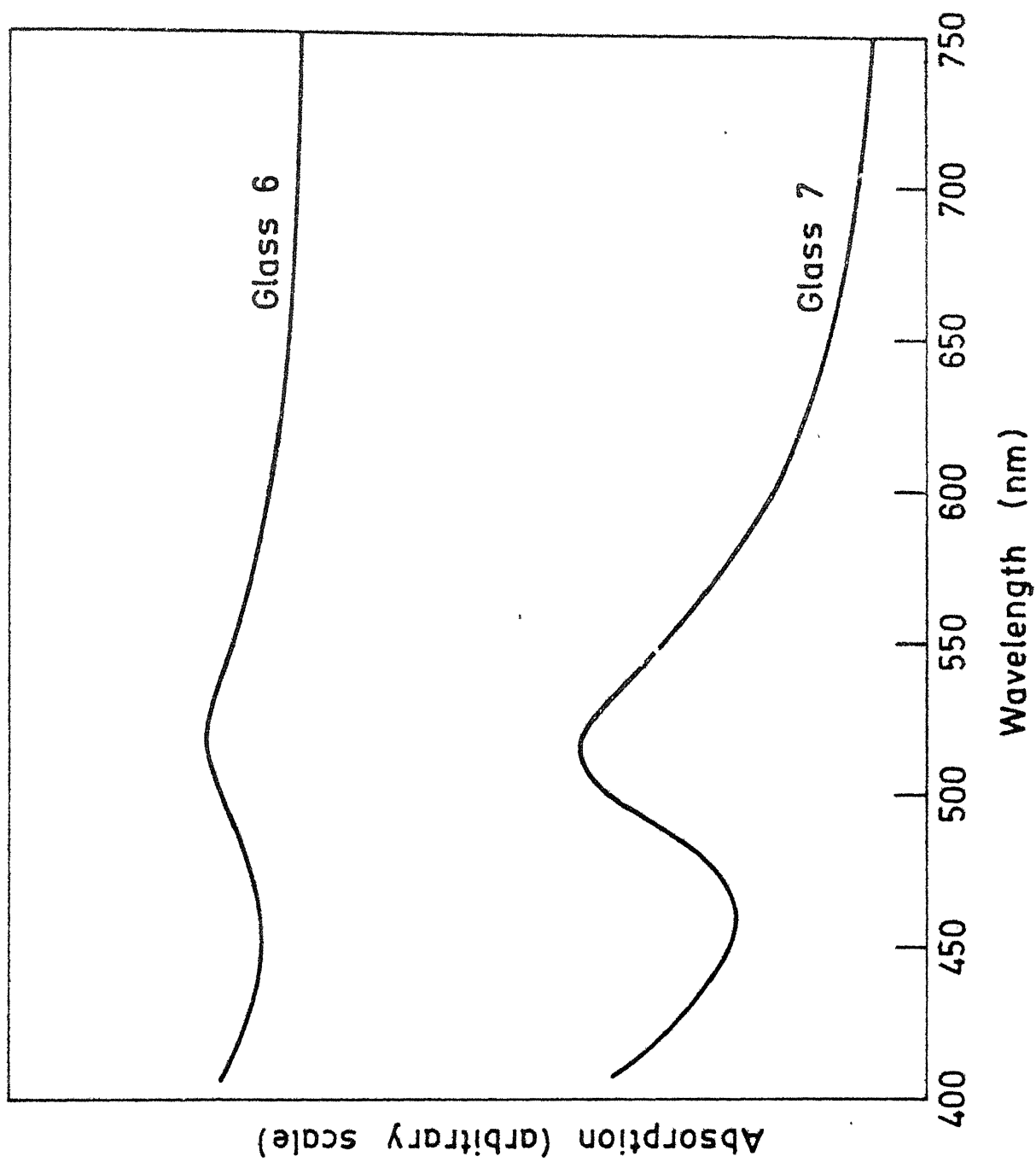


Fig. 2.20. Optical absorption of glasses.

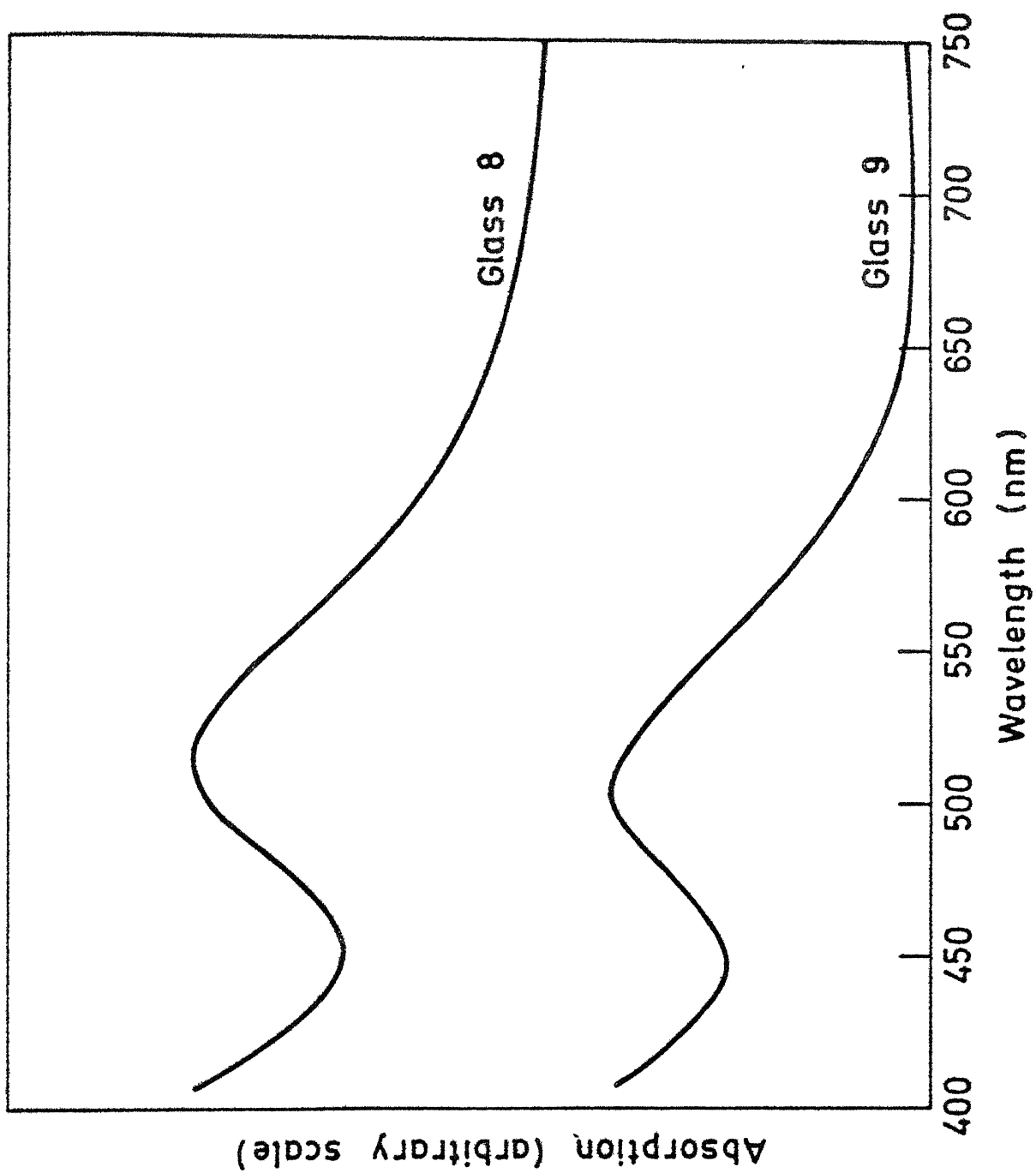


Fig. 2.21. Optical absorption of glasses.

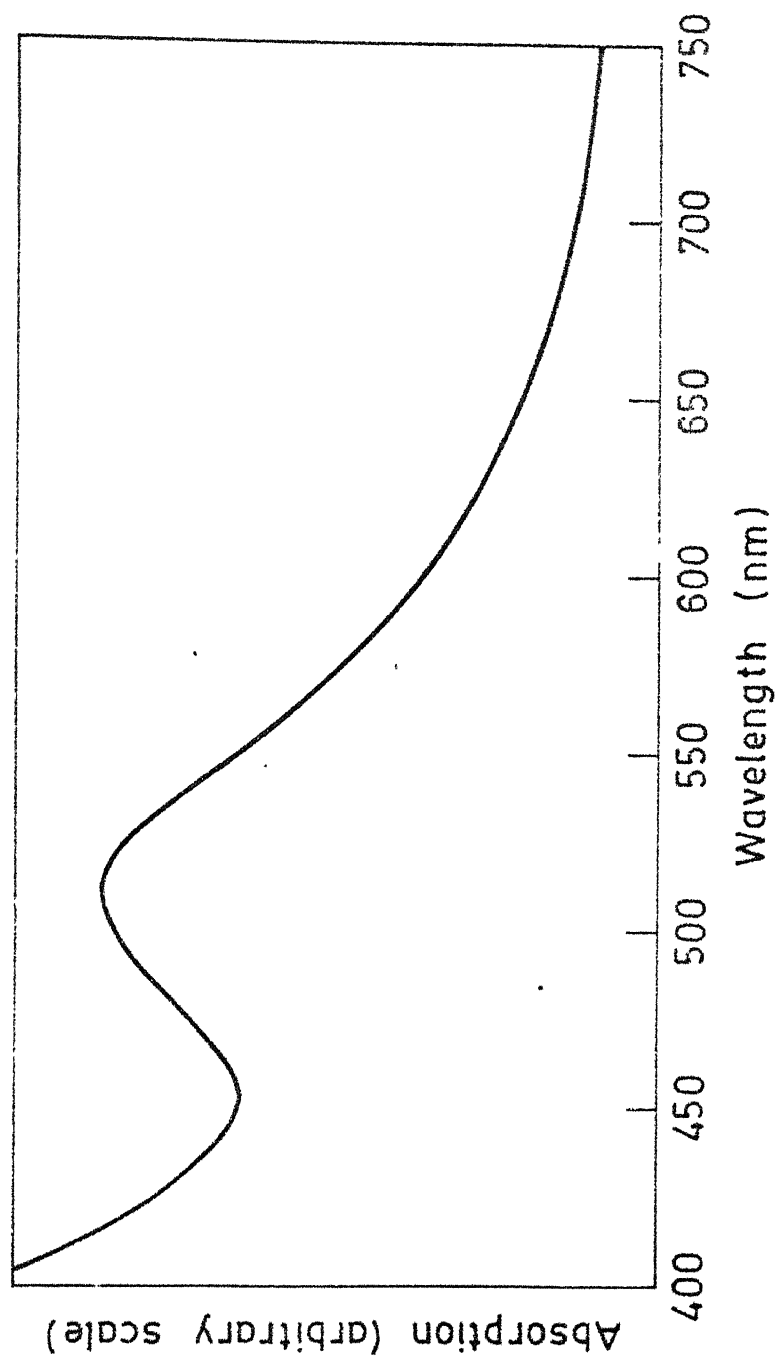


Fig. 2.22. Optical absorption of glass 10.

intensity around 500 nm has been found to be higher in case of ZnO containing glasses.

In general, the colour of Set A glasses is stronger than that of Set B glasses due to higher Bi_2O_3 content in the former. With the addition of ZnO, the colour of Set A glasses gradually turns brown. For Set A glasses, absorption peak around 500 nm has been found to broaden and become stronger with the increase in ZnO content in the glasses (Figures 2.17 to 2.19). As Set A glasses contain more Bi_2O_3 than Set B glasses, the probability of getting Bi^{3+} ion clusters (other than pairs) will be more in the case of the former. So with the increase in packing of the structure (that is, with the addition of ZnO), more Bi^{3+} clusters of different sizes are expected to form. This will give rise to a broad absorption of light and will impart brown colour to the high ZnO containing glasses. However, detailed structural studies are needed to find out the exact mechanism(s).

2.4 Conclusion

It has been found that GeO_2 can be replaced to some extent by ZnO in bismuth germanate glasses. In case of 60 GeO_2 .40 Bi_2O_3 glass, up to 15 mol % GeO_2 can be replaced by ZnO and for 80 GeO_2 .20 Bi_2O_3 up to 20 mol % GeO_2 can be replaced by ZnO without inducing crystallization. The glasses containing highest amount of ZnO (that is 15 mol % in case of 40 mol % Bi_2O_3 containing glass, and 20 mol % in case of 20 mol % Bi_2O_3 containing glass) will devitrify at the top surface above a certain thickness.

From IR transmission studies, it has been found that the partial substitution of ZnO for GeO_2 improves though slightly, the IR transmittance of the glasses at higher wavelengths. The total cut-off as well as 50% cut-off wavelengths of ZnO containing glasses are slightly higher than the glasses containing no ZnO. As expected, the total cut-off wavelengths of high Bi_2O_3 containing glasses (Set A) are higher than that of low Bi_2O_3 containing glasses (Set B).

The partial substitution of ZnO for GeO_2 lowers the molar volumes of the glasses. This is reflected in the density values of the glasses, which have been found to increase with the increase in ZnO content of the glasses.

Except glass 4, the replacement of GeO_2 by ZnO increases the microhardness of the glasses. Glass 10 (containing 20 mol % ZnO) has been found to show maximum hardness value amongst the glasses we studied.

All the glasses are very resistant to water. The effect of ZnO substitution on the durability towards 3 N HCl

has been found to be variable. In case of low Bi_2O_3 containing glasses (Set B), addition of ZnO has improved the durability except for glass 9 (containing 15 mol % ZnO). But glasses containing high Bi_2O_3 (Set A) show poor durability after addition of ZnO. Glass 5 (containing 15 mol % ZnO) is an exception, which shows a marked improvement in durability and is the most durable glass (towards 3 N HCl) of the lot.

From the DTA studies, it has been found that none of the glasses will devitrify below 500°C and the devitrification temperature of low Bi_2O_3 containing glasses (Set B) is somewhat higher than that of Set A glasses containing higher Bi_2O_3 . Glass 1 ($60 \text{ SiO}_2 \cdot 40 \text{ Bi}_2\text{O}_3$) and glass 6 ($80 \text{ GeO}_2 \cdot 20 \text{ Bi}_2\text{O}_3$) do not show any sign of devitrification.

With the addition of ZnO, the colour of the glasses has been found to deepen. In case of high Bi_2O_3 containing glasses (Set A), ZnO addition has been found to broaden the absorption peak around 500 nm.

So from all these studies, it can be concluded that except one or two cases, the partial substitution of ZnO for GeO_2 in bismuth germanate glasses ($60 \text{ GeO}_2 \cdot 40 \text{ Bi}_2\text{O}_3$ and $80 \text{ GeO}_2 \cdot 20 \text{ Bi}_2\text{O}_3$) improves the IR transmission, chemical durability and hardness of the glasses.

These glasses (containing ZnO) are also expected to possess a very good thermal shock resistance, because addition of ZnO to GeO_2 glass has been found to lower the thermal expansion coefficient of the glasses. ⁽⁶¹⁾

The minor water absorption band around 2.5-3.5 μm can be removed by melting in vacuum or in a flowing dry atmosphere. Halide additions can also be tried.

Surface coatings can be employed as antireflection aids to minimize high reflection losses of these glasses. To get the best effect, the refractive index of the coating should be equal to the square root of the substrate refractive index and the thickness should be equal to the quarter of the wavelength at the position where peak transmission is desired.⁽³⁾

Considering all the aspects, glass 10 ($60 \text{ GeO}_2 \cdot 20 \text{ Bi}_2\text{O}_3 \cdot 20 \text{ ZnO}$) can be said to be the best of the lot showing good IR transmission, chemical durability and hardness. This glass seems to be an excellent candidate for use as IR transmitting windows.

REFERENCES

- (1) Hackforth, H.L. (1960), Infrared Radiation, pp. 4, 107, 138, McGraw-Hill Book Co., Inc., New York.
- (2) Hudson, R.D., Jr. (1969), Infrared System Engineering, John Wiley and Sons, New York.
- (3) Donald, I.W. and McMillan, P.W. (1978), J. Mat. Sci. 13, 1151.
- (4) Rao, C.N.R. (1963), Chemical Applications of Infrared Spectroscopy, p. 9, Academic Press, New York.
- (5) Simon, I. in Modern Aspects of the Vitreous State (Ed. J.D. Mackenzie) (1960), Vol. 1, p. 126, Butterworth & Co. Ltd., London.
- (6) Donald, I.W. and McMillan, P.W. (1978), J. Mat. Sci. 13, 2301.
- (7) Chin, G.Y., Van Uitert, L.G., Green, M.L., Zydzik, G.J. and Kometani, T.Y. (1973), J. Amer. Ceram. Soc. 55, 369.
- (8) Kirchner, H.P. (1971), J. Canadian Ceram. Soc. 40, 15.
- (9) Doherty, J.E., Tschinkel, I.G. and Copley, S.M. (1973), Amer. Ceram. Soc. Bull. 52, 681.
- (10) Norberg, M.E., Mochel, E.C. and Garfinkel, H.M. (1964), J. Amer. Ceram. Soc. 47, 215.
- (11) Bloor, A.S., Phillips, S.V. and Partridge, G. (1976), Paper presented at Society of Glass Technology Meeting at St. Andrews.
- (12) Jamieson, J.A., McFee, R.H., Plass, G.N., Grube, R.H. and Richards, R.G. (1963), Infrared Physics and Engineering, p. 253, McGraw-Hill Book Co. Inc., New York.
- (13) Lippincott, E.A., Valkenburg, A.V., Weir, C.E. and Bunting, E.N. (1958), J. Res. Nat. Bur. Std. 61, 61.
- (14) Adams, J.H. in Kirk-Othmer Encyclopedia of Chemical Technology (1980), Vol. 11, p. 793, John Wiley and Sons, New York.
- (15) Florence, J.M., Glaze, F.W. and Black, M.H. (1955), J. Res. Nat. Bur. Stand. 55(4), 231.
- (16) Blau, H.H. (1955) U.S. Patent 2,701,208.

- (17) Neilsen, S., Lawson, W.D. and Fray, A.F. (1961), *Infrared Phys.* 1(1), 21.
- (18) Cleek, G.W. and Hamilton, E.H. (1962), U.S. Patent 3,022,182.
- (19) Cleek, G.W. and Hamilton, E.H. (1964), U.S. Patent 3,119,703.
- (20) Phillips, B. and Scroger, M.G. (1965), *J. Amer. Ceram. Soc.* 48, 398.
- (21) Burton, C.D.S. and Reid, A.M. (1965), U.S. Patent 3,188,216.
- (22) Leitz, E. (1968), *Fr. Patent* 1,549,090.
- (23) Dumbaugh, W.H. (1970), U.S. Patent 3,531,305.
- (24) *idem* (1973), U.S. Patent 3,769,047.
- (25) *idem* (1975), U.S. Patent 3,911,275.
- (26) *idem* (1976), U.S. Patent 3,982,952.
- (27) Hodogaya Chemical Co. Ltd. (1980), *Jpn. Kokai Tokkyo Koho JP* 8,060,041.
- (28) Tokyo Shibaura Electric Co. Ltd. (1981), *Jpn. Kokai Tokkyo Koho JP* 8,188,844.
- (29) Furukawa Electric Co. Ltd. (1981), *Jpn. Kokai Tokkyo Koho JP* 8,172,404.
- (30) Agency of Industrial Sciences and Technology (1982), *Jpn. Kokai Tokkyo Koho JP* 57,145,049.
- (31) Agency of Industrial Sciences and Technology Sumita Optical Glass Manufacturing Co. Ltd. (1982), *Jpn. Kokai Tokkyo Koho JP* 57,209,849.
- (32) Boudot, J.E. and Mazeau, J.P. (1982), *Fr. Demande FR* 2,499,546.
- (33) Khalilev, V.D., Koveschnikova, I.D. and Vakhrameev, V.I. (1984), *Fiz. Khim. Stekla*, 10(4), 499.
- (34) Colburn, S.C. and Miller, R.A. (1968), *Proceedings of the Symposium on Electromagnetic Windows, Vol. 1*, AD 841,562.
- (35) Cleek, G.W. and Scuderi, T.G. (1955), *J. Amer. Ceram. Soc.* 42, 599.
- (36) Adams, R.V. (1961), *Phys. Chem. Glasses* 2(2), 50.

- (37) Riebling, E.F. (1974), J. Mat. Sci. 9, 753.
- (38) Topping, J.A., Cameron, N. and Murthy, M.K. (1974), J. Amer. Ceram. Soc. 57(12), 519.
- (39) Nassau, K. and Chadwick, D.L. (1982), *ibid*, 65(4), 197.
- (40) *idem* (1982), *ibid*, 65(10), 486.
- (41) Volf, M.B. (1961), Technical Glasses, p. 36, Sir Isaac Pitman and Sons Ltd., London.
- (42) Zarzycki, J. (1957), Verres. Refract. 11, 3.
- (43) Riebling, E.F. (1963), J. Chem. Phys. 39, 1889, 3022.
- (44) Murthy, M.K. and Kirby, E.M. (1964), Phys. Chem. Glasses 5, 144.
- (45) Kolesova, V.A. (1979), Fiz. Khim. Stekla 5(3), 367.
- (46) Kamiya, K., Sakka, S. and Yoko, T. (1982), Res. Rep. Fac. Eng. Mie Univ., 7, p. 107.
- (47) Bishay, A. and Maghrabi, C. (1969), Phys. Chem. Glasses (10(1), 1.
- (48) Kokubo, T., Naito, S. and Tashiro, M. (1979), Yogyo Kyokaishi 87(9), 453.
- (49) Malmros, G. (1970), Acta Chem. Scand. 24, 384.
- (50) Aurivillius, B., Lindblom, C.I. and Stenson, P. (1964), Acta Chem. Scand. 18, 1555.
- (51) Abrahams, S.C., Jamieson, P.B. and Bernstein, J.L. (1967), J. Chem. Phys. 47, 4034.
- (52) Williams, A.F. (1979), A Theoretical Approach to Inorganic Chemistry, p. 171, Springer-Verlag Berlin, Heidelberg.
- (53) Ainsworth, L. (1954), J. Soc. Glass Tech. 38, 501.
- (54) Tarte, P. and Preudhomme, J. (1970), Spectrochim. Acta, 26A, 2207.
- (55) Weyl, W.A. and Marboe, E.C. (1962), The Constitution of Glasses — A Dynamic Interpretation, Vol. 1, pp. 57, 384, 377, 55, Interscience Pub., New York.
- (56) Morey, G.W. (1954), The Properties of Glass, p. 421, Reinhold Publishing Co., New York.
- (57) Scholze, H. (1959), Glastech. Ber. 32(3), 81.

- (58) Adams, R.W. and Douglas, R.W. (1959), J. Soc. Glass Tech. 43, 147T.
- (59) Wilburn, F.W. and Dawson, J.B. in Differential Thermal Analysis (Ed. R.C. Mackenzie) (1972), Vol. 2, p. 229, Academic Press, London.
- (60) McMillan, P.W. (1979), Glass Ceramics, p. 131, Academic Press, London.
- (61) Shelby, J.E. (1983), J. Amer. Ceram. Soc. 66(6), 414.

CHAPTER 3

THERMALLY GENERATED DARKENING OF OXIDE GLASSES*

* A paper based on this work has been accepted for publication in *Phys. Chem. Glasses*.

ABSTRACT

A new darkening effect has been observed in oxide glass powders of a wide range of composition when heated in the temperature range 400°C-600°C with a trace amount of water. Generation of blackening is inhibited when excess water is present. The behaviour is not dependent on the atmosphere in which the heat treatment is carried out. The darkened samples bleach when heated up to 850°C under ordinary atmosphere or treated with oxidising agents. Transmission electron microscopic studies do not reveal any precipitated crystalline phase within the darkened glass matrix. The latter also do not give any specific EPR signal. A model has been proposed which ascribes the darkening to the formation of nonparamagnetic colour centres. The latter forms due to a simultaneous dehydration and reduction reaction, in which, trace amount of water acts as a catalyst.

3.1 Introduction

Normally transparent crystals and glasses often appear coloured because of the presence of colour centres within them. Colour centres originally referred specifically to intrinsic defects in alkali halides, broadly speaking, the term now embraces all defects, impurities, or more complex imperfections which give rise to absorption in the visible region of the electromagnetic spectrum.^(1,2) In our discussion, we will use the term colour centre for describing defects associated with electron(s) or hole(s) in vacancies.

Weyl and Marboe⁽³⁾ have classified the inorganic chromophors, which can induce colour to crystals and glasses, into eight groups. These have been listed in Table 3.1. A better way of classification is that of Nassau⁽⁴⁾ as given in Table 3.2. From these tables, it is clear that, except a few special cases, glasses/crystals which are normally transparent and do not contain any colour producing impurity can exhibit colour due to the presence of colour centres only.

The common methods of colour centre generation in crystals and glasses can be summarised as follows.

In alkali halides, colour centres can be generated in three ways.⁽⁵⁾

- 1) Irradiation with X-rays, fast electrons, neutrons, or high energy protons generate defects. The temperature at which the irradiation is made determines the type of defects that are produced. Optical irradiation and heat treatment can bleach (transform) the centres.

TABLE 3.1 Classification of chromophors in inorganic systems (3)

Chromophors	Products (with brief comments)
1. Atoms and molecules	Lazurite {sodium aluminium silicate and sulphide} (S_2 molecule), Blue sulphur glass (S_2 , $(S_x)^{2-}$), Selenium pink glass (Se atoms), etc.
2. Ions of the transition elements	Rhodonite {manganese silicate}, Malachite {basic copper carbonate}, Cobalt nickel and other transition metal ion containing coloured glasses, etc.
3. Mutual deformation of colourless ions	Orpiment {arsenic trisulphide}, Cadmium sulphide containing glasses, etc. (ions like Hg^{2+} , Cd^{2+} and Pb^{2+} can exhibit colour when combined with anions of high polarizability like S^{2-} , I^- , etc.)
4. Valency interaction	Magnetite $\{Fe_3O_4\}$, Blue iron glasses etc. (The interaction of two states of valencies of the same element like Fe^{2+} and Fe^{3+} in magnetite can give rise to colour)
5. Induced valency	Red feldspar {alkali aluminosilicates} (Fe^{4+} impurities in Si^{4+} sites), Praseodymium yellow (Pr^{4+} impurities in CeO_2) etc. (Fe^{4+} , Pr^{4+} are unknown in normal conditions, but in special cases, crystals can force them to such valence states)

Contd....

TABLE 3.1 (continued)

Chromophors	Products (with brief comments)
6. Asymmetrical units	A variety of brown coloured finely subdivided quartz, leached vycor etc. (The colour centre may be a strongly distorted SiO_4 tetrahedron or even a group which contains a singly charged O^- ion $\{\text{Si}^{4+}(\text{O}^{2-}/2)_3\text{O}^-\}$).
7. Electron transfer by radiation	Smoky quartz, blue rock salt, irradiated glasses etc. (Colour centres are formed due to irradiation)
8. Metals	Gold ruby glass, copper ruby glass etc. (The colloidal colour in this case is strongly dependent on the size of the metal particles).

TABLE 3.2 Types of colour in minerals⁽⁴⁾

Colour cause	Typical minerals	Formalism
1. Transition metal compounds	Malachite (basic copper carbonate), Almandite (iron-aluminium garnet)	Crystal field theory
2. Transition metal impurities	Emerald (Cr^{3+} in beryllium aluminium silicate), ruby (Cr^{3+} in Al_2O_3)	Crystal field theory
3. Colour centres	Fluorite (CaF_2 , electron colour centres), smoky quartz (SiO_2 , hole colour centre)	Crystal field theory
4. Charge transfer	Blue sapphire ($\text{Fe}^{2+} - \text{Ti}^{4+}/\text{Fe}^{3+} - \text{Ti}^{3+}$), Vanadinite ($\text{V}^{5+} - \text{O}^{2-}$)	Molecular orbital theory
5. Organic materials	Graphite (π electrons), amber (organic pigments)	Molecular orbital theory
6. Conductors	Copper, silver	Band theory
7. Semiconductors	Galena (Pbs), Pyrite (FeS_2)	Band theory
8. Doped semiconductors	Yellow diamond (nitrogen impurity), blue diamond (boron impurity)	Band theory
9. Dispersion	'Fire' in high dispersion gem stones such as diamond, zircon etc.	Physical optics
10. Scattering	Moonstone albite etc. (light scattered from colloidal particles give rise to bluish tinge)	Physical optics

Contd...

TABLE 3.2 (continued)

Colour cause	Typical minerals	Formalism
11. Interference	Iridescent chalcopyrite (the colour originates from interference in thin films and is dependent on film thickness, the refractive index of the film and the nature of the incident light)	Physical optics
12. Diffraction	Opal (the colour originates from the interference of light waves by a diffraction grating produced by periodic spacings as in opal, Irish agate etc. The colour depends on grating spacing and the angle of observation)	Physical optics

2) Heating of a crystal to several hundred degrees in an atmosphere of the alkali metal vapour produces crystals with a stoichiometric excess of alkali metal. If the crystal is rapidly cooled from this temperature, the F-centre (electron trapped in a negative ion vacancy) is the prominent defect (additive colouration). Similarly, heating in halogen vapour followed by quenching can give rise to hole colour centre.

3) Passage of an electrical current (dc) through samples held at several hundred degrees, generate colour centres (radiolytic colouration). F-centres are generated at the cathode and move into the crystal under the action of the applied electric field.

Though radiolytic and additive colouration can be made in alkaline earth oxides, X-irradiation induced electron colour centres cannot be formed in such oxides except when the anion vacancies are generated by plastic deformation prior to radiation.⁽⁶⁾ This is due to larger binding energies of ions in alkaline earth oxides in comparison to alkali halides (high energy proton irradiation can generate electron colour centres in alkaline earth oxides).

Trapped electron centres have been found in explosively shocked magnesium oxide without irradiation.⁽⁷⁾ Also some surface defect centres have been observed after grinding alkaline earth oxides, sulphides and selenides.⁽⁶⁾ These defect centres absorb (chemisorption) oxygen very quickly.

Defect centres have also been generated in BeO, ZnO, SiO₂, GeO₂, BaTiO₃ etc.⁽⁸⁾ In case of highly covalent

structure like silica, because of the rigid character of the binding forces, it is understandable that electromagnetic radiation is not capable of causing structural defects, at least not by any simple mechanism — in fact, defects caused by ionizing radiation originate at imperfections present before irradiation.⁽⁹⁾ These defects are normally associated with impurities.⁽⁹⁾ In case of smoky quartz, hole colour centres have been found near Al^{3+} impurities.⁽⁴⁾

In glasses, colour centres have been produced after irradiating them with X-ray,⁽¹⁰⁾ γ -rays⁽¹¹⁾ and high energy particles.⁽¹²⁾ After irradiation, paramagnetic electron colour centres,⁽⁹⁾ hole colour centres,⁽⁹⁾ as well as non-paramagnetic electron colour centres⁽¹³⁾ (due to pairing of electrons captured on a nonbridging oxygen vacancy near a modifier ion) have been observed in glasses.

A new darkening effect has been observed by us in the case of glass powders treated with trace amounts of water and subsequently heated to specific temperatures. The effect seems to be general in that a large number of glass systems have exhibited this property. In this chapter, the results obtained on a systematic investigation of this phenomenon are presented. A model based on colour centre formation is also proposed to explain the observed behaviour.

3.2 Experimental

The compositions of the glasses studied are given in Table 3.3. Silicate, borate and phosphate glasses with varying amounts of network modifying oxides like alkali and alkaline earth oxides, and intermediate oxides like alumina were prepared for our studies. The compositions were so chosen as to find out the effect of different components on the darkening process and at the same time to establish the fact that this darkening effect occurs in a wide variety of glass compositions. While the glass no. 1 was the commercial product Vitrosil, the others were prepared from reagent grade chemicals by melting suitable mixture of oxides in an electric furnace at temperatures in the range 1050° to 1350°C using alumina crucibles. Some glass samples were annealed in the temperature range of 350° to 500°C. Glass no. 7, however, was made from analytical grade chemicals and to ensure that there was no alumina contamination, a platinum crucible, instead of alumina, was employed. Both annealed as well as quenched glass samples were used for the experiments.

Glass pieces were washed in acetone. Some samples were also washed in benzene and they were subjected to grinding process in an agate (also in a porcelain) mortar and pestle. Unwashed glass samples were also used. The ground powder batches after grading in ASTM sieves were placed on an alumina (also in a glass) base. Small amount of distilled/deionized water was then added to the powder. The best way to add water, the amount of which seemed to be

TABLE 3.3 Glass compositions in mol %

Glass no.	SiO ₂	B ₂ O ₃	GeO ₂	P ₂ O ₅	Al ₂ O ₃	BaO	PbO	MgO	CaO	Sb ₂ O ₃	Na ₂ O	Li ₂ O	CeO ₂ over 100 mol % glass
1	100												
2			100										
3		60				40							
4		60			20	20							
5		60			15			15			10		
6		66			4					15		15	
7		75						10			15		
8	60						40						
9	60						20				20		
10	60						20				20		
11	60						20						2
12	72								20				
13	56				3				10		15		
14	41				4				10		30		
15					4				10		45		
16				88	2			10					
			75	15							10		

critical, was to put one or two drop(s) at one side of the powdered sample so that a continuous gradation of water content was attained. This procedure ensured proper amount of water at least in some regions of the powder. Subsequently, samples were heated to 400-600°C slowly. Heat treatment was repeated by directly introducing the samples inside the furnace at specific temperatures and kept for 15 minutes to 1 hour. Heat treatment was also given in various atmospheres viz., dry oxygen, dry hydrogen, dry argon and steam. Experimental arrangement for the heat treatments in controlled atmosphere is given in Figure 3.1. The heat treatments were carried out in a wire wound electrically heated muffle furnace. Samples were kept inside a quartz tube which was covered by a mullite muffle. A thermocouple was held near the sample and was connected to a temperature controller at the other ends. Fused calcium chloride was used for drying oxygen, hydrogen and argon gases. Similar heat treatments were imparted to the samples by adding excess water (so as to form a slurry like mass) and also by grinding them in water itself. Relative humidity of the atmosphere was noted by a standard hygrometer.

The samples were subsequently observed against white background to find any colour change. This was especially needed when the base was not alumina (which is white in colour) and the darkening effect was little and highly localized. The samples after darkening were heated up to 850°C and also treated with water (at room temperature as well as boiling), NaOH solution (hot as well as cold),

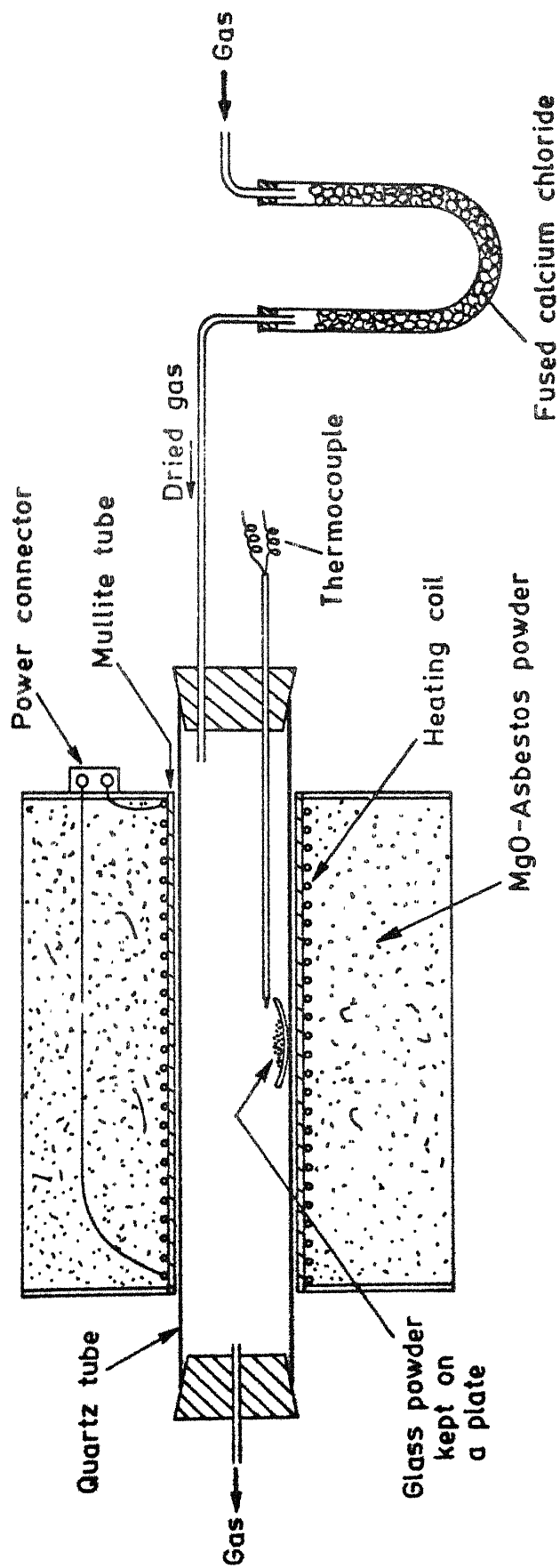


Fig. 3.1. Experimental arrangement for heat treatment in controlled atmosphere.

concentrated H_2SO_4 , concentrated HNO_3 and a mixture of chromic acid and sulphuric acid respectively to see their individual effects on the colour, if any.

Samples for transmission electron microscope (TEM) studies were prepared by the conventional technique (as described in Chapter 1) using carbon supported copper grids. Selected area electron diffraction and the microstructure of characteristic samples (white as well as dark regions) were recorded in a Phillips EM301 TEM, operated at 100 KV. In order to identify the crystalline phase (if any) in the glass samples, radii of diffraction rings were measured from the negative by using a graduated eye piece with an accuracy of 0.1 mm. The interplanar spacings were calculated from the relation given below:

$$\text{Camera constant} = r \cdot d_{hkl}$$

Here r is the radius of the diffraction ring and d_{hkl} is the interplanar spacing of the (hkl) plane giving rise to the diffraction ring.

The value of camera constant was determined from the diffraction pattern of a gold sample taken as standard, under identical conditions. Using this camera constant value and from the radii of the diffraction rings, d_{hkl} values for the crystalline phase were calculated.

Electron paramagnetic resonance studies were carried out in a Varian E109 EPR spectrometer for both the darkened and virgin powders using a quartz tube.

3.3 Results and Discussions

The effect of heat treatment on glass powder of different compositions is summarised in Table 3.4. Quenched as well as annealed samples of each composition showed identical behaviour after the heat treatment. Also the effects observed were independent of the atmosphere (oxygen, argon and hydrogen respectively) in which the treatment was carried out. When excess water was added to the glass powder of different compositions to make a slurry the darkening effect was drastically reduced or found absent altogether. A heat treatment of the glass powder in steam also did not show any darkening effect. For high values of relative humidity ($> 90\%$), colour changes were observed in some glasses even without the addition of trace quantity of water.

Particle size of the glass powder had a pronounced effect on the darkening. In most cases the optimum size was found to be $44\text{ }\mu\text{m}$ (A.S.T.M. -325 mesh), though for glass no. 9, even particles as large as $210\text{ }\mu\text{m}$ exhibited this behaviour.

The darkened samples could be bleached by subjecting them to temperatures in the range $600\text{--}850^{\circ}\text{C}$. The bleaching temperatures for different glasses are given in the last column of Table 3.4. Temperature ranges have been given as the bleaching temperature is dependent on the time of heating in the sense that, at relatively higher temperature, the samples will be bleached in few minutes, whereas at lower temperature, an hour may be needed for complete

TABLE 3.4 Summary of heat treatment effects on various glasses

Glass no.	Amount of water added to glass powder (wt %)	Heat treatment temperature (°C)	Effects observed/remarks	Bleaching temperature (°C)
1 & 2	~15	400-600	No colour change	-
3 & 4	~15	400-500	Light grey semifused mass (The colour seemed to be confined on the surface).	650-750
5	~15	400-500	Black (or dark grey) colour at the boundary of the powder and the base and localised black (or dark grey) regions on the surface. Removal of the top layer showed that the colour was mainly confined to the surface.	700-850
6	~15	~400	Initially there was darkening on the surface and the boundary but if kept for a longer time around the heat treatment temperature, crystallization took place and the dark regions disappeared.	400-450
7	~15	400-500	Same as glass no. 5	700-850
8	~15	400-600	No colour change	-
9	~15	400-500	Pronounced darkening. The semifused mass turned dark black.	600-650

Contd.,..

TABLE 3.4 (continued)

Glass no.	Amount of water added to glass powder (wt %)	Heat treatment temperature (°C)	Effects observed/remarks	Bleaching temperature (°C)
10	~15	400-500	Reasonable darkening	600-650
11 & 12	~15	400-600	No colour change	-
13	~15	400-500	Grey semifused mass (The colour seemed to be confined on the surface).	650-700
14	~15	400-550	No colour change	-
15	~15	400-500	Same as glass no. 13	650-700
16	~15	400-500	Same as glass no. 5	700-850

bleaching. It is evident that this temperature is low for glasses having a low melting temperature and vice versa.

The darkening cannot be removed by treating the samples with boiling water, NaOH solution and concentrated sulphuric acid respectively. The darkening however disappears slowly over a period extending from 24 to 96 hours in H_2O_2 solution. The bleaching effect was found to be much faster (few hours only) with concentrated nitric acid and a mixture of chromic acid and sulphuric acid. It is therefore evident that bleaching can be affected by oxidising agents only.

Electron micrographs either of virgin or darkened samples did not show any precipitated phases within them. A typical electron micrograph of the glass samples has been given in Figure 3.9. In the case of glass no. 9, however, fine lead particles were found dispersed in the glass matrix. This case has been dealt with separately below.

EPR studies did not show any difference between the virgin and the darkened specimens. In fact, no specific EPR signal was found in the case of the latter.

As discussed before, in the inorganic systems, colour may be attributed to various mechanisms. In our case, the darkening effect was found in a wide variety of glasses of different constituents. The mechanisms, therefore, should be based either on the formation of colour centres as a result of heating or related to some specific changes in the physical structure of the glass particles induced by heating, which could give rise to optical

absorption by the principle of physical optics (e.g., scattering, interference). The latter alternative can be ruled out because the physical structure is not dependent on the oxidising agents, which alone can bleach the colour. Therefore, the formation of colour centres due to heat treatment can possibly explain the darkening process. Further, the EPR results indicate that the colour centres formed by heat treatment should be of a nonparamagnetic type. The following model is therefore proposed to explain the formation of nonparamagnetic colour centres in the present case.

It is well known in catalysis that in silica-alumina systems, aluminium atoms replacing silicon can give rise to a Lewis acid centre (electron acceptor).⁽¹⁴⁾ Si-OH and Si-O-Si groups on the surface of silica as well as Al-OH and Al-O-Al groups on the surface of alumina are not strongly acidic. Aluminium atoms embedded in silica structure can display very strong acidity. The electrophilic property of the aluminium atoms thus placed on the surface may be traceable to the electrical asymmetry of the $\text{Al}^{3+}:\text{O}:\text{Si}^{4+}$ groups. It is believed that the electron pair in the Al:O bond is shifted toward more highly charged silicon ion (as indicated by arrows in Figure 3.2).⁽¹⁵⁾ Alumina-boria and magnesia-silica catalysts have also been found to contain such acidic sites.⁽¹⁵⁾ Similar types of acidic sites are expected on the surface of many glasses especially when they contain intermediate oxides like Al_2O_3 . Even in the absence of intermediate species, if the network forming cation (e.g., boron) can assume different coordination in the glass (e.g.,

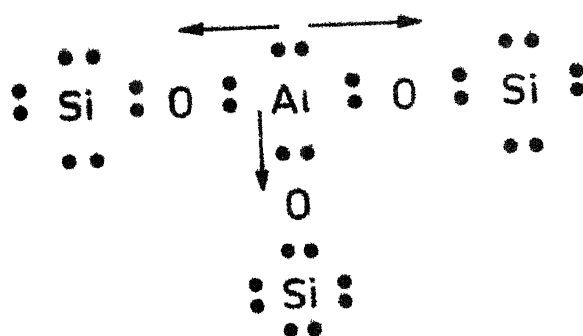


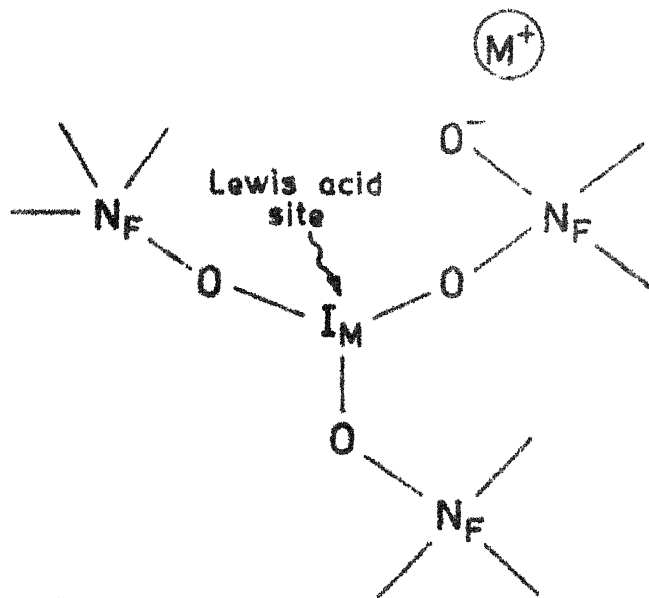
Fig. 3.2. Schematic representation of Lewis acid site in aluminosilicate.

due to the addition of alkali oxides), creation of such sites are possible. Grinding of a solid induces defects⁽¹⁶⁾ as well as strain within it. This can give rise to differently coordinated cations on the surface.⁽¹⁷⁾ Such deviations are more facilitated in disordered structures like glasses.

Figure 3.3 shows schematically the atomic arrangements in a specific region of the glass particle surface. Nonbridging oxygen has been shown near the modifier ion. Figures 3.4 and 3.5 show the effect of water addition on the atomic arrangements at the surface. OH^- ion will attach itself to the Lewis acid site and H^+ will combine with nonbridging oxygen. Figures 3.6, 3.7 and 3.8 show the three possible configurations of various atoms after removal of one molecule of water from the glass during heat treatment.

The configuration shown in Figure 3.6 is energetically unfavourable. Network forming cation (e.g., Si) when tetrahedrally coordinated, cannot be bonded to another network forming cation via two oxygen ions⁽¹⁸⁾ on crystal chemical considerations.

Figure 3.7 describes a situation where thermal motion will cause oscillation of the bond (of nonbridging oxygen) between N_F and I_M ions to meet the electrophilic requirements of the Lewis acid site in I_M and screening demand of N_F . But the surface structure in actual case is highly distorted and the swinging motion of the nonbridging oxygen may be hindered to some extent.



N_F — Network former ion (like Si)
 I_M — Intermediate ion (like Al)
 M — Modifier ion (like Na)

Fig. 3.3. Schematic representation of the atomic arrangements in a specific region of the glass surface.

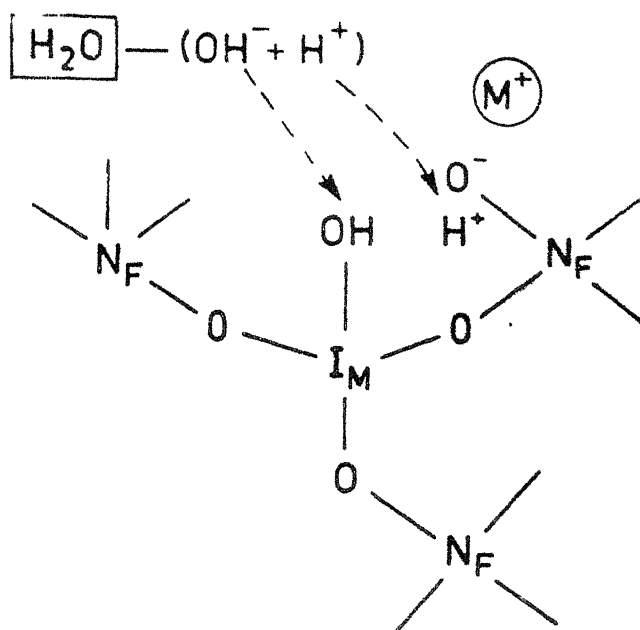


Fig. 3.4

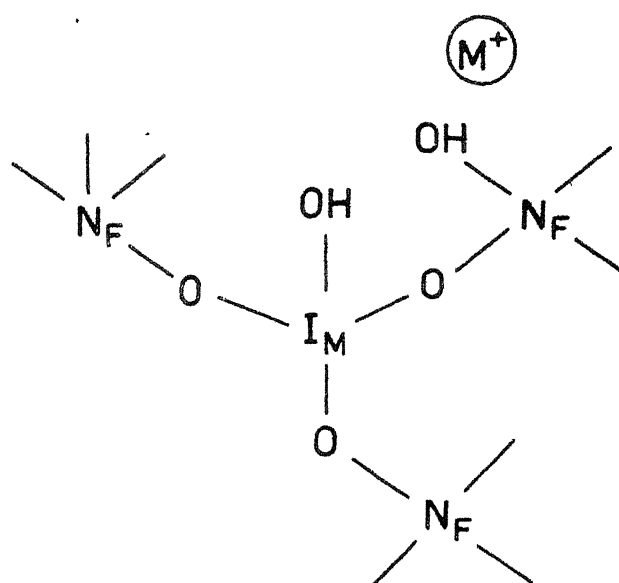


Fig. 3.5

Schematic representation of the effect of water addition on the atomic arrangements at the surface.

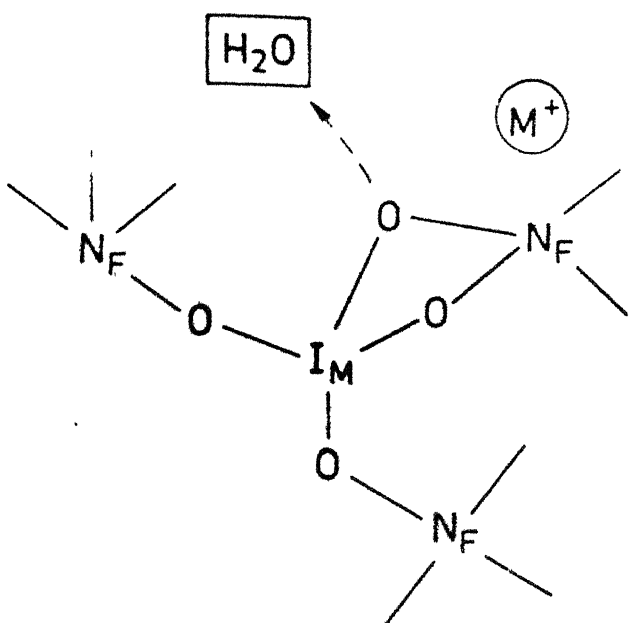


Fig. 3.6

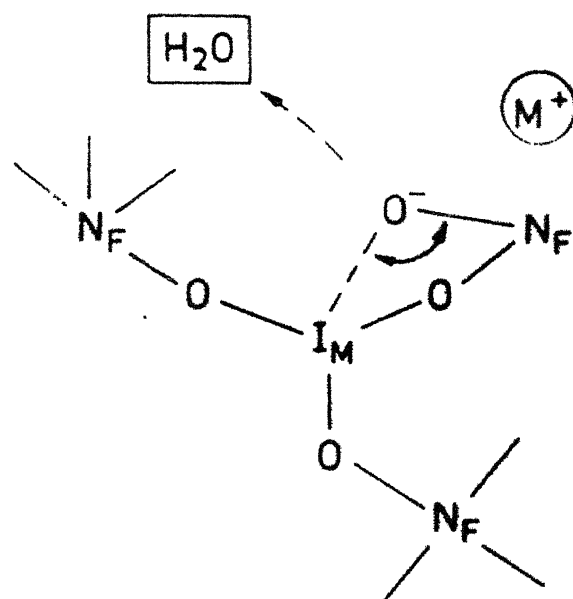


Fig. 3.7

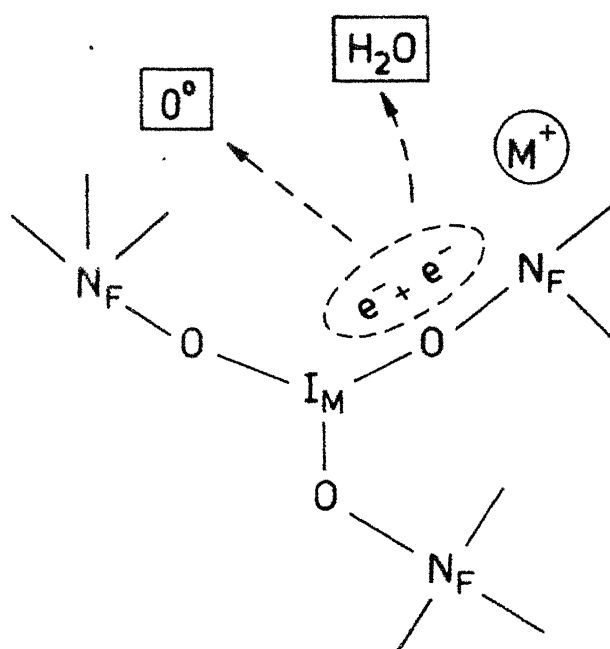


Fig. 3.8

Schematic representation of three configurations of various atoms that may emerge following heat treatment.

In Figure 3.8, where the third alternative structure has been shown, it is assumed that the thermal vibration (and catalytic action of water, described below) has helped to remove the nonbridging oxygen and two electrons are left at the vacant site to maintain the local charge neutrality. These electrons are comparatively free and can meet the electrophilic requirements of I_M atom and at the same time can screen the N_F atom properly. This structure thus seems energetically more favourable than the one shown in Figure 3.7.

Water seems to act as a catalyst in this process. Actually water and oxygen removal take place simultaneously and when dehydration and reduction occur at the same time, the former influences the latter. This demonstrates coupling effect and one such example is the dehydration-reduction of goethite (α -FeOOH) to magnetite (Fe_3O_4).⁽¹⁹⁾

Hence the process can be divided into three steps. Figure 3.3 is the initial stage. Figures 3.4 and 3.5 show the second stage after addition of the water. The final stage, as given in Figure 3.8, results due to the heat treatment. Such oxygen ion vacancies (on the surface) containing even number of electrons can give rise to nonparamagnetic colour centres. Since these electrons will be more stable in some specific vacancy sites usually close to a cation, and since at the same time the environment of the electrons will not be the same in different regions (due to the disordered structure), a variety of energy levels will be available for such electrons. So, radiation will be

absorbed uniformly throughout the visible spectrum. This will result in a general darkening effect, rather than development of a specific colour.

These electrons (at the vacancy sites) are generally stabilized by modifier ions. Presence of one or more electrons trapped on or near a modifier cation or a cluster of modifier cations has been observed in glasses after irradiation. (13,20)

No darkening or colour change was observed during heat treatment of the glasses in the bulk form. The darkening effect was found to be mainly limited on the surface of the powder. This can be easily explained by taking into account the well known fact that surface is chemically more reactive. The interface of a solid and a gas or the boundary between a solid, a liquid and a gas is the seat of an asymmetry that can enhance chemical reactivity in many cases. (21) Also, as stated previously, grinding will introduce defects and strain and these factors will increase the reactivity. So the darkening effect, in the present case, is more pronounced (observable) on the surface and accordingly the finer the particles the more intense is the effect.

This behaviour seems to be restricted to the glassy states only and is supported by the observations of heat treatment of glass no. 6. Here, the glass composition was so chosen that, initially after melting, it would form a glass, but after heat treatment, it would ceramise. In this case (as given in Table 3.4) during heat treatment black regions were formed on the surface, but, if the heat treatment

was carried out for a longer time (nearly for an hour) around that temperature, so as to allow ceramisation, the black colour vanished. The reasons for the absence of this effect in crystalline materials appear to be twofold. Firstly, sufficient number of nonbridging oxygen atoms are required to produce the darkening effect (according to the proposed model) and this can be easily ensured in the case of glasses. Secondly, the inherent disordered structure of glasses favours the formation of suitable colour centres.

Water in excess, other than what is required for the catalytic activity, can have a very pronounced effect on the darkening. The possible reasons could be as follows: Firstly, excess water can break the N_F-O-N_F (or N_F-O-I_M) bonds⁽¹⁵⁾ and so can change the surface structure drastically. Secondly, modifier ions may be leached out by water. Thirdly, at the heat treatment temperature, ion migration can be pronouncedly facilitated for a surface containing a high proportion of OH ions,⁽²²⁾ reducing thereby the surface defects, strains and consequently the formation of colour centres.

The ambient atmosphere (air, hydrogen, argon or oxygen) does not appear to have any appreciable effect on the darkening process. The formation of colour centres is a coupling type of reaction (at high temperatures) occurring at some specific regions on the surface where minute amount of water acts as a catalyst. If appropriate amount of water is added, then colour centres will be formed irrespective of the environment, but it is difficult to compare the concentration of colour centres formed in different environments as

they are nonparamagnetic in nature.

The bleaching of darkened surface by oxidising agents is due to the injection of oxygen atoms at the vacant sites resulting in the loss of colour centres. Mixture of chromic and sulphuric acids, being a strong oxidising agent, bleaches the colour faster than H_2O_2 which is a relatively weak oxidising agent. The bleaching time (average) in the latter case is nearly thirtysix hours, whereas for the chromic acid and sulphuric acid mixture, the bleaching time is a few hours only. The bleaching rate is intermediate in the case of HNO_3 . However, it should be noted that if the surface forms a viscous mass (which happens for some low melting point glasses at the heat treatment temperature), some of the darkened regions will be entrapped within fine pores beneath the surface. In such cases, oxidising agents will not be able to reach those areas and the colour bleaching will be somewhat incomplete.

At high temperatures, when the glass powders form a low viscous mass and high mobility of surface atoms causes drastic changes in the surface structure, colour centres are expected to be destroyed. This is because, in the new environment at high temperature, electrons at the vacant sites will be largely exposed (i.e. less screened) as well as more mobile. So, either, they will absorb oxygen atoms from the air to accommodate them in the structure (as a bridging or nonbridging oxygen), or, else, free electrons may be removed/bound in some structural flaws in the glass. Accordingly, we observed that dark regions vanished at

higher temperatures and the bleaching temperature was lower for low melting point glasses and vice versa consistently with the above model.

Now the effect of glass compositions on the darkening phenomenon (Tables 3.3 and 3.4) will be discussed in the light of the present model. From the previous discussion, it is clear that at least the following two factors, which are mainly controlled by glass composition, should be considered to get the darkening effect. Firstly,^a sufficient number of nonbridging oxygens are required which need the presence of an equivalent amount of modifier species. Secondly, to get strong Lewis acid sites, intermediate species (like aluminium) or network forming ions capable of changing their coordination easily (like boron) are needed.

It is therefore obvious that according to the present model, glass no. 1 (vitreous silica) and glass no. 2 (pure GeO_2) should not show any colour change. This is confirmed by our experimental data. Glass no. 8 also does not show any colour change. This may be partly due to the ability of Pb^{2+} ions to act as network formers (consequently lowering the number of nonbridging oxygens) and partly to higher polarizability of Pb^{2+} ions which can accommodate the nonbridging oxygens in a better way and can increase their stability. This is more appreciable in case of glass no. 9 where by replacing half of the PbO by Na_2O , very good darkening was observed. This case is also interesting from another point of view. It is expected that some of the electrons, remaining in the vacant sites,

should be captured by easily reducible Pb^{2+} ions to give lead atoms. This conjecture was supported by TEM studies of darkened powders for this glass. In the microstructure, fine dark particles were visible (Figure 3.10) and corresponding diffraction pattern contained haloes characteristic of amorphous materials or particles of very small size. However, after getting heated by the electron beam inside the microscope, the small dark regions agglomerated (Figure 3.11) and produced a diffraction ring pattern (Figure 3.12). By analyzing the data with respect to rings from a standard gold sample, the phase was identified to be metallic lead (Pb). Table 3.5 gives a comparison of the calculated d_{hkl} values for our sample and standard d_{hkl} values for cubic lead. So this observation also supports the proposed model. In this glass, the dark colour obtained after heat treatment seems to be partly due to metallic lead and partly due to colour centres.

In glass no. 10, some CeO_2 was added to see its effect on the darkening process. Interestingly, this glass also showed reasonable darkening. But the extent of darkening appeared to be somewhat less than that of glass no. 9. This is because some of the electrons left by oxygen atoms may be taken by cerium ions (some of them are in Ce^{4+} state) to change their oxidation state. Hence the concentration of colour centres will be somewhat reduced.

In glass no. 11, where instead of Na_2O , CaO has been added, no colour change was observed. Calcium ions being doubly charged (and of higher field strength than alkali

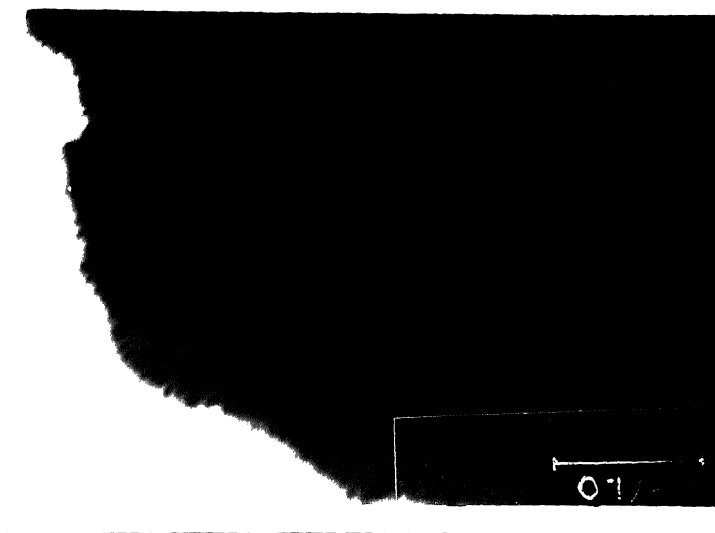


Figure 3.9 A typical transmission electron micrograph of the glass samples

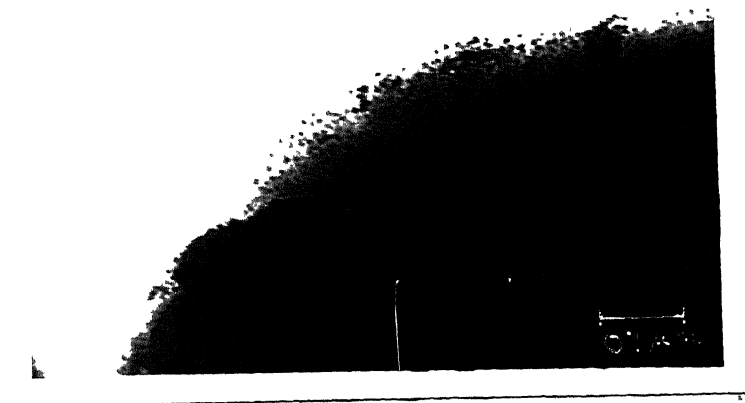


Figure 3.10 Transmission electron micrograph of glass no. 9.



Figure 3.11 Microstructure of glass no. 9 after being heated for a few minutes with the electron beam inside the TEM.

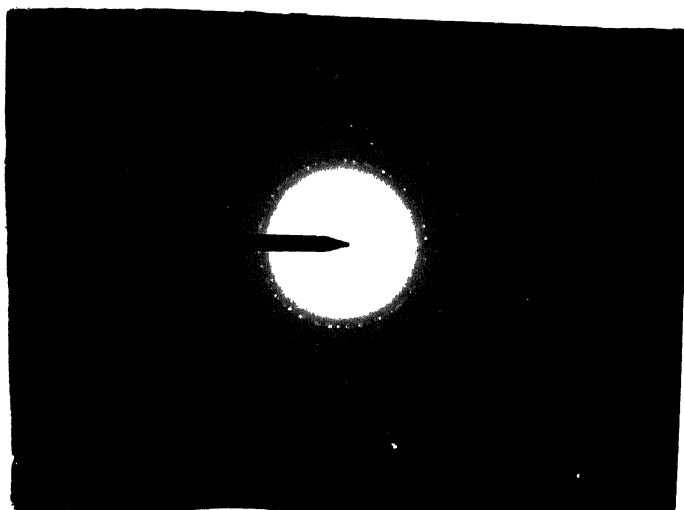


Figure 3.12 Representative electron diffraction pattern of regions emerged in glass no. 9 after electron beam heating of the sample inside the TEM indicative of the presence of the cubic phase of lead (Pb).

TABLE 3.5 Standard d_{hkl} values for cubic lead and d_{hkl} values calculated from SAD pattern of glass no. 9 after electron beam heating of the sample inside the TEM

Standard data for cubic lead			Calculated d_{hkl} values for glass no. 9
hkl	I/I ₁	d Å	
111	100	2.855	2.88
200	50	2.475	2.44
220	31	1.750	1.77
311	32	1.493	1.50
222	9	1.429	-
400	2	1.238	-
331	10	1.136	-
420	7	1.107	-
422	6	1.011	-
511	5	0.953	-
440	1	0.875	-
531	9	0.837	-
600	4	0.825	-

metal ions),⁽²³⁾ will interact strongly with nonbridging oxygens and will inhibit their removal. So, no colour centre will be formed in this situation.

Glass no. 12 (soda lime silica) does not show any colour change. In this case, higher amount of network forming oxides (and hence less number of nonbridging oxygens) and lower amount of intermediate oxides can account for the formation of very poor density of colour centres with almost no visible change. By lowering the amount of silica and by increasing the alkali content (glass no. 13), however, the darkening could be observed.

The reason for the absence of colour in case of glass no. 15 is however different. This glass is highly hygroscopic. During grinding, it absorbs enough moisture to become wet. As mentioned above, water in excess destroys the process of colour formation. So no colour change was observed in this glass.

Other glasses of Table 3.3 satisfy (at least to some extent) the aforesaid requirements of darkening and exhibit the effect in varying degrees (see Table 3.4).

3.4 Conclusion

Powdered oxide glasses over a wide range of compositions exhibit a darkening effect when subjected to a heat treatment with addition of a trace amount of water. The dark colour can however be bleached by some oxidising agents as well as by heating the samples to a temperature around 850°C. This behaviour is believed to arise due to the formation of nonparamagnetic colour centres. The latter forms in the glasses due to a simultaneous dehydration and reduction reaction, in which a trace amount of water acts as a catalyst. A model proposed on the basis of Lewis acid sites concept, common in the theory of catalysis, can satisfactorily explain the important parameters related to the darkening effect observed.

In the field of catalysis, this darkening effect could be exploited for useful purpose. It is well known that glass powders are used as catalyst in many important industrial processes^(24,25) (e.g., petroleum cracking). As the surface defect structure is an important parameter for the catalytic activity of a catalyst, so by increasing the surface defect of the glass powder (i.e. after darkening by our method) better catalytic activity is expected, which in turn will increase the efficiency of the chemical processes involved.

REFERENCES

- (1) Henderson, B. (1972), *Defects in Crystalline Solids*, p. 69, Edward Arnold Ltd., London.
- (2) Schulman, J.H. and Compton, W.D. (1962), *Colour Centres in Solids*, Pergamon Press, Oxford.
- (3) Weyl, W.A. and Marboe, E.C. (1962), *The Constitution of Glasses — A Dynamic Interpretation*, Vol. 1, pp. 292, 30, Interscience Pub., New York.
- (4) Nassau, K. (1978), *Amer. Mineral.* 63, 219.
- (5) Compton, W.D. (1974) in *The Encyclopedia of Physics* (Ed. R.M. Besancon), p. 147, Van Nostrand Reinhold Co., New York.
- (6) Henderson, B. and Wertz, J.E. (1977), *Defects in the Alkaline Earth Oxide*, pp. 8, 135, Taylor and Francis Ltd., London.
- (7) Gager, W.B., Klein, M.J. and Jones, W.H. (1964), *Appl. Phys. Lett.* 5, 131.
- (8) Hughes, A.E. and Henderson, B. (1972) in *Point Defects in Solids* (Ed. J.H. Crawford, Jr. and L.M. Slifkin), Vol. 1, p. 397, Plenum Press, New York.
- (9) Lell, E., Kreidl, N.J. and Hensler, J.R. (1966) in *Progress in Ceramic Science* (Ed. J.E. Burke), Vol. 4, pp. 4, 12, 43, Pergamon Press, Oxford.
- (10) Nurnberger, C.E. and Livingston, R. (1937), *J. Phys. Chem.* 41, 691.
- (11) Kernohan, R.H.A. and McCammon, G.M. (1952), *Bull. Amer. Phys. Soc.* 27(2), 8.
- (12) Levy, P.W. (1960), *J. Amer. Ceram. Soc.* 43, 389.
- (13) Beekenkamp, P. (1966), *Philips Res. Rep. Suppl.* 40 (Chap. 4).
- (14) Thomson, S.J. and Webb, G. (1968), *Heterogeneous Catalysis*, p. 146, Oliver and Boyd, London.
- (15) Ryland, L.B., Tamele, M.W. and Wilson, J.N. (1960) in *Catalysis* (Ed. P.N. Emmette), Vol. 7, pp. 54, 85, 38, Reinhold, New York.
- (16) Boldyrev, V.V., Bulens, M. and Delmon, B. (1979), *The Control of the Reactivity of Solids*, p. 117, Elsevier, Amsterdam.

- (17) Weyl, W.A. (1950), Trans. N.Y. Acad. Sci. 12, Series II, No. 8.
- (18) Grimshaw, R.W. (1971), The Chemistry and Physics of Clays and Allied Ceramic Materials, p. 97, Ernest Benn, London.
- (19) Garcia-Gonzalez, M.L., Grange, P. and Delmon, B. (1977). in Reactivity of Solids (Ed. J. Wood, O; Lindqvist, C. Helgesson and N.C. Vannerberg), p. 755, Plenum Press, New York.
- (20) Griscom, D.L. (1971), J. Non-Crystalline Solids 6, 275.
- (21) Weyl, W.A. and Marboe, E.C. (1967), The Constitution of Glasses — A Dynamic Interpretation, Vol. 2, Part 2, p. 1022, Interscience Pub., New York.
- (22) Winfield, M.E. (1960) in Catalysis (Ed. P.H. Emmette), Vol. 7, p. 153, Reinhold, New York.
- (23) McMillan, P.W. (1964), Glass-Ceramics, p. 16, Academic Press, London.
- (24) Sabatier, P. (1965) in Catalysis Then and Now (Trans. E. Emmet Reid), Part II, p. 811, Franklin Publishing Co. Inc., Englewood, New Jersey.
- (25) Alex Mills, G. and Cusumano, J.A. (1979) in Kirk-Othmer Encyclopedia of Chemical Technology, Vol. 5, p. 52, John Wiley and Sons, New York.